[redacted] UNCLASSIFIED

019077

WT- 727

Copy No. 162 A

C 162A

Operation UPSHOT-KNOTHOLE

NEVADA PROVING GROUNDS

March - June 1953

Project 3.8

AIR BLAST EFFECTS ON UNDERGROUND STRUCTURES

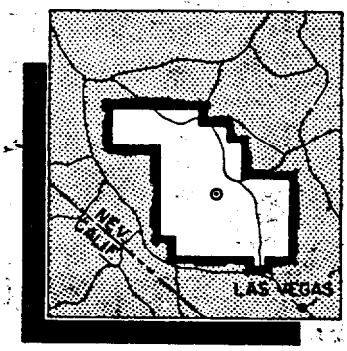

[redacted]

HEADQUARTERS FIELD COMMAND, ARMED FORCES SPECIAL WEAPONS PROJECT
SANDIA BASE, ALBUQUERQUE, NEW MEXICO

[redacted] UNCLASSIFIED

[redacted]

WT-727

This document consists of 138 pages
No. 102 of 285 copies, Series A

OPERATION UPSHOT-KNOTHOLE

Project 3.8

AIR BLAST EFFECTS ON UNDERGROUND STRUCTURES

REPORT TO THE TEST DIRECTOR

by

N. M. Newmark
G. K. Sinnamon
University of Illinois

January 1954

[redacted]

Protective Construction Branch
Engineering Division, Military Construction
Office Chief of Engineers
U. S. Army

[redacted]

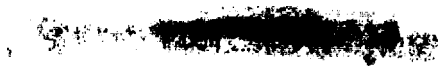

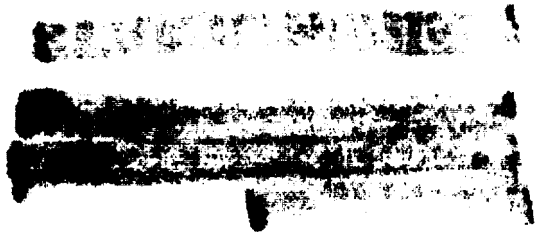

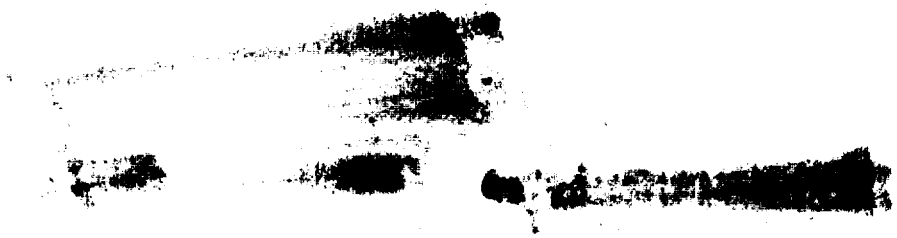

ABSTRACT

This report describes the results of a test to determine the nature of forces transmitted through earth to buried structures from the explosion in air of an atomic bomb. The structures were primarily reinforced concrete boxes having a large number of simply supported steel beam strips forming their roofs. Three structures were included in the program, having respectively 1 ft, 4 ft, and 8 ft of earth cover over the beam strips, and each of the structures had a number of individual beam strips, with several strips of each of three different degrees of flexibility to provide information concerning the effect of flexibility of the structure on the loading transmitted to it. All of the beam strips had the same span, namely 8 ft.

The structures were tested in two shots, the first producing an overpressure level of about 15 psi, and the second about 63 psi. *No damage* or permanent deformation was expected in the first shot, and none was observed. As a matter of fact, the pressures attained in this shot were considerably smaller than those expected and the records obtained provided only qualitative information in most cases.

In the second shot, the pressures were of about the order of magnitude expected in the design, and the pressure wave had the expected highly irregular pulse shape characteristic of the precursor region. The positive phase duration of the main pulse was about 0.15 sec. It was preceded by a precursor pulse of about one fourth the magnitude of the maximum pressure pulse, lasting for about 0.05 sec.

Only small permanent deflections were obtained in the test, although the transient deflections *were of an* order of magnitude sufficient to give appreciable readings. The design criteria selected for the test structures were adequate. However, it was intended that the steel in all of the roof beams would have the same physical properties. Unfortunately the "plastic" beams, intended to be considerably *weaker* than the "intermediate" and the "elastic" beams, were fabricated from substitute material having a considerably higher yield point than that in the other beams. This material was not available for laboratory tests before the field tests were made. In spite of this difficulty, the general aims of the project were achieved, and both the plastic and the intermediate beams experienced some plastic deformation.

The analyses of the test data indicate the following conclusions:

(1) In well-compacted silty subsoil of the type at the test site, there is no effective attenuation of a pressure pulse applied at the surface with depth through the subsoil, when the pressure is transmitted to a structure in the soil. The transient as well as the permanent strains and deformations of the beam strips were of about the same order of magnitude at all three depths, and showed only a slight decrease for the 8 ft depth compared with the others. This indicates that for deflections of less than 0.5 per cent of the span, and for depths of cover less than the span length, the dynamic "arching" phenomenon is negligible and the beneficial effect of added cover is primarily that due to the added mass of such a cover.

(2) For underground structures having a net density less than that of the displaced soil, the overall accelerations of the structure act to reduce the influence of the pressures applied to the top of the structure. However, this influence is not large, and may be neglected in design.

(3) The lateral pressures exerted on vertical faces of a buried structure, produced by pressures applied at the top surface of the soil, are of an order of magnitude of 15 per cent of the vertical pressures on the surface, for well-compacted silty soils of the type at the test site.

(4) The pressures exerted upward on the base or floor slab of buried structures, are very nearly of the same magnitude as the downward pressures on the ground surface.

Theoretical considerations indicate that these conclusions are not unreasonable for other types of soil except that the horizontal pressures might be larger in other soils. It is also reasonable to expect that the conclusions are conservative for larger deflections approaching more nearly the collapse limit. However, because experimental verification is lacking in the range near collapse, it is recommended that advantage be taken of any opportunity to obtain further verification of these conclusions by subjecting the same structures to additional atomic bomb blasts. Valuable information would be obtained from further tests with pressure levels ranging from 75 psi upward. Information of practical usefulness would be obtained even though only permanent deformations were measured by means of before and after surveys, provided that a pressure-time record of the overpressures at the ground surface is measured during the shot. However, valuable basic data could be obtained by transient measurements of deflection and strain in further tests, with instrumentation similar to that provided in the tests described herein.

[redacted]

REWORD

This report is one of the reports presenting the results of the 78 projects participating in the Military Effects Tests Program of Operation UPSHOT-KNOTHOLE, which included 11 test detonations. For readers interested in other pertinent test information, reference is made to WT-782, Summary Report of the Technical Director, Military Effects Program. This summary report includes the following information of possible general interest.

a. An over-all description of each detonation, including yield, height of burst, ground zero location, time of detonation, ambient atmospheric conditions at detonation, etc., for the 11 shots.
b. Compilation and correlation of all project results on the basic measurements of blast and shock, thermal radiation, and nuclear radiation.
c. Compilation and correlation of the various project results on weapons effects.
d. A summary of each project, including objectives and results.
e. A complete listing of all reports covering the Military Effects Tests Program.

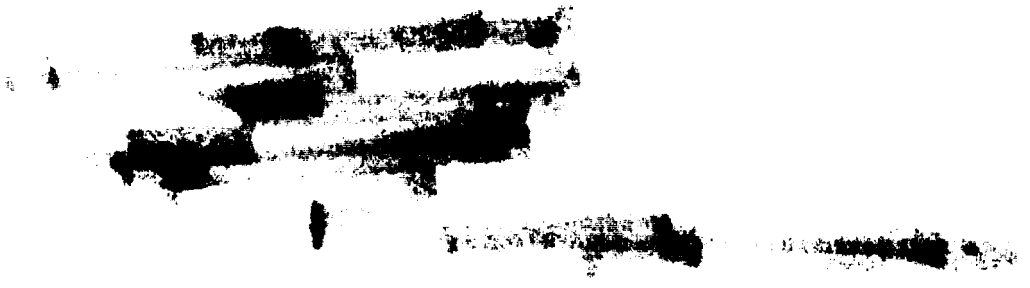

ACKNOWLEDGMENTS

The work reported herein was planned and carried out by personnel of the Structural Research Laboratory of the University of Illinois, under contract DA-49-129-eng-239 with the Office-of the Chief of Engineers, U. S. Army. The project was under the general direction of N. M. Newmark, Research Professor of Structural Engineering, and under the immediate supervision of G. K. Sinnamon, Research Assistant Professor of Civil Engineering.

The project officer for Project 3.8 was Mr. W. J. Matthews, Protective Construction Branch, Office of the Chief of Engineers. The authors wish particularly to acknowledge Mr. Matthews' continual assistance and advice in all phases of the work.

The field inspection and operations for this project were supervised by Professor Sinnamon with the assistance of other members of the staff of the University of Illinois and the help of Mr. Matthews.

The analyses of the test data were made by E. R. Bretscher, Associate Professor of Civil Engineering, with the aid of D. A. Day, Assistant Professor of Civil Engineering. The laboratory tests of control specimens and coupons were made under the direction of W. E. Black, Professor of Theoretical and Applied Mechanics, and the inspection of the soil compaction and all the laboratory tests of the soil properties were made by H. O. Ireland, Research Assistant Professor of Civil Engineering.

The writers wish to express appreciation to a number of persons who contributed materially to the success of the operational phase of project 3.8. LT. R. M. Longmire and Mr. Sam Cox of the U. S. Navy Bureau of Yards and Docks assisted in the inspection of the construction operations. Commander C. E. Langlois and Lt. Col. J. P. Dawley of Program 3 DWET, CDR. L. N. Saunders and Lt. Col. J. J. Haley of the Division of Engineering and Construction DWET were helpful in the general administration of the program. Mr. J. J. Meszaros of the Ballistic Research Laboratories and his staff on Project 3.28.1 were responsible for all of the instrumentation. Mr. W. J. Hall, Mr. W. Egger, Assistant Professors R. J. Mosborg and J. E. Stallmeyer of the University of Illinois, in addition to the other staff members whose responsibilities and association with the program have been described, contributed materially to the general operations of the work and to the production of the data for this report.

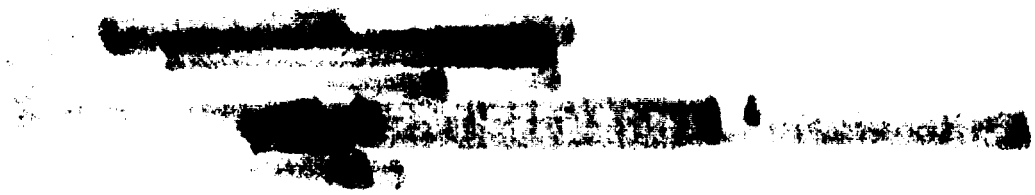

CONTENTS

ILLUSTRATIONS

TABLES

[redacted]

CHAPTER 1

INTRODUCTION

1.1 OBJECTIVES

The general purpose of this project was to obtain the necessary basic data from which to develop criteria for the economical and efficient design of underground protection from air blast forces.

The specific objectives were: (1) to investigate the nature of the forces transmitted from an air burst of an atomic bomb through the earth to underground structures; (2) to determine the variation of these forces with the depth of transmission through the earth and with the flexibility of the structural elements subjected to the forces; and (3) to study the response of simple structural elements of different stiffnesses subjected to the transmitted dynamic forces.

1.2 BACKGROUND

1.2.1 General Comments

The results of previous weapons effects tests and the experience in Japan[1] appear to indicate that even relatively shallow earth cover over light shelters provides substantial protection against blast. The exact nature of this protection is uncertain. There are three principal ways in which the earth cover can act: (1) to increase the mass of the structure and consequently to reduce its response to the applied loading; (2) to reduce or attenuate the magnitude of the forces acting on the structure by absorbing the energy of these forces in the deformation of the soil; and (3) to change the pattern of distribution of the forces on the structure by either changing the effective shape of the structure (as for example by rounding off an angular structure above ground with a mound of earth as in the covered arch structures in the

1. The Effects of Atomic Weapons, U. S. Govt. Printing Office, 1950, P 389-390.

[redacted]

GREENHOUSE program), or by permitting transfer of forces around but not through the structure.

All of these actions are affectedly the flexibility of the structure as well as by the physical and mechanical properties of the earth cover. This program was therefore designed to obtain information concerning the pressure transmission through different depths of soil to structures having different degrees of flexibility.

1.2.2 Arching

When forces are applied to a non-uniform soil mass, the less stiff parts of the soil deform most. The relative deformations of the soil permit shearing stresses to be developed which transmit part of the stress from the flexible elements to the stiffer adjacent elements. This phenomenon in soil is called "arching." Arching can occur when any element is introduced into a mass of soil if the element has a stiffness different from that of the surrounding soil. Consequently an underground structure, which interrupts the continuity of the mass of soil in which it is placed, changes the transmission of force because of its difference in stiffness from the surrounding soil, and is subjected to forces on its various faces which differ from the forces on the corresponding planes in the free, undisturbed earth mass. If the structure is stiffer than the surrounding soil the forces in general will be greater, and if it is less stiff the forces in general will be less than in the free earth. The former phenomenon is sometimes called "reverse" arching.

Arching in soils occurs under static loads, and has been the subject of experimental and theoretical studies in the field of soil mechanics. From these studies, under static conditions, it can be concluded that the vertical stresses due to the weight of the soil or due to superimposed static loads can "arch" around a yielding or flexible horizontal element. The relief of pressure on the element depends on the ratio of the depth of earth above it to the span or size of the area. Beyond a certain value of this ratio, no increase in arching takes place. Normally the degree of arching is very nearly at its maximum value for a depth approximately equal to the span of the flexible element.

No previous studies of arching under dynamic conditions have been reported.

1.3 TEST PROGRAM REQUIREMENTS

Because of the lack of dependable information on the transmission of dynamic pressures through soil, and because of the almost complete lack of information on arching under transient loading conditions, this test program had to be planned so as to give as much information as possible of a basic nature. It was necessary to lay out the program in such a way as to obtain comparative results for different degrees of flexibility of the underground structures, and for different depths of cover relative to the span of these structures. The decision was made

to include very stiff structures, moderately flexible structures, and extremely flexible structures which would undergo a good deal of inelastic or permanent deformation.

For each of these degrees of flexibility, it was desirable to provide a depth of cover so slight as to prevent arching almost completely, a moderate depth of cover which would permit only moderate arching, and a depth of cover about equal to the span of the structure so as to allow arching to develop almost fully.

The selection of these different degrees of flexibility was dictated by other requirements as well. Because of the uncertainty in the transmission of pressure through the earth, as well as the uncertainty as to the magnitude of the surface forces expected from the blast, it was necessary to provide some range in the design of the structures so as to permit the obtaining of valid data even for extreme conditions of variation from the predicted test phenomena.

In order to avoid ambiguity in the interpretation of the data, it was necessary to make the test structures as simple as possible. To this end, it appeared desirable to make all of the structures similar rectangular chambers of reinforced concrete, and to provide the variations in the roofs of the chambers only. Such structures could be designed to have the same general characteristics as typical underground protective construction. The simplest type of roof covering for the test structure appeared to be simply supported beams, in which the different stiffnesses could be obtained simply and conveniently with a number of parallel beam strips, graded in size and flexibility, but each one independent in action from the action of neighboring elements.

Although it would have been desirable to have had another major variable in the program, namely, the soil properties, it was impossible to include such a variable in the program at the test site selected, and accordingly the test was planned for only one soil type.

To aid in the interpretation of the data, it was desirable to have complete and accurate measurements of the soil properties, and to control the properties of the backfill to the extent that a reasonable degree of uniformity was obtained in the moisture content, degree of compaction, and other variables affecting the soil behavior.

In order to obtain the maximum amount of useable information from the test program, it was necessary to instrument the structures completely enough so that all of the necessary information could be obtained from survey measurements and measurements of transient structural response and pressures. These data were required not only for specific quantitative results, but for internal checks of the consistency of the data in order to give some assurance of validity to the test results. To define completely the forces acting on the structures and the structural response, it was *necessary* to determine the pressures acting on the earth surface, and on the top, bottom and sides of each of the test structures. The pressure measurements had to include separate values for each of the different degrees of flexibility in each structure. For comparative purposes, pressures in the free earth were required as well.

In order to describe completely the response of the roof beam

strip elements of the structures, it was necessary to measure both deflections and strains in these elements. As a check of consistency of these values and to assist in the determination of the relations between the forces on the different surfaces of the test structure, the reactions of the beam strips on the concrete test chambers were also required. To permit a complete analysis of the data, measurements of the accelerations of the entire test chambers were necessary.

To provide a check on the transient measurements, and to permit the determination of response in the plastic range if the responses became extremely large, survey measurements had to be planned to determine the *overall* deformations after the test.

CHAPTER 2

DESCRIPTION OF TEST STRUCTURES

2.1 DESIGN CRITERIA

2.1.1 Pressures and Durations

In order to make the results of this study applicable to structures in regions where maximum protection is desirable, it was decided to place the test structures at a location where pressures of the order of 60 to 80 psi would be reached. Preliminary estimates of the maximum pressure to be expected for the size of the bomb to be used indicated that this pressure range was feasible. Consequently, the structures were designed on the basis of an expected pressure of 60 psi, with a possible variation in either direction of 20 psi from the expected value.

At the time the design was made, accurate estimates of rise time and of duration of positive phase were not available. Examination of pressure records for pressures in the range considered, and for bomb sizes in the range from 10 to 20 KT, indicated that the pressure-time diagram after the precursor would be roughly triangular in shape with a rise time to maximum pressure ranging from nearly zero to possibly 20 millisec or more, and with an initial rate of decay from the maximum corresponding to an effective duration of about 300 millisec or less. The total positive phase duration was expected to be approximately twice this figure, but substantial departure from the nearly linear rate of initial decay would be expected to occur much later than the time at which the structures would have reached their maximum deflection.

Shortly after the designs were completed, the test data for Operation TUMBLER became available, and permitted a more accurate prediction of the expected phenomena. However, no change in the design would have been required with the use of the TUMBLER data for precursor and main pulse duration, so long as provision had to be made for a possible variation in expected peak pressure of 25 per cent.

The effect of a finite rise time was expected to be relatively negligible for large responses of the structures, but this effect was

recognized to be extremely important for structural responses in the elastic range or just beyond this range.

The design criteria selected were based on the best available estimates at the time the designs were prepared, with an allowance for inaccuracy of the predictions. However, because of the sensitivity of these structures to variations in pressure and positive phase duration, it proved to be impossible to provide for as wide a range as was desirable in the degrees of flexibility for all possible combinations of rise time, peak pressure, and duration. Therefore, it was decided to standardize on an effective duration of 300 millisec., an instantaneous rise. and a range in peak pressure from 40 to 80 psi, to cover the probable variations, as well as to avoid complete failure of the elements of the structures. Of these variables, the pressure range is by far the most important.

2.1.2 Variation of Flexibility

The desired variations of flexibility in the test structures were provided in the roofs of the test chambers by making the roofs of simply supported steel beam strips. By choice of the makeup of the strips a wide range in flexibility could be achieved. For each structure it was decided to provide three different flexibilities of the roof beams. These were designated as "elastic" or E strips "intermediate" or M strips, and "plastic" or P strips. The criteria governing the design of these beam strips were taken as follows:

For either of the extremes in the expected loading it was desired that at least one set of beam strips would remain elastic, and at least one set would get part way into the plastic range. In order for the plastic beam strips to yield at the lower range of loading it was impossible that they would be able to sustain the higher loading without extremely large deflections. Therefore, it was considered necessary to provide a safety support to limit their deflection to about 6 in. in order to prevent collapse of the structure and consequent loss of records. For the extreme high loading, the intermediate beam strips were not intended to have a deflection exceeding 4 to 6 in., and for the extreme low loading these strips were expected to remain elastic.

Variations in the yield point of the steel used in the beam strips could cause variations in their response. Ranges of variation from the expected yield values were considered in the design of the structures to the extent that it was possible to do so with such extremely sensitive elements.

From the laboratory tests of the beam strips reported in Chapter 5 it was found that because of a substitution of material the P beam strips had a much higher yield point than the M beam strips, resulting in their having about the same capacity at yielding. If they had been of the same material as the M beam strips, as intended, the capacity of the P beam strips would have been considerably less at yielding, and their dynamic deflections would have been much larger. It is considered that the design criteria were well selected, however, as the deflections achieved in the field test were in the yield range

for the P beam strips and for some of the M beam strips in spite of all the uncertainties which had to be considered in the design.

2.1.3 Choice of Structures and Layout

The general layout of the test structures was governed by the design criteria selected, and by economic considerations involved in the selection of structures covering as wide a range of variables as possible with the least number of separate elements. Three different degrees of roof flexibility were chosen as explained above. Similarly, to include the entire range of variation in the phenomenon of arching, three different depths of cover were chosen also. In order to avoid extraneous phenomena which might be caused by subjecting the structures and the instruments mounted thereon directly to the blast, it was decided to provide at least 1 ft of earth cover over the shallowest structure. The span of the roof beams then had to be selected so that negligible arching would occur with a cover of 1 ft. For the deepest structure, a depth of *cover* equal to the span would provide virtually complete development of arching (under static conditions). Considerations of economy in excavation and backfilling operations indicated that an 8 ft span, and corresponding depth, could be used. Moreover, the necessity of working in the structures, and of mounting equipment in them, required a span of this order of magnitude. The depth of the chambers was determined by considerations of headroom within them. With the extreme depths of cover of 1 ft and 8 ft selected in this way, an intermediate depth of cover of 4 ft was selected arbitrarily.

Since each of the three different degrees of flexibility was to be provided at each of the three depths of cover, provision had to be made for each test chamber to be roofed with a series of beam strips having graded properties. Because the flexibilities of the classes of beam strips were different, it was necessary to provide some transition from each test element to the next one of a different flexibility. This transition was provided by using a minimum of three parallel beam strips for each degree of flexibility. The central one of the three strips was designated as the test strip and all measurements were taken on it. The adjacent beams of the group were primarily for the purpose of providing a transition in flexibility to the next test strip.

However, because of the fact that the plastic beam strips were adjacent to the very stiff end walls of the structure, one additional transition strip was provided between the test strip for the plastic beams and the end wall. This gave a total of four plastic beam strips in each chamber. The total length of the test *chambers was* determined by the number of roof beam strips selected.

To insure that all of the structures would be subjected to the same pressure pulses, they were located in the same region in a group, such that each was at the same distance as the others from the expected ground zero.

In order to make the structures easier to instrument and to construct, it was decided to make the roof beam strips of steel. It was expected that the properties of the steel would be more uniform and the

test data would be simpler to analyze and easier to interpret if the beams were of steel rather than of reinforced concrete. Furthermore, in order to permit direct comparisons of the effect of depth of cover, it was decided that each structure, at each depth, should have identical roof beam strips.

Since the strength and flexibility of the supporting structure was not a primary variable in these tests, the decision was made that the test chambers supporting the roof beam strips would be made of reinforced concrete, heavily reinforced to avoid any major deformation during the test.

2.2 DESCRIPTION OF STRUCTURES

2.2.1 Concrete Test Chambers

In order to provide for the desired level of ground pressures, the test structures were located, as shown in Fig. 2.1, close together on an arc of 900 ft radius from the intended ground zero. Access to each structure was provided through a vertical shaft extending to a horizontal passage leading into one end of each structure. The structure having a 1 ft depth of cover had its own access way. For the other two structures a common shaft located between the structures provided access to both through separate passageways.

Each of the concrete test chambers was identical in design, with overall outside dimensions of 10 ft 2 in. by 21 ft 2 in. in plan, and 8 ft 3 in. in depth. A sketch of the structure is shown in Fig. 2.2. The sidewalls of the chambers were 19 in. thick, the end walls 15 in. thick and the floors 12 in. thick.

A photograph of Structure 3.8c before the roof was added is shown in Fig. 2.3. The anchor bolts for the attachment of the roof beam strips are visible in the figure. The figure also shows the parapets on the sidewall which provide protection for the ends of the beam strips. The tops of the parapet walls are on a level with the tops of the beam strips. The side and end walls of the test chambers are keyed into and dowelled to the base slab.

Because of the great length of the side walls, a partition wall was placed at about midlength with a large central opening to permit access between the two parts of the concrete structure. A supporting beam was placed down the middle of the structure, 6 in. below the plastic beam strips, to provide a safety support.

All concrete walls had vertical and horizontal reinforcement in both the inner and the outer faces. All the walls were designed for large pressures, so that under the expected conditions the deflections of the walls and of the floor slab would be negligible. Equivalent static loads for the design of the base slab were taken as 40 psi, and for the walls 60 psi. For these static design pressures, the allowable stresses were taken as 1.33 times the normal value or 26,700 psi for the reinforcing steel, and 1.5 times the normal value or about 2000 psi for the concrete.

The percentages of reinforcing steel in the base slab and end

walls are approximately 0.65 to 0.75 per cent in each direction on each face, and for the side walls 0.5 to 1.0 per cent in each direction on each face, with the lower percentages of steel in the directions and regions where the flexural stresses were considered to be smallest.

The base slab, the end walls, and the side walls were investigated for critical shearing stresses and were found to be adequate without any special provision for shear.

2.2.2 Roof Beam Strips

Each of the 10 beam strips for the roof of each test chamber was composed of two closely spaced I-sections attached by welding to a common cover plate 1/2 in. thick. For the plastic beam strips, the I-sections were made by welding two 7 in. channels back-to-back. The details of the design of each beam strip are shown in Fig. 2.4. A cross-section of each type of strip shows the makeup of the beam strips. The elevation view in the figure indicates the transverse diaphragms used to insure integral action and to strengthen the beam at the points where holes were placed for the mounting of pressure gages directly on the beam strips.

The dimensions and properties of the various beam strips are summarized in Table 2.1. The moments of inertia and other section properties are computed for the actual width of the beam strip. However, the loadings on the strips are assumed to cover the distance from the center of the space between adjacent strips on one side to the center of the corresponding space on the other side, which is 3/4 in. greater than the width of the cover plate. The beam strips are 96 in. long between the centers of their supports, and effectively overhang their supports by 2 in. at each end, making a total length of 100 in.

To provide the desired conditions of nearly free rotation at the ends of the beam strips, the ends were supported on shoes made of T-sections cut from rolled I-beams. A photograph showing the supports at both ends of a typical beam strip, Beam CP2, is included in Fig. 2.5. This figure also shows a detailed view of each of the supports, to indicate the method of increasing the flexibility of the supports by the horizontal grooves placed in the supporting elements.

In Fig. 2.5 it can be seen that the end diaphragm of the beam strip is inclined at an angle to the vertical web of the support. This inclination was chosen so as to permit rotation of the ends of the beam during large deflections of the beam strip. The lower flange of the supporting T is welded to a bearing plate and holes are provided for anchor bolts embedded in the walls of the concrete test chambers.

As shown in Fig. 2.5, at one end of the beam strip the web of the T-section has a section of reduced thickness, formed by horizontal transverse grooves, which acts in effect as a hinge. This end is designated as the "fixed" end. At the other support, the web of the T has two such sections or hinges, one being 6 in. above the other. These reduced sections have a thickness of 0.25 in. at their minimum section, and were designed as elasto-plastic hinges. That is, the

sections were intended to resist only small bending moments but are capable of resisting large vertical forces, either upward or downward. The end of the beam having the shoe with two hinges is designated as the "expansion" end.

With the supporting shoes described, the beam strips are practically free to rotate at their ends but receive sufficient restraint against longitudinal movement to prevent collapse at the ends. The webs of the shoes were designed to permit the measurement of vertical strains as a means of determining end reactions. To determine the reactions from the strains the areas of the webs are required. These areas, as well as the average widths and thicknesses of the webs at the sections where vertical strains were measured, are given in Table 2.4.

A 3/4 in. opening between the cover plates of adjacent beam strips was provided to permit them to deflect independently. A diagram of the arrangement of the beam strips in the roof of a test chamber is shown in Fig.2.6. A view of the process of placement of the beam strips in the roof of Structure 3.8c is shown in Fig. 2.7. To prevent the infiltration of the backfill through the openings, a canvas cover was looped between the beam strips and placed over the entire roof. This canvas covering is shown in Fig.2.8. Also shown in this figure are the filler strips used to bridge the narrow gap between the beam strips. These strips are light T-sections which were made to be inserted into the spaces between the beam strips. The flange of the T-section bears on the cover plates of the adjacent beam strips as shown in the figure.

The larger gap at the ends of the beam strips, between these ends and the top of the parapet wall, is bridged by a similar section consisting of a channel with flanges turned downward, welded to a light plate. These sections are inserted into the end spaces and infiltration of the backfill in this region is prevented by the canvas covering.

2.3 SOIL CONDITIONS

The soil in the Frenchman Flat area where the three structures for Project 3.8 were constructed is a tan silt with a trace of clay. In its natural state this soil is very friable. It is horizontally stratified, has vertical joints which are local zones of weakness, and contains many voids. Limited tests of the undisturbed soil in this area gave values of 86.6 lb per cu ft for the dry density, 10.6 per cent for the water content, and 95.9 lb per cu ft for the wet density.

For the purposes of this project it was not required that specific soil properties be attained but that the properties of the soil be reasonably uniform and accurately known. Since a considerable amount of backfill material was required it was decided to investigate the use of the soil from the Frenchman Flat area for backfilling. Accordingly, two samples of the soil were obtained. One of these was taken from the top 6 in. and another from a depth of 5 ft. These samples were subjected to the standard Proctor compaction test and the results are

shown in Fig.2.9. The maximum dry density as obtained from these tests varied from about 96.4 to 108.2 lb per cu ft and the corresponding water content varied from about 17.2 per cent to 23.5 per cent, based on dry weight. The least maximum dry density on these tests was less than 90 per cent of the largest, and the shape of the compaction curves indicated that this soil was sensitive to small changes in water content. From these tests it was decided that the excavated material could be used for backfilling around the structures if it were compacted in place at a water content slightly on the dry side of the optimum value. If a water content equal to the plastic limit *were* used, the test indicated that a dry density greater than 90 per cent of the maximum value could be achieved.

The compacted specimens of the surface material were trimmed to a suitable size and subjected to tests to determine their unconfined compressive strength. The results of these tests are also shown in Fig. 2.9. *This curve* shows that the maximum strength is obtained at about the optimum moisture content and that the strength on the dry side of optimum does not change as rapidly with changes in water content as the strength on the wet side of optimum. The maximum unconfined compressive strength obtained in these tests was 4.17 tons per sq ft.

Tests were also made on an undisturbed sample of the soil in the immediate vicinity of the test structures. Only one reliable water content determination could be made for the sample, yielding a value of 10.6 per cent, corresponding to a wet density of 95.9 lb per cu ft. The unconfined compressive strength determined on three samples gave results of 1.1, 2.1, and 4.3 tons per sq ft. The dry densities ranged from 85 to 100 lb per cu ft.

In order to investigate the effect of drying on this material a specimen of soil from each of the two depths was compacted on the wet side of optimum moisture. These samples were air dried for an extended period of time and then subjected to unconfined compression tests. The sample from the surface tested 34.4 tons per sq ft. The water content at the time of the test was 3.27 per cent. The sample from a depth of 5 ft tested 19.7 tons per sq ft and had a water content of 3.96 per cent. Since these soils gain tremendous strength on drying it was *necessary to* make arrangements for taking representative samples of the compacted fill material near the time of the field tests to investigate the strength of the fill.

The excavation for the three structures was carried out carefully to permit the base slabs to be poured directly on the undisturbed soil. After completion of the construction of the concrete chambers and the placement of the beam strips and canvas covers, the excavated material was used for backfilling. This material was thoroughly mixed to the proper water content by spreading, sprinkling, and windrowing the material until it was at a uniform moisture content approximately equal to the plastic limit of the material. The backfill was placed in layers of about 4 in. loose thickness and generally compacted by pneumatic hand tampers, except that a rubber-tired roller was used over Structure 3.8c after 5 ft of hand-tamped material was in place. Since the excavations for these structures had nearly vertical slopes which were

located within about 3 ft of the structure, this vertical surface adjacent to Structures 3.8b and 3.8c was interrupted by cutting a bench parallel to the structures, at a depth of about one-half of the total depth of cover and a width equal to the depth of the bench, in order to eliminate a possible shear plane at the juncture between the backfill and the undisturbed soil faces.

Numerous field density tests were performed during the backfilling operation. The results of these tests are shown in Table 2.2. The average water content at the time of placement was 21.5 per cent at an average dry density of 94.9 lb per cu ft and a wet density of 115.1 lb per cu ft.

Shelby tube borings were taken at two locations immediately before Shot 9. The results of these tests are shown in Table 2.3. These tests show that the water content had decreased to an average value of 18.4 per cent which would indicate a reduction of the wet density to about 112 lb per cu ft. The average value of the unconfined compressive strength determined from these borings was 8.3 tons per sq ft. This strength is considerably more than the value of 1.1 to 4.3 tons per sq ft determined for samples of the undisturbed soil. However, this was to be expected since the backfilling operation eliminated the vertical joint planes and the horizontal stratification found in the natural soil. It is possible that similar joint planes or planes of weakness were introduced in the backfill by the disturbance created by Shot 9.

2.4 INSTRUMENTATION

2.4.1 General

The instrumentation for Project 3.8 consisted of: (1) the transient measurement of pressures, strains, deflections and accelerations with electronic equipment, (2) the measurement of permanent strains in the beam strips with mechanical strain gages, and (3) the measurement of permanent deflections of the beam strips and relative motion of the structures with a precise surveyor's level. Most of the electronic instrumentation was performed by the Ballistic Research Laboratories as a part of Project 3.28.1. The recording equipment used by them was the Webster-Chicago Tape Recording type which had been modified by Crescent Industries of Chicago, Illinois. Each of the recording units was capable of recording the intelligence from 22 gages on a 1 in. magnetic tape. The intelligence from each tape was transferred to oscillograph records for study by running the tape through play-back equipment. By using this method records having almost any desired time basis could be reproduced after a test was completed.

Since the recording equipment used was a phase-sensitive type on which long leads could not be used, all of the recording equipment and the power supply for the 3.8 structures were located in an instrument shelter approximately 150 ft west of the test structures. The gages were connected to the recorders by shielded cables which were buried a minimum of 18 in. below the ground surface. The location of

the recorders and test structures so close to ground zero gave rise to irregularities in many of the records for Project 3.8 which were not found in similar records produced by the same type of equipment located at a greater distance from ground zero. Because of these irregularities considerable effort was expended in the assimilation and interpretation of the test data. A more detailed description of the details of the instrumentation system and the methods used in reducing the data is given in Appendix A.

2.4.2 Pressure Measurements

Twenty-six earth pressure gages of the Carlson-Wiancko type were used to measure the pressure at various points on the structures and in the free earth. Five of these gages were located on the beam strips in each structure as shown in Fig.2.6. These gages were mounted on the test beam strips in holes provided for them on the center-line of the cover plates. The diaphragm casing of each gage rested directly on top of the cover plate. Two pressure gages were mounted on each of the intermediate and plastic test strips, *one gage* being close to the quarter point of the span and the other close to the center of the span. The fifth gage was placed as close to the support of the elastic test strip as practical in order to obtain pressure readings with as little influence of deflection as possible. The gage locations used were chosen to give an indication of the dynamic load distribution along the beam strip span and to show any tendency of arching of the soil.

Six earth pressure gages were used to determine pressures on the bottoms and walls of the concrete supporting structures. The pressures on the bottom of the floor slabs of Structures 3.8a and 3.8b were measured by gages installed in the section of the floor slab where the thickness was increased to take the load from the support of the safety beam. This location was chosen since it protected the gages from damage and limited any appreciable effect of deflection.

Structure 3.8a had three gages mounted in the end wall on the outside surface. These gages were 2 ft, 4 ft 9 in., and 7 ft 6 in. from the earth's surface. One gage was mounted in the end wall of Structure 3.8c, 11 ft 9 in. from the earth surface.

Figure 2.10 shows the location of the earth pressure gages buried in free earth to measure the vertical component of stress only. These gages *were* placed in a large excavation which was originally made to provide access to the deepest structure. The soil beneath and above the gages was compacted by the same method used in compacting the soil over the test structures. Therefore the gages should give information on the attenuation of pressure as it travels through soil having the same properties as that above the structures. The gages were put in place with the pressure diaphragm facing upward, in contrast to the orientation used by previous investigators in experiments with similar gages. The gages were placed face downward in a removable form and then earth was compacted for several inches above the back of the gage. After the top of the compacted soil was struck off, the form was removed and the compacted block of soil placed with the gage facing up in

a carefully prepared excavation. The space around the block of soil containing the gage was then backfilled carefully and tamped with an air tamper. Four inches of loose soil was then placed over the gage and compacted very carefully. Figure 2.11 shows an earth pressure gage being placed in the removable form and Fig. 2.12 is a view of a block of soil containing the gage after it has been removed from the form.

Air pressure gages were used to measure the pressures inside the structures and at the earth surface. One gage was placed in each of the structures to determine if the pressure increased an appreciable amount due to leakage through the access shafts. An air pressure gage was mounted in a small block of concrete near the entrance to Structures 3.8b and 3.8c to measure the air pressure 6 in. above the earth surface. Two additional air pressure gages in flush type mounts located at either end of the structures were provided by Stanford Research Institute for Shot 10 only. The location of these gages is shown in Fig. 2.10.

2.4.3 Strain Measurements

Electric *resistance* strain gages of the SR-4 type were used to measure the transient strains in the flanges of the test beams at the center of the span and the reactions transmitted to the supporting structure. Seventeen transient strain measurements were made in each structure. Gages were located to measure the strain on the inside of each of the flanges of both I-beams for the M and P test beams and on only one of the I-beams of the E test beam. The strain in each flange was measured by mounting one gage perpendicular to and one gage parallel to the span on both sides of the web. These four gages were wired to form a resistance bridge, the output of which should be proportional to the longitudinal strain in the flange. Eight gages were mounted in a similar manner on each support of each test beam. On each support four of the gages were mounted on each side and all eight gages were wired into a resistance bridge in such a way that the output of the bridge would be a measure of the axial load on the support. Four additional gages were mounted *on* the expansion end support of the intermediate beam and wired into a similar bridge so that there would be two independent measurements of the load transmitted to this support. This extra measurement was made because of the importance of obtaining this record, and for a check on the results.

Mechanical strain gages were used to measure permanent strains on all the beam strips. At the mid-point of all 30 of the beam strips four pairs of gage points 2 in. apart were located in general as follows: 1 pair on the bottom of each I-beam bottom flange along the center line, and 1 pair on the outside edge of the bottom face of each I-beam top flange. When this was not possible on the bottom flange of an I-beam owing to the weld on the plastic beam strips or the installation of some experimental gages, two pairs of gage points were located symmetrically about the web near the edges of the flange. On all of the intermediate and plastic test beam strips the gage points on the

bottom flange were placed in continuous lines to the quarter points of the span. Readings were taken on each pair of gage points with a 2 in. Whittemore gage and a 2 in. direct reading gage which had a much larger range. Both gages were used since the strains in some of the beams could be so large near the center of the span that they would be beyond the range of the Whittemore gage.

2.4.4 Deflection Measurements

The transient deflection of the center diaphragm of each test beam was measured with respect to the concrete supporting structures. Four gages *were* used in each structure. One gage was mounted *on* the concrete pedestal under the elastic test beam to measure the deflection of the center of this beam, and one gage was mounted on the floor of the structure under the plastic test beam to measure the deflection of its center. Two gages were mounted on the central concrete diaphragm under the intermediate test beam to measure deflection. These two gages were set to measure two different ranges of deflection of the intermediate beams since the deflection of this test beam was the most unpredictable. The gage used to measure the deflection of the elastic beam and one of the gages used to measure the deflection of the intermediate beam were of the linear differential transformer type. The other gages were a potentiometer type gage which had been developed by the Ballistic Research Laboratories. The potentiometer was rotated by a length of piano wire connected to the bottom of the test beam and maintained under a load of 60 lb by a heavy spring in the gage.

To provide information on the overall deflection of the structures with respect to the undisturbed soil, and on the permanent deflections of the beam strips with respect to the concrete supporting structures, a comprehensive set of level readings was taken with a surveyor's precise level. Bench marks were located at various depths in the undisturbed soil as shown in Fig. 2.10, and at the bottom of the two access shafts. These were used to determine the movement of the structures with respect to various bench marks in the soil. Eight additional bench marks located in the side walls of each structure were referenced to the bench mark at the bottom of the access shaft. Readings taken on these benchmarks gave a picture of the overall vertical motion of the concrete supporting structures. In addition, level readings were taken at three points on each lower flange of each of the beam strips. *One* point was located as near to the end of the span as the side wall would permit and the other point was located at the center of the span. These readings permitted the determination of the permanent deflection of the center of each beam strip with respect to its ends. Where it was impossible to locate points at the center, because of obstructions such as the safety beam under the plastic beam strips, two points as near as possible to the center of the span on each flange were used.

TABLE 2.1 - Dimensions and Properties of Beam Strips

Quantity	Beam Strip Type		
	P	M	E
Rolled Sections Used, each side	two 7C9.8	8I23	15I50
Width of 1/2 in. Plate, in.	21.25	20.25	23.25
Total Width Supported, in.	22	21	24
Total Moment of Inertia, in.^{4}	162.0	232.8	1462
Distance to Neutral Axis, in.			
top flange	2.19	2.67	5.79
bottom flange	5.31	5.83	9.71
Max. Stress, 100 psi Load, ksi**	83.1*	60.6*	18.4
Max. Defl., 100 psi Load, in.			
neglecting shear	0.501	0.333	0.0605
including shear	0.542	0.366	0.0764
Equiv. Dead Load, psi			
1 ft. cover	1.1	1.1	1.3
4 ft. cover	3.4	3.4	3.6
8 ft. cover	6.5	6.5	6.7
Dead Load Stress, ksi**			
1 ft. cover	0.9	0.7	0.23
4 ft. cover	2.8	2.1	0.66
8 ft. cover	5.4	4.0	1.23
Dead Load Defl., in.			
1 ft. cover	0.0058	0.0041	0. 0010
4 ft. cover	0.0184	0.0125	0.0027
8 ft. cover	0.0352	0.0239	0.0051
Fundamental Period T, millisec.			
steel section only	11	11	5
1 ft. cover	21	18	9
4 ft. cover	38	32	15
8 ft. cover	53	44	20

* Assuming linear elastic action

** The abbreviation ksi is the standard notation for kips (kilopounds) per sq in., or 1000 lb per sq in.

2.4.5 Acceleration Measurements

Four accelerometers to measure vertical acceleration components only were used in each of the structures, two of them being mounted on each of the side walls near the central concrete diaphragm. One of the gages on each of the walls was an electronic type, the output of which was recorded by the equipment in the instrument shelter. The two accelerometers, whose output was recorded in the instrument shelter, had widely different ranges. Two ranges were used because of the large uncertainty in the expected accelerations. The other gage on each wall was the self recording ERA type of accelerometer which was used only as back-up instrumentation.

TABLE 2.2 - Field Density Tests of Backfill Material Taken During Backfill Operation

Structure	Depth, ft	Water Content, (%)	Dry Density, lb per cu ft	Wet Density, lb per cu ft
3.8a	0.5	21.3	87.9	107.0
	1.8	20.6	98.0	118.1
	3.0	21.1	102.0	124.0
	4.8	21.8	102.0	124.2
	5.5	24.7	102.0	126.2
	5.8	17.7	90.0	102.0
3.8b	0.0	20.4	97.0	117.0
	0.75	22.5	99.2	122.0
	1.5	20.5	85.6	103.0
	4.0	25.2	96.6	121.0
	9.2	23.5	94.6	117.0
3.8c	0.0	17.5	93.4	109.9
	0.0	19.1	90.9	108.4
	0.0	19.3	99.2	113.0
	0.0	19.8	99.3	119.0
	0.0	20.3	95.3	114.7
	1.5	20.2	89.5	108.0
	2.75	23.5	95.8	119.0
	2.8	22.5	98.6	120.2
	3.75	21.0	89.8	108.2
	4.4	25.6	94.5	119.5
	5.75	18.6	92.9	110.0
	5.75	23.7	92.0	114.0
	9.7	22.8	94.0	116.0
	12.25	24.8	90.1	113.0
	14.5	21.2	98.2	119.0
Ave.		21.5	94.9	115.1

TABLE 2.3 - Strength of Compacted Fill Immediately Before Shot 9

Boring	Depth, ft	Unconfined Compr. Strength, tons per sq ft	Water Content, (%)
B	2	10.2	16.9
	5	5.9	19.4
	8	7.85	19.2
C	2	8.15	17.3
	5	8.0 (est.)	19.2
	8	9.5	18.3
Ave.		8.3	18.4

TABLE 2.4 - Dimensions of Web of Beam Supports

Beam Strip	End	Web Dimensions		
		Width, in.	Thickness, in.	Area, sq in.
E	Fixed	16.00	0.77	12.3
	Exp	16.00	0.65	10.4
M	Fixed	12.75	0.50	6.38
	Exp	14.00	0.50	7.00
P	Fixed	13.25	0.50	6.63
	Exp	14.50	0.50	7.25

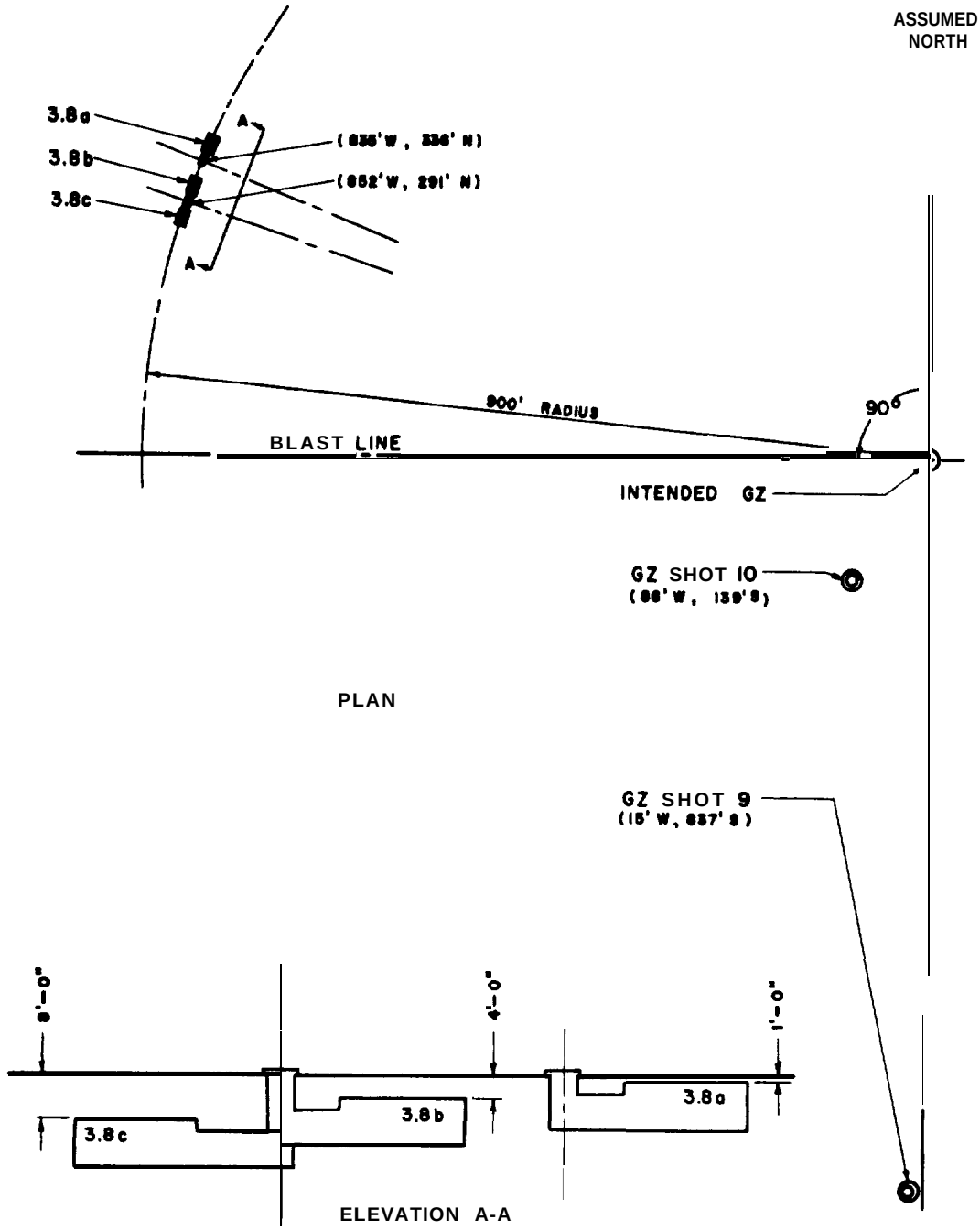

Fig. 2.1 Location of Structures

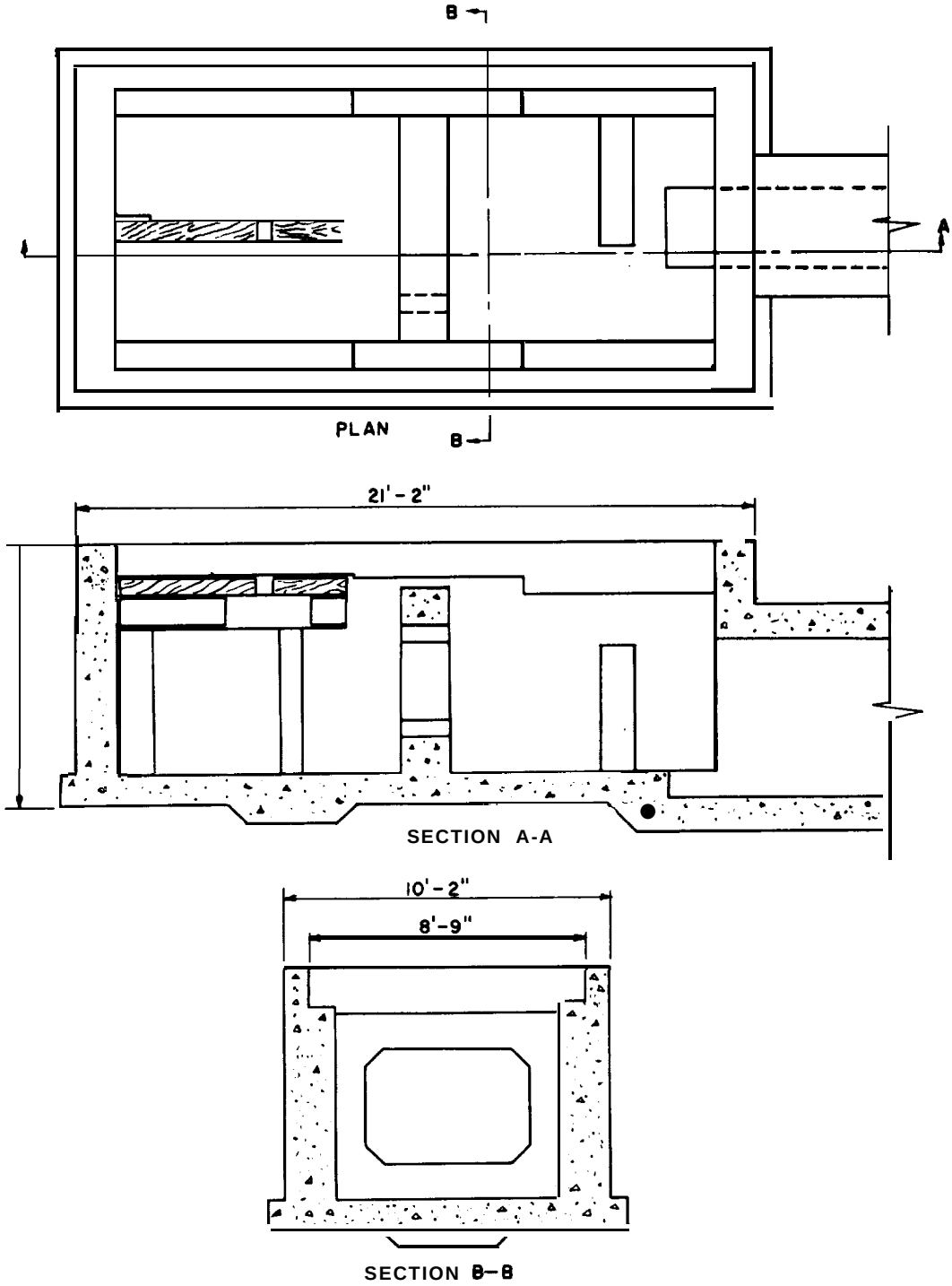

Fig. 2.2 Concrete Test Chambers

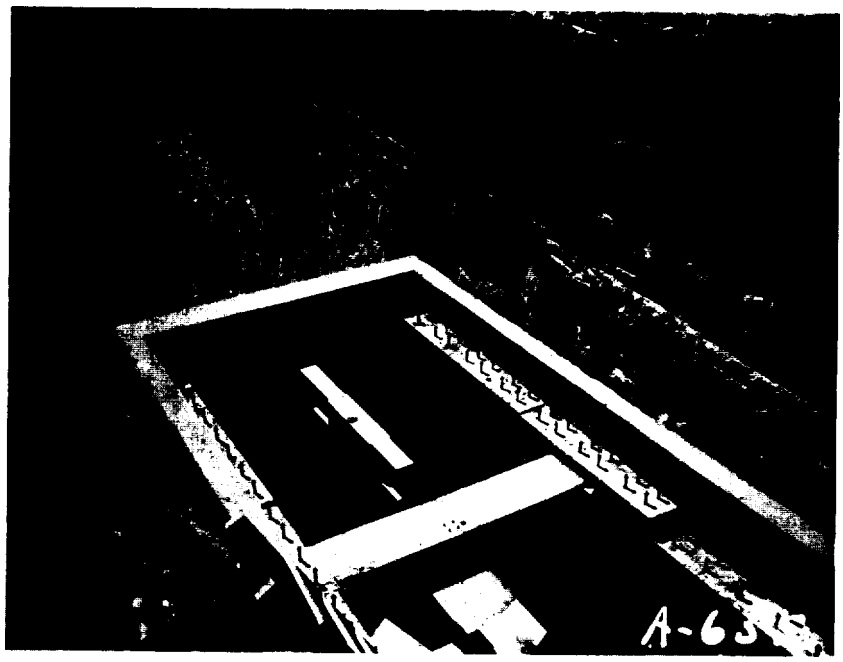

Fig.2.3 Structure 3.8c During Construction

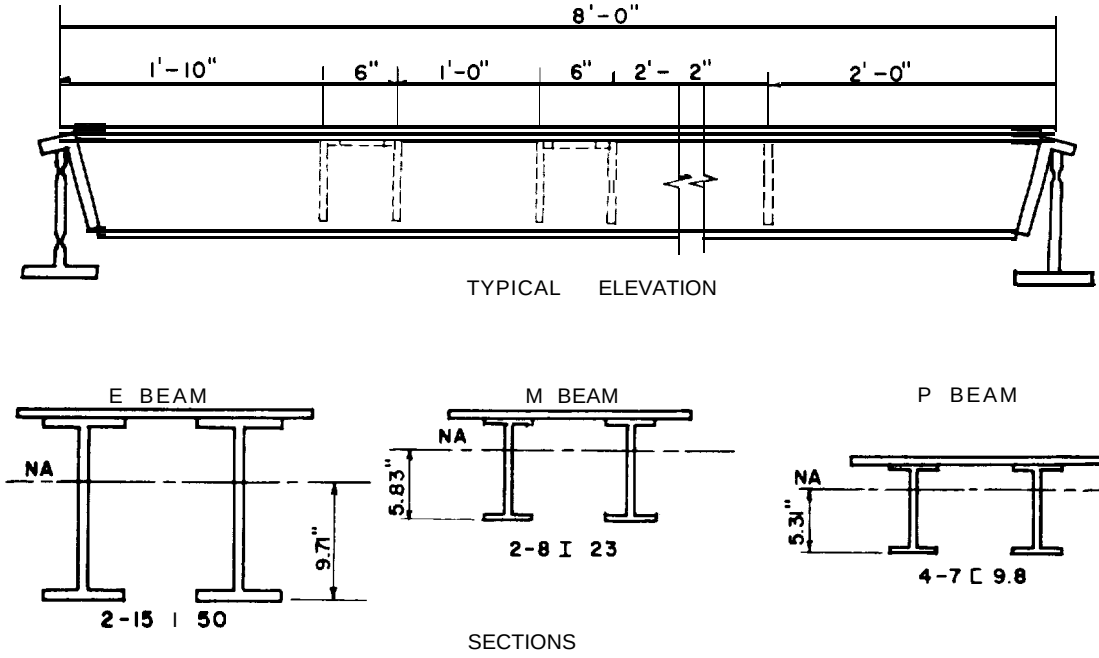

Fig. 2.4 Elevation and Sections of Beam Strips

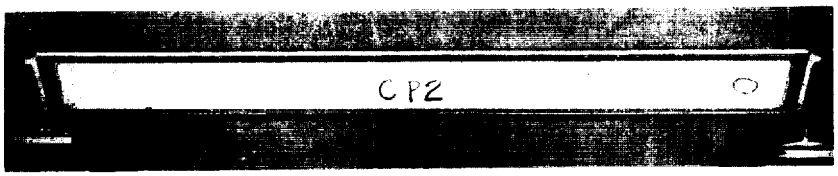

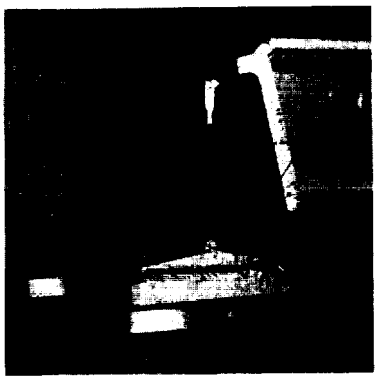

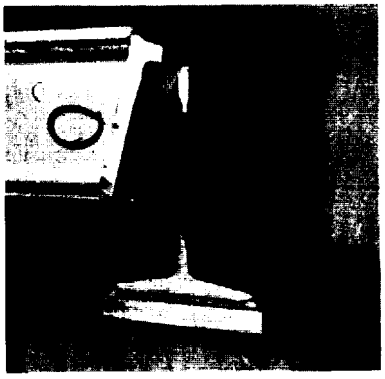

Fixed Shoe

Expansion Shoe

Fig. 2.5 Beam Strip CP2 and Supporting Shoes

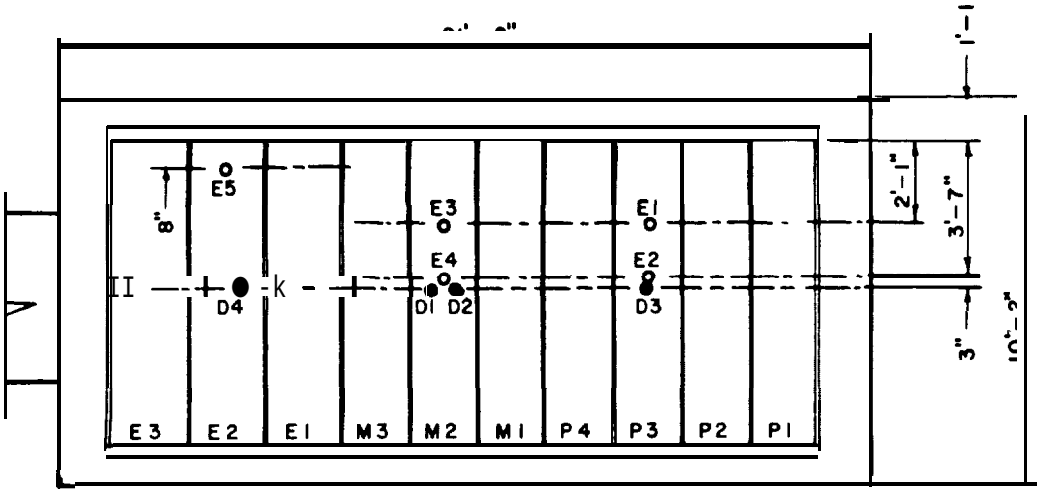

o EARTH PRESSURE GAGES

● DEFLECTION GAGES

Fig.2.6 Arrangement of Beam Strips in Roof and Location of Gages

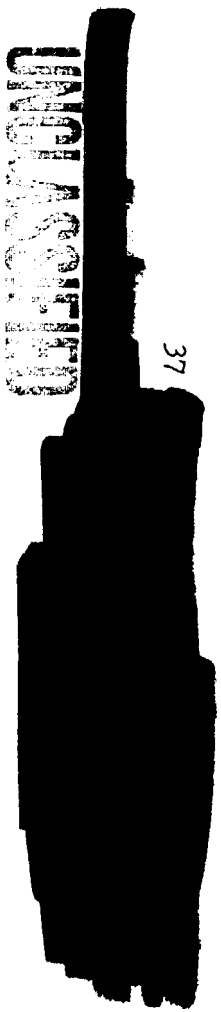

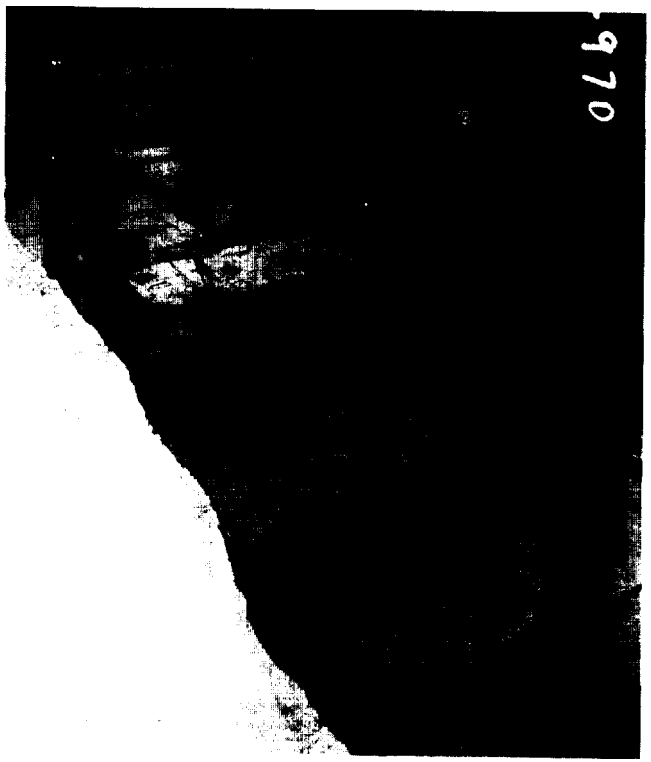

Fig. 2.7 Placing of Beam Strips in Roof on Structure 3.8c

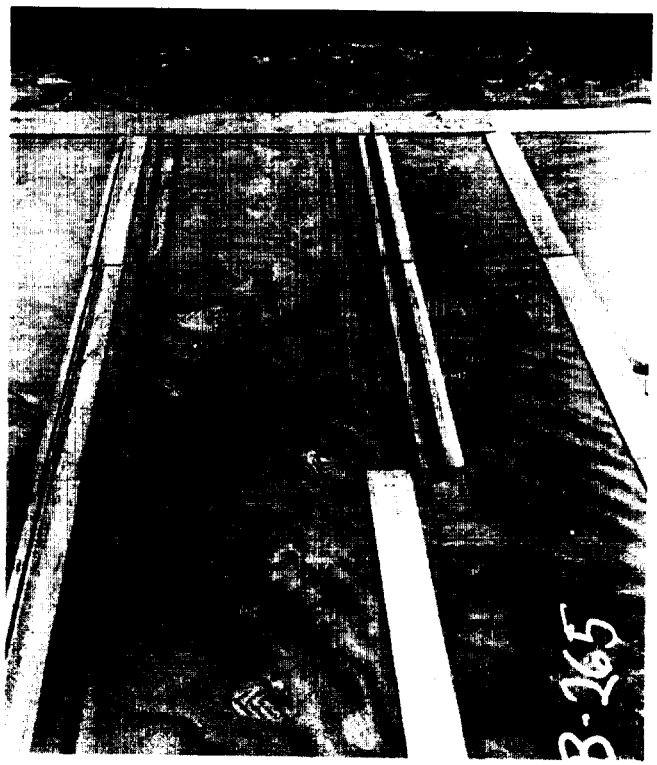

Fig. 2.8 Canvas Cover over Strips

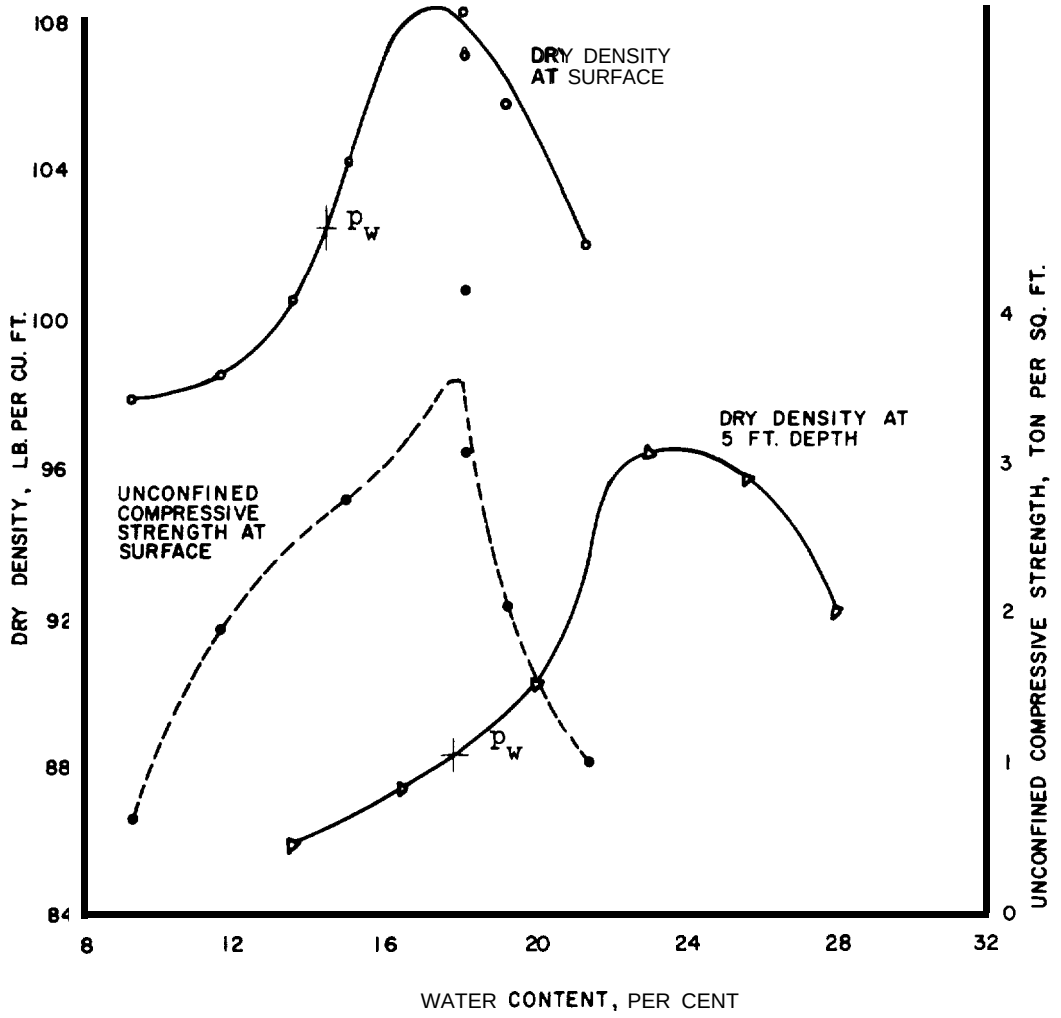

Fig. 2.9 Soil Properties at Location of 3.8 Structures

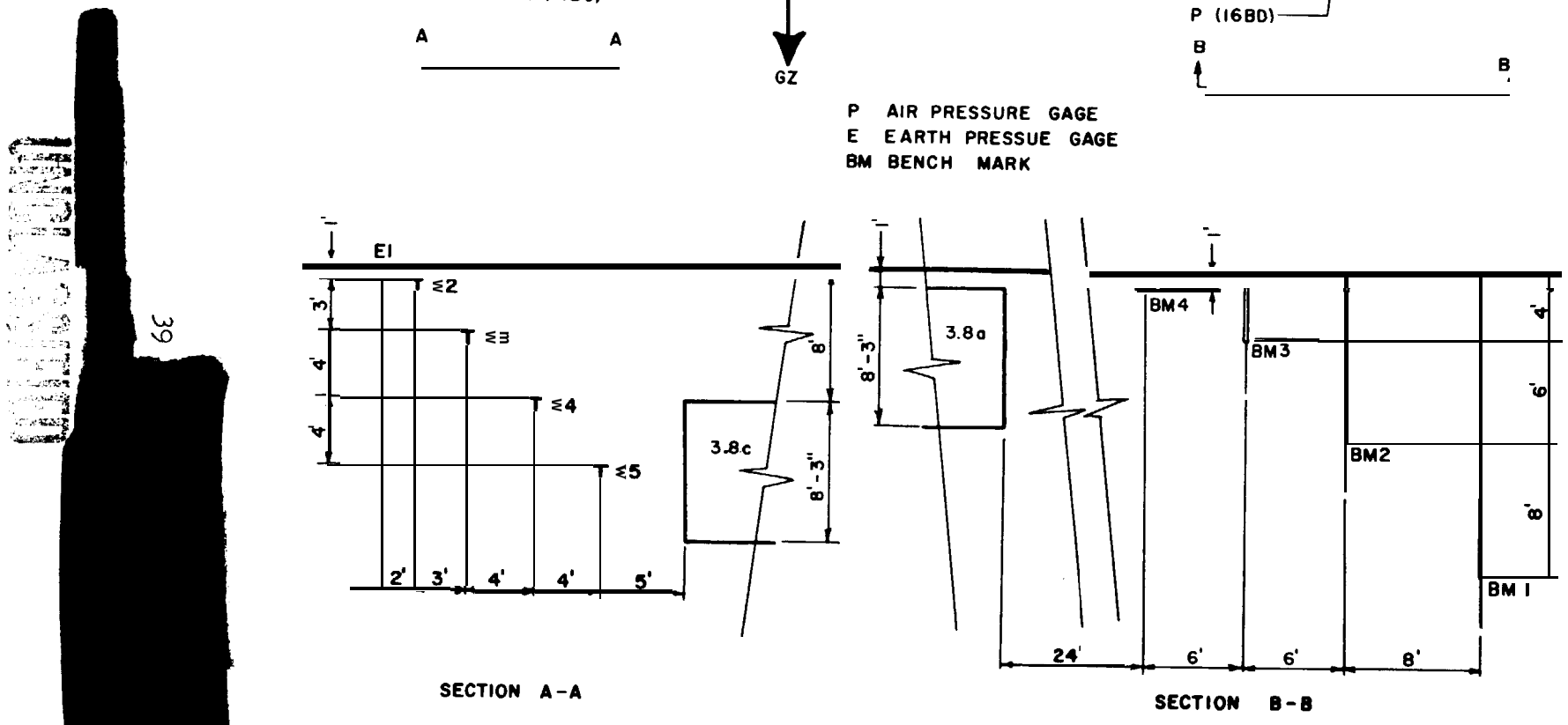

Fig. 2.10 Location of Earth Pressure Gages and Bench Marks

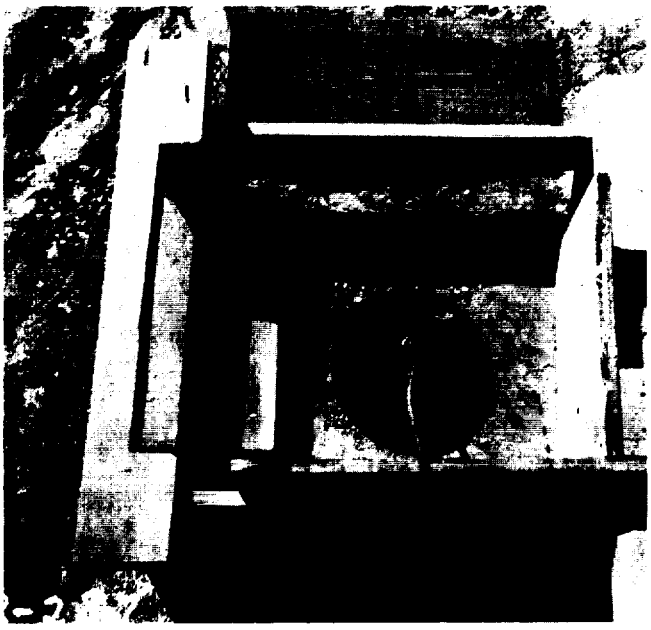

Fig. 2.11 Placement of Earth Pressure Gage in Form

Fig. 2.12 Earth Pressure Gage in Cube of Soil

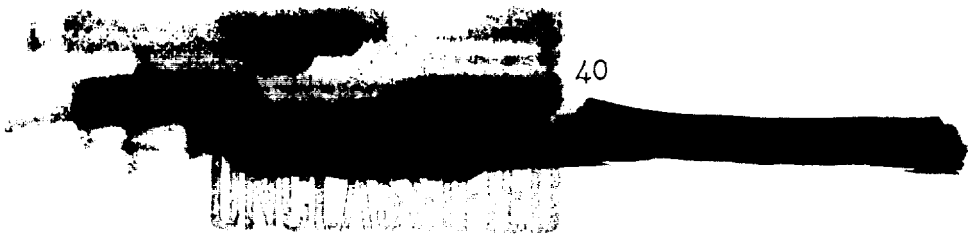

CHAPTER 3

GENERAL DESCRIPTION OF STRUCTURAL BEHAVIOR DURING TESTS

3.1 PRESSURES AT GROUND SURFACE

Because of the plan of the test program, the structures in Project 3.8 were subjected to two shots, Shot 9 and Shot 10. For the first of these it was not expected that any damage would occur, or that even plastic behavior would be initiated in any part of the structures. However plans were made to take readings on this shot primarily to obtain information as to the behavior of the structure in the elastic range and to check out the general program of instrumentation and observations. The primary test of the structure was intended to be made with Shot 10.

The air pressures on the ground surface for these two shots are shown in Figs.3.1 and 3.2. Because of a failure in the recording equipment, the surface pressure measurement near the 3.8 structures was not obtained for Shot 9. However, the curve shown in Fig.3.1 was reconstructed from other data at approximately the same range from the ground zero of the shot. The air pressure pulse on this shot was conventional, with a fast rise to a peak of about 15 psi, and a positive phase duration of about 700 millisec., with an initial rate of decay after the peak corresponding to an effective triangular pulse of a duration of about 400 millisec. The low peak pressure, only about two-thirds of the predicted value, arose from the fact that there was a large bombing error which changed the ground range from the planned value of about 900 ft to approximately 1400 ft.

In Shot 10, the pressures were very nearly of the same maximum value as those which had been expected, and the pressure time relation was very irregular, having the initial plateau characteristic of the precursor region. The initial plateau was of the order of 50 to 60 millisec. in length, with a peak pressure, nearly constant over this time of about 16 psi. Just before the main pulse, there was a drop off in pressure nearly to a zero value. This was followed by a slow rise, 15 to 20 millisec. in length, to a peak value of about 63 psi. The duration of the main pulse was about 150 millisec. in length, corresponding to a decay rate consistent with an equivalent triangular pulse of about 100 millisec. duration. This was considerably shorter than

the design value.

All of the departures in the shape of the pressure curve from a conventional curve were of such a nature as to produce in general a smaller effect on the structure than would be produced by the conventional blast curve. The length of the precursor shock, the slow rise following the precursor, and the effective duration of the positive phase of the main pulse, are factors which must be taken into account in considering the measured response of the structures.

3.2 VISIBLE RESULTS

Qualitative results of the blasts were observed as soon as the area could be entered. There was little evidence of any effect whatsoever from Shot 9 except for some small amount of cracking of the surface of the fill over the structures and other similar surface disturbances in the soil. A photograph of the soil surface over Structure 3.8c is shown in Fig. 3.3. The cracks in the fill are plainly evident. After Shot 10 there was additional evidence of settling of the surface, slight void spaces around the entranceways, and some evidence of a rise in the surface over Structure 3.8a.

After Shot 10 it was almost immediately evident that Structure 3.8a had been subjected to considerable motion within the soil. The roof covering had apparently raised several inches and fallen back into place. Some of the tee-fillers were no longer entirely within the slots between the beams, and in several areas the canvas loops were pulled out from between the beams and stretched taut. However, in spite of this evidence of general motion, there was no visible effect on the structure and no visual evidence of any appreciable permanent deflection or permanent strain in the beam strips, even in Structure 3.8a. The deeper structures showed no evidence even of relative motion and no indication of any serious overstress.

3.3 RECORDS OF TRANSIENT EFFECTS

Because of a failure of part of the recording equipment in Shot 9, only a part of the instrumented channels produced records. However even these records are not very useful because of the fact that the gage settings had to be planned for a higher pressure than that which was actually reached in Shot 9.

In Shot 10, excellent dynamic records were obtained on a majority of the instrument channels. Some minor difficulties were experienced, and some of the records do not seem to be completely reliable, but on the whole, the results obtained appear about as good as can be expected for dynamic measurements under field conditions.

3.4 SURVEY MEASUREMENTS

The survey measurements made of these structures were intended to show quickly the general nature of the response in terms of permanent effects, and to permit a check on the dynamic measurements of transient

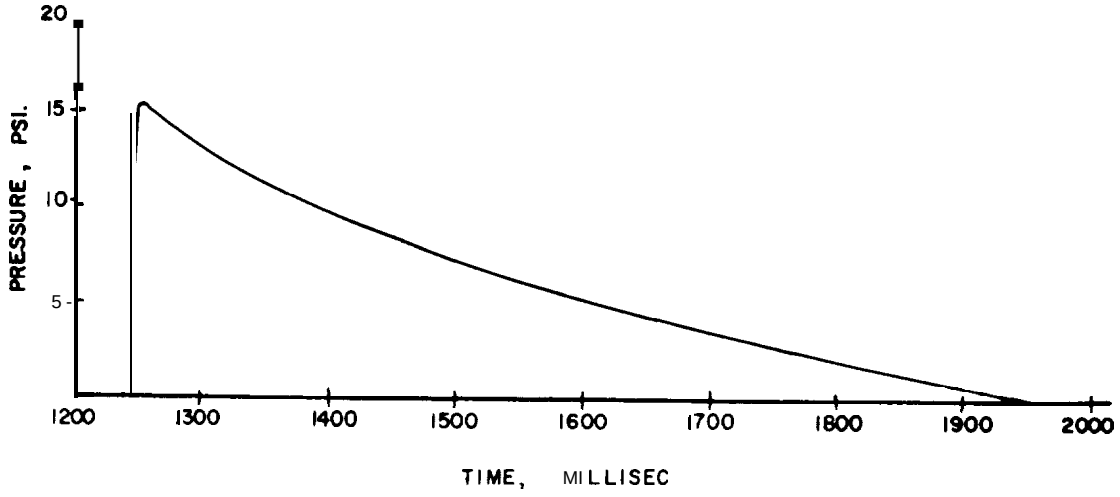

Fig.3.1 Pressure on Ground Surface - Shot 9

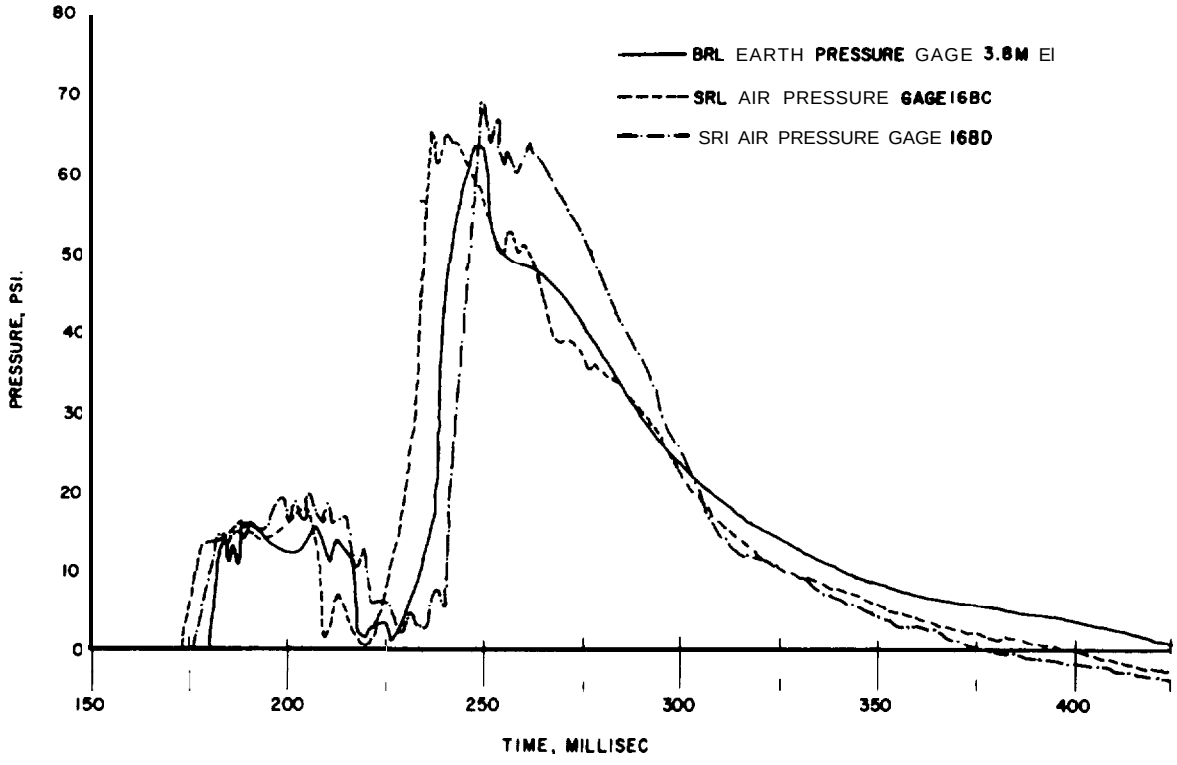

Fig. 3.2 Pressure on Ground Surface - Shot 10

quantities since the final values recorded should agree with those indicated by the survey. However, the survey measurements could not be made with the precision that was possible for the dynamic measurements, and consequently where the permanent deflections and strains are not relatively large, the quantities measured in the survey are not dependable. In spite of the limitations of the survey, it was quickly established by the survey measurements that there were no permanent deformations in Shot 9 and little permanent displacement or strain in the structures after Shot 10. The elastic beam strips showed no permanent deformations, and the plastic and intermediate beam strips only *very* slight permanent strains and almost negligible permanent deflections.

The survey measurements of relative displacement of the structures and of various levels in the free earth indicated that there was practically no relative settlement of the deeper structures, and some slight residual upward motion in the shallowest structure.

Fig.3.3 Surface Cracks in Soil after Shot 9

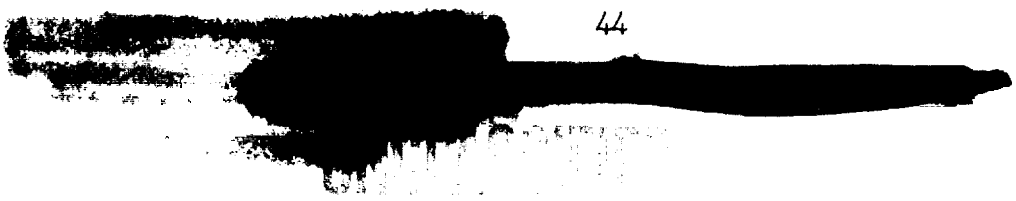

CHAPTER 4

ANALYSIS OF TRANSIENT MOTION OF SIMPLE BEAMS

4.1 BASIC CONCEPTS

4.1.1 Fundamental Relations

The general analysis of the transient motions of a beam subjected to dynamic loads is a complicated problem. However, the structures with which this program is concerned are all simply supported beams carrying essentially a uniform load varying only with time, and the beams are of constant cross section. These conditions permit a number of simplifying approximations to be made.

Where a beam remains elastic in its response to a dynamic load, the problem resolves itself into an evaluation of the motions of the beam in its various "modes" of vibration. Each mode is excited to a different degree, in general, by the component of the loading in that mode and by the variation of the intensity of loading with respect to time. The complete response of the beam is the sum of the responses in all of its modes.

The mode shapes for a uniform hinged-end beam are sine curves of varying integral numbers of waves in the span length. The periods of the various modes vary inversely as the square of the number of waves. Since it is possible to define any loading as a trigonometric series and particularly as a series of sines only, the loading over the span length can easily be divided into the modal loadings. For uniform loading this partition of the loading into the modal shapes is merely the expression of a uniform quantity into a series of sines, and the series contains terms only for odd integral values of the modes with the coefficients varying inversely as the modal number.

If we designate the number of the mode by the symbol i, the intensity of loading in the various modes varies as $1/i$, the moments as $1/i^3$ and the deflections as $1/i^5$, for static loadings. For a load which is suddenly applied and which remains constant, the maximum effects on the beam are essentially the same as twice the static effects for each mode separately, but the absolute maximum values which are combinations of the modal values may be reached in different ways. It can be proved that under these conditions neglecting all but the

first mode of the deflection shape cannot possibly produce an error of more than 0.45 per cent and the probable error is much less than this. The corresponding figure for the error in the bending moment or in the stress is 5.18 per cent for the extreme maximum error and the probable value is less than this.

However, if the loading is applied instantaneously as a pure impulse, lasting an infinitesimal time, then the responses are somewhat different in character, the modal deflections being excited in a proportion varying inversely as the third power of the mode number, and the moments inversely as the first power of the mode number. Under these circumstances, the error in the deflection produced by neglecting all but the first mode may reach 5.2 per cent, whereas the error in the bending moment may be infinitely large. However, if one takes any finite duration of loading, or if one considers the effect of damping, the errors approach those for a constant load suddenly applied; and *in any* case, if the loading lasts for a time comparable to the period of the fundamental mode, then for all practical purposes, it acts as if it lasts indefinitely long. Since most of the cases with which this program is concerned refer to loads lasting somewhat longer than the period of the fundamental mode, it can be seen that the neglect of all but the first mode in the deflection shape is a reasonable assumption. Other types of approximation of the shape of the deflection tune in a single mode are possible. However, other approximations lead to results which cannot be easily studied in terms of the error produced by the approximation.

The methods of analysis for simple one-degree-of-freedom structures are much simpler, for determining dynamic response, than the corresponding methods for systems with multi-degrees-of-freedom. Consequently, one of the procedures for making a rapid approximate analysis is to develop an equivalent single-degree-of-freedom system for the more complicated structure. Methods of doing this are available by use of energy concepts. However, it must be remembered that the equivalent system determined in such a fashion is only an approximation and does not necessarily represent the structure in the best manner. Moreover, although a reasonably accurate representation can be made for purely elastic, and in some cases for purely plastic behavior of the structure, in the intermediate range it is not usually convenient to develop a simple replacement structure which represents the actual structure faithfully. The degree of departure, however, in the case of the simply supported beam subjected to a uniform transient load, is not serious .

4.1.2 Notation

The following notation is used in general throughout this report:

a = acceleration

E = modulus of elasticity

i = number designating order of mode considered or subscript applying to i th mode

I = moment of inertia of beam per unit of width of cross-section, in units of length cubed

k = effective spring constant of beam, per unit of plan area

kips = kilopounds, used to designate a unit of 1000 lb

ksi = kips per square inch

L = span length of beam between simple supports

m = mass per unit of plan area of beam

$\bar{m}$ = equivalent mass of replacement system

n = subscript designating end of n th time interval

p = pressure applied to ground surface or to beam, also pressure at center of beam

$\bar{p}_i$ = pressure for i th mode of vibration

p_o = maximum pressure in precursor pressure pulse

Pm = maximum pressure

q = resistance of beam, measured *in same* units as pressure

q_e = yield value of q

s = static deflection for load p, $s = p/k$

t = time

t_o = effective length of precursor pressure pulse

t_1 = effective duration of equivalent triangular pressure pulse

t_m = time to reach maximum deflection

t_r = effective rise time of pressure pulse, from zero to maximum, considered as an equivalent linear rise

T = period of vibration of a simple system

T_1 = fundamental period of vibration, or first mode period

T_i = natural period of vibration of beam, in i th mode

v = velocity

x = coordinate of length along beam axis

Y = deflection at any point of beam

y = deflection of center of beam

y_e = yield deflection

y_m = maximum deflection

α = parameter relating variables in numerical integration procedure = $\frac{4\pi^2\gamma^2}{T^2}$

β = parameter in numerical integration routine, generally taken as zero or as 1/6

γ = time interval

4.1.3 Equivalent Single-Degree-of-Freedom Systems

The differential equation which governs the transient motion or the static deflection of a beam, neglecting the influence of damping, is the following:

$$EI \frac{\partial^4 Y}{\partial x^4} + m \frac{\partial^2 Y}{\partial t^2} = p(x,t) \qquad (4.1)$$

When the loading is uniform along the length of the beam the quantity on the right-hand side of the equation is a function only of t and does not depend on x. When the beam deflects in one of its mode shapes, namely

$$Y_i = y_i(t) \sin \frac{i\pi x}{L}, \qquad (4.2)$$

then when equation 4.2 is substituted into equation 4.1 an ordinary differential equation results which governs the deflection of the center of the beam in terms of the component of loading in the i th mode. The latter is given by the relation

$$\bar{p}_i = p_i(t)\sin\frac{i\pi x}{L} \tag{4.3}$$

where

$$\sum_{i} \bar{p}_i = p(x,t)$$

Under these circumstances the ordinary differential equation takes the following form:

$$m\frac{d^2y_i}{dt^2} + \frac{i^4\pi^4 EI}{L^4}y_i = p_i(t) \tag{4.4}$$

However, it can be readily seen that equation 4.4 is the same as the equation for the motion of a single-degree-of-freedom system having a mass m, an applied force p_i, and a spring constant which is the coefficient of y_i In the second term of the equation. The natural period of vibration, therefore, corresponds to the following formula:

$$T_i = \frac{2L^2}{i^2\pi}\sqrt{\frac{m}{EI}} \tag{4.5}$$

The motion of the beam in its fundamental mode is given by the solution of equation 4.4 when i has the value 1. For a uniform load applied to the beam the coefficients in equation 4.3 for the loading pi have the following form:

$$p_i = \frac{4p}{i\pi}\sin\frac{i\pi}{2} \tag{4.6}$$

It follows therefore that for the first mode the maximum intensity of loading is $4/\pi$ times the uniform intensity of loading on the beam.

A relation between the deflection y and a uniformly distributed resistance q can be written by taking p = q, letting y_i be a constant in equation 4.4, and substituting $p_1 = q_1 = 4q/\pi$, from equation 4.6. One derives the result:

$$q = ky = \frac{\pi^5 EI}{4L^4}y \tag{4.7}$$

However, the value of spring constant defined by this equation differs by only 0.39 per cent from the value obtained directly for a uniformly loaded beam,

$$q = \frac{384\ EI}{5L^4}\ y\ , \tag{4.8}$$

and therefore the latter value is used in the calculations for this report.

With the value of q defined by equation 4.7, that of p defined by equation 4.6, with i = 1, and if equation 4.4 is multiplied through by the factor $\pi/4$, it can be rewritten as follows, dropping the subscript i = 1:

$$\frac{\pi}{4}\ m\ \frac{d^2y}{dt^2} + ky = p \tag{4.9}$$

This equation can be interpreted as defining a single-degree-of-freedom equivalent system to the beam, in which the deflection of the equivalent system is the same as that of the center of the beam, the mass of the equivalent system is equal to $\pi/4$ times the mass per unit of length of the beam, and the loads and resistances of the equivalent system are equal to the uniformly distributed pressures or resistance considered to be acting on the beam. The period of vibration of the equivalent system and of the fundamental mode of the beam are identical. In other words, the equivalent mass $\bar{m}$ is related to m by the equation

$$iii = \pi m/4 \tag{4.10}$$

when the deflection has the shape of a sine curve, and all other quantities are the same for the two systems. Alternatively, one can keep the masses the same and increase the loads and resistances by the factor $4/\pi$.

A sketch of the actual beam and of its replacement system is shown in Fig. 4.1a, and b respectively. In Fig. 4.1c the equivalent mass is considered as a free body with the force p and the resistance q acting on it. The upward resistance q is measured in the same terms as the downward loading and is accordingly the uniform force which is required to produce the given displacement under static conditions. The sine curve of deflection is shown in Fig. 4.1d.

4.1.4 Yielding and Resistance of Beams

As the beam yields, the shape of its deflection curve

approaches a triangle rather than a sine curve, and there is a more or less abrupt break in the slope of the deflection curve at the point where the plastic hinge occurs at the middle of the beam. If the beam does actually deflect as a triangle, as in Fig. 4.1e, with the two sides of the triangle remaining undeformed, the corresponding equation of motion for the beam can be written in the form:

$$\frac{2}{3} m \frac{d^2y}{dt^2} + q_e = p \qquad (4.11)$$

In this equation the quantity q_e is the yield value of the resistance, or it is that uniform load which applied to the beam would produce the yield point deflection of the middle.

From a comparison of equations 4.11 and 4.9 it can be seen that the effective mass of the beam is reduced after yielding, from $\pi m/4$ to $2m/3$ or alternatively the loads and resistances are increased, relatively from $4/\pi$ to $3/2$. The relative increase in acceleration, for other conditions the same, after yielding compared with before yielding, is therefore:

$$\frac{3/2}{4/\pi} = 1.178 \qquad (4.12)$$

This increase in acceleration is required in order to preserve the nature of the replacement structure at the limiting condition for plastic behavior in the beam, when the deflection curve is actually triangular in shape.

Observations of the deflection of actual beams loaded beyond initial yielding, as well as analyses of beams on the basis of an idealized elasto-plastic relation between moment and curvature, indicate that the actual deflection curve beyond yielding is a combination of curves similar to those in Fig. 4.1d and e. If the elastic part of the distortion remains unchanged as plastic action increases the total distortion, the effective increase in acceleration as a function of deflection shows a gradual rather than a sudden increase. For example, in Fig. 4.2, the accelerations arising only from the resistance q are plotted as a function of deflection y. The lower horizontal line indicates the value at which yielding begins. The upper horizontal line indicates the resistance acceleration increased by the factor of 17.8 per cent corresponding to equation 4.12. The curved transition was computed by means of an accurate relationship derived from the principle of conservation of energy, for a deflection curve for the beam consisting of two parts: (1) a sine curve of magnitude corresponding to the beginning of yielding; (2) a triangle for all additional deflection. However, the accurate relation can be approximated very closely by the relation:

$$\frac{\text{modified acceleration after yielding}}{\text{acceleration at beginning of yielding}} = 1.18 - 0.18y_e/y \quad (4.13)$$

Both the resistance and the loading accelerations, after yielding, are to be increased by exactly the same factor. However, it can be shown that neglecting the increase entirely changes the maximum deflection by at most 18 per cent, and probably by much less for practical conditions.

The limits on the maximum deflection can be obtained by considering two extreme cases. The first case is that where yielding occurs immediately as a rigid-plastic system. Then it is readily seen that all of the accelerations, both from the loading and from the resistance, are increased in exactly the same proportion. Under these conditions, the maximum deflection of the system is increased also by the same proportion, namely 18 per cent, and the time to reach maximum deflection is unchanged. The increase in maximum deflection is less than 18 per cent if the beginning of yielding is delayed, but it occurs still in the range where the accelerations from the resistance forces are less than those from the external loading.

The other extreme is obtained if all of the loading on the system is applied before yielding begins, or if the loading is essentially an impulsive loading. Under these circumstances the response is decreased because only the resistance is acting during the yield phase of the structure's response. The decrease in response is readily determinable from a consideration of energy concepts. The energy input into the structure is determined by the loading pulse, which is not modified. The energy absorbed by the structure is the area under the resistance-deflection curve, which can be considered to be modified by a direct increase in the vertical scale of resistance, by 18 per cent, since the mass must be held constant to avoid changing the kinetic energy of motion. Then it follows that to keep the energy absorption constant requires a reduction of slightly less than 18 per cent in maximum deflection if the resistance is increased by 18 per cent over the entire yield range.

These changes in maximum deflection are extreme limits. They are applicable only under the conditions where the maximum possible change in acceleration occurs, and where other rare and unusual circumstances govern. In general, the differences in maximum deflection produced by the change in effective mass (or load or acceleration) at yielding is less than 18 per cent, because of the phenomenon described in Fig. 4.2 where it is shown that the change in the effective value of acceleration does not occur abruptly at yielding but rather gradually, as the deflection increases. For these reasons, it does not appear to be desirable or necessary to make any allowance for the change in the effective accelerations accompanying yielding of the beam.

4.1.5 Deformations Due to Shear

The ordinary theory of flexure of beams does not take into account the influence of the shearing stress on the deflection nor on the distribution of stress on the cross section of the beams. However, the influence on deflection is not entirely negligible for beams with thin webs. The influence of shear on the deflection of the beam strips in the roof of the test structures can be determined quite readily.

The influence of the flexural stresses on the deflection of the beam strips is indicated by the coefficients shown in Table 2.1. The deflection coefficients shown in this table give the change in the deflection at the center of the beam for a change in loading applied over the entire surface of the beam strip, and are given in such a way that the deflection is determinable in inches from the loading in psi. These coefficients are obtained from the usual relationships for simply supported beams by the formula shown in equation 4.8.

The effect of the shear in the web on the deflection is to increase the deflection by an amount proportional to the ordinates of the moment diagram of the beam. The shearing deflection at the middle of the span is equal approximately to the moment at the middle divided by the area of the webs of the beams and by the shearing modulus of elasticity. The web areas used in the calculation should be the net areas of the webs between the flanges, and are computed by taking the thickness of the webs multiplied by the total depth of the rolled sections less the average thicknesses of both flanges. With this method of calculation, the effect of shear is to increase the deflections for the various beams by the following percentages:

For the P beams, 8.4 per cent
For the M beams, 10.0 per cent
For the E beams, 26.2 per cent.

These increases apply in the elastic range. The influence of shear on the deflections in the plastic range is smaller, because the yielding of these beams occurs primarily in the flanges but the webs do not yield in shear extensively. Moreover, the deflections are large enough in the plastic range so that the corrections would be either minor or probably not valid because of lack of certainty as to the effective values of the constants after yielding begins.

The modified values of the coefficients for determining deflections of the beams, taking into account the influence of shear, are also given in Table 2.1. The reason for the correction being so much greater for the elastic beams is because of their much greater depth. The flexural stresses are much smaller and the shearing stresses relatively larger in beams of greater depth.

In the various calculations in this report, the influence of shear is considered in the deflections and in all of the various physical constants determining the behavior of the beams, including the natural periods of vibration of the beams. These influences are

determined approximately by considering that the beams behave as if their total deflection arose from flexure alone. In other words, the spring constants for the beams are used for the total deflection as if this total deflection were the deflection of a simple system in which shearing stresses did not play a part.

4.1.6 Effects of Dead Load

Although the dead load forces on the roof beam strips are small, they are not negligible. The dead load stresses and deflections of the various beam strips are shown in Table 2.1. In general, the stresses are less than 5400 psi and the deflections less than 0.035 in. However, the fact that the beams at the different depths of cover bad different dead load stresses and deflections makes it necessary to consider these differences in the analyses of their behavior. In general this was done by the following procedure:

Where the beams remained elastic, the influence of the applied loading was computed as a change in the stress and deflection conditions in the beam, and the dead load stresses and deflections were added to the dynamic deflections and stresses to give total values. However, these totals are not reported because of the fact that only the changes were measurable during the tests. Consequently, for those structures which remained elastic, the tabulated values are for the live load increment only.

However, for those structures which yielded under the dynamic loads, the influence of the dead load was to reduce the effective yield strength. In this regard, the dead load stresses acted as residual stresses *or* as initial stresses. Consequently, the structure was treated as if its yield resistance were decreased by the amount of the dead load effect, the increment in stress or deflection computed, and then the dead load stresses added to the computed transient values. The increment in deflection, however, was generally used in order to compare with the observed values.

4.2 METHODS OF ANALYSIS

4.2.1 Numerical Integration

Methods of analysis for simple one-degree-of-freedom systems as well as for more complicated systems are discussed in detail in a number of papers by N. M. Newmark[1,2,3]. Only a very brief summary of

---

1. Methods of Analysis for Structures Subjected to Dynamic Loading, Report to Physical Vulnerability Division, Directorate of Intelligence, U. S. Air Force, 17 November 1949.
2. Analysis and Design of Structures Subjected to Dynamic Loading, Proceedings of the Conference on Building in the Atomic Age, MIT, June 1952, p34-47.
3. Computation of Dynamic Structural Response in the Range Approaching Failure, Proceedings of the Symposium on Earthquake and Blast Effects on Structures, Earthquake Engineering Research Institute and UCLA, June 1952, p 114-129.

the recommended procedures is given here. With the use of the numerical integration procedures described in Ref 1 and 3 one may take time intervals as long as one-sixth the period of a simple system without introduction of serious errors. The errors decrease rapidly if one takes smaller time intervals. The time intervals can be lengthened materially as the structure gets into the inelastic range.

By application of the technique described in Ref 3 one can derive readily a recurrence formula for the deflections y of an elasto-plastic system in terms of preceding deflections, as a function of an integration parameter β, and the following quantities:

$\alpha = 4\pi^2\gamma^2/T^2$
γ = time interval
s = p/k = "static" deflection for force p

The subscripts n - 1, n, and n + 1 are used to designate successive time intervals.

The general equation for ordinary conditions is:

$$y_{n+1} + \alpha\beta \left\{y_{n+1}, y_e\right\} = 2y_n - \alpha(1 - 2\beta)\, y_n, \left\{y_e\right\} - y_{n-1} - \alpha\beta \left\{y_{n-1}, y_e\right\} + \alpha\beta\, s_{n+1} + \alpha(1 - 2\beta)\, s_{n-1} \qquad (4.14)$$

In this equation the symbol $\left\{y_n, Ye\right\}$ indicates that the smaller of the two quantities in the brackets is to be used; that is, y_n is used when y_n is less than y_e, otherwise ye is used. When p is discontinuous, and therefore s is discontinuous, the values of s_{n+1} and s_{n-1} to be used are those on the side nearest the nth point, and the value of s_n is the average of the two values at the nth point. At the starting point, where n = 0, if the initial velocity and displacement are zero, the relation becomes:

$$y_1 + \alpha\beta \left\{y_1, Ye\right\} = \alpha(1 - 2\beta)\, s_o/2 + \alpha\beta\, s_1 \qquad (4.15)$$

Both equations 4.14 and 4.15 become particularly simple when $\beta = 0$:

$$y_{n+1} = 2y_n - \alpha \left\{y_n, Ye\right\} - y_{n-1} + \alpha\, s_n \qquad (4.16)$$

$$y_1 = \alpha s_o/2 \qquad (4.17)$$

Although somewhat *more* accurate results can be obtained with $\beta = 1/6$, for small time intervals (less than 0.1T) the increase in accuracy is not important and the increased simplicity of equation 4.16 is readily apparent.

Special consideration can be given to a better starting procedure for the calculations, or to the use of $\beta = 0$ for the coefficients of y and $\beta = 1/6$ for the coefficients of s, but the gain in accuracy is trivial. For general use, however, equations 4.14 and 4.16 must be modified to take account of reversals in direction of motion after plastic action occurs, if the true maximum deflection is reached after an intermediate peak value. For such cases, or in general for other special cases, the original relations of Ref 3 should be used.

In the case of motion after a maximum deflection has been reached in the yield region, the recovery is elastic, and equation 4.16 for the special case of $\beta = 0$ can be modified by a change only in the term in brackets. This change replaces y_n in the brackets by the expression:

$$y_n - y_m + ye \qquad (4.18)$$

The smaller of either expression 4.18 or ye is to be used rather than the smaller of the terms y_n or y_e, for motion in the pseudo-elastic region following recovery from a maximum deflection. Since an intermediate maximum may be reached before an absolute maximum, the use of expression 4.18 may be required occasionally, especially with pulses of slow rise time or those having precursor plateaus. It is evident that after a decreasing deflection begins again to increase, plastic action begins again as soon as y_n reaches or exceeds the previous maximum y_m.

4.2.2 Gyrogram for Elastic Range

There are some advantages to be gained in the elastic range by the use of the graphical construction which has been termed the "gyrogram." This is described in Ref 2, and a simple illustration is given here, in Fig. 4.3. For any time interval γ, however long, for which the load p is constant, the motion is described by a rectangular plot of deflection y against the quantity $2\pi v/T$ where v is the velocity. The relations among y, v, and γ are as indicated in the figure. From the initial conditions at point b a circular arc is swung having a center at c, located at a distance s = p/k from the origin. The quantity s is the so-called static deflection for the force p. Then at any time interval γ after the time corresponding to point b, the motion is described by a point such as d on the circle arc bd, with a central angle $2\pi\gamma/T$ in the sense indicated.

For any variation of loading, an equivalent series of uniform step pulses can be determined, and the construction is readily carried out in stages, with a different center for each step pulse. The maximum value of y is readily measured, or the time can be determined, and the corresponding velocity, when a deflection ye corresponding to yielding is reached.

4.2.3 Conjugate Beam Concept

The relations among loads, resisting forces, velocities and displacements are best described in the graphical representation shown in Fig. 4.4. The accelerations due to the loading and to the resistance are plotted as functions of time in Fig. 4.4a. The difference between the curves is the net acceleration. The velocity-time relation, in Fig. 4.4b, is the first integral of the acceleration curve, and the displacement, in Fig. 4.4c, is the integral of the velocity curve. It follows by analogy, therefore, that the accelerations can be considered as loads on a conjugate cantilever beam with distance analogous to time, having a free end at the origin ($t = 0$) and with the sign convention that the conjugate beam loading is upward when the loading accelerations p/m exceed the resistance accelerations q/m. Then the velocities correspond to shears in the conjugate beam, and the displacements to moments in the conjugate beam.

It is apparent from this concept that the maximum deflection is reached when the areas Al and A_2 in Fig. 4.4a are equal, and the maximum deflection is equal to the moment of the couple formed by these equal areas.

Where yielding occurs, if the elastic part of the resistance curve is traced out by numerical methods or by use of the gyrogram, then the maximum deflection is obtained by the simple process of determining the maximum moment in the conjugate beam.

4.2.4 Effect of Support Movements

If the simple one-degree-of-freedom system studied in the foregoing sections is attached to a moving support, where the motion of the mass relative to the support is denoted by y, as before, and where the support motion is denoted by u, the maximum relative motion of the mass is computed in the same way as for the case of a stationary support, but for a modified loading. The modified loading is merely the given loading p less the product of the mass m and the acceleration d^2u/dt^2 of the moving support. If the product of the mass m and the acceleration of the support is very small compared with p, then the effect of the support motion on the maximum relative deflection will be small also.

4.2.5 Methods Used in Analysis of Fieldtest Data

The field test structures were analyzed to determine the theoretical maximum responses for the various measured surface loading

conditions. The analyses were carried out in general as follows:

The values of mass, loading, and resistance were defined as described in Section 4.1. The pressures were determined for 5 millisec. intervals from the record of surface pressures. Equivalent uniform pressures were computed for each interval as the average pressure for that interval. A gyrogram was then constructed to obtain the maximum deflection and the time to reach the maximum deflection. Where the structures were assumed to become plastic, the gyrogram construction was terminated at the corresponding yield point deflection, and the numerical integration procedure was followed to the maximum deflection, still using time intervals of 5 millisec.

For the calculations made to take into account the support movements, the values of the measured acceleration of the concrete chambers were used to correct the accelerations determined from p/m. The corrected accelerations were used in drawing the gyrograms or in the numerical integrations beyond yielding.

In the calculations, in order to simplify the work for the large number of analyses, the following procedure was used to take into account the effect of yielding. The accelerations due to the resisting forces were considered to vary linearly with deflection beyond the point of original yielding, up to a value of 1.20 times the yield resistance. The values used are shown in Fig. 4.2 by the dotted line extending from the unmodified value (corresponding to the yield resistance) to the higher modified value. The accelerations due to the loading were increased by the same factor to a value of 1.20 times the Unmodified value, beginning at the time when the modified yield value of resistance was reached. The loading was not increased for the interval during the varying modification of the yield resistance.

Although this procedure is slightly inaccurate, the results are not in error by more than a few per cent. The calculations were made by Professor E. R. Bretscher of the Department of Civil Engineering during the latter part of July and in August, 1953, before the more precise procedures were developed. As information developed regarding the inaccuracies in the measured data upon which the calculations were based, it became evident that it was not worthwhile to repeat the calculations, as the increase in accuracy would not be warranted by the available information on pressures.

4.3 EFFECTS OF VARIOUS PARAMETERS

4.3.1 Simplified Loading Considered

In the analyses discussed herein a number of parameters are considered and their effects and results studied in order to lead to a better understanding of the nature of their influence on the behavior of the structures in the tests. Because of the fact that the field tests could cover only a limited number of variables, an extension of the results is not possible without the data outlined in this chapter. It is also desirable to have available the analytical data described herein as a basis for interpretation of the test results. Many of the

field test data are subject to difficulties in interpretation because of the very great influence on the numerical values of the data obtained arising from small differences in the test conditions. It will be found, for example, that small errors in measurement, or in the determination of the fundamental physical constants, can cause extremely large errors in the predicted responses. Consequently, an extensive survey of this phenomenon appears desirable by analytical methods.

In the discussion in this chapter, a simplified loading condition is assumed, corresponding to the diagram shown in Fig. 4.5, in general however without the initial flat portion of the pressure curve. In most cases the pressure-time diagrams considered are triangular in shape with a rise time which is finite and which maybe large compared with the period of the structure. The duration of the pressure pulse is held constant for a number of different rise times including an instantaneous rise. Analyses were made by means of the numerical procedures described in the preceding section. The results are given in Table 4.1. Various comparisons can be made from these data . The influences of the magnitude of the peak pressure acting on the structure, the yield resistance of the structure, the duration of the loading, and the rise time, are all discernible in terms of their effect on the maximum deflection of the structure. In the tabulated data, the maximum deflection is related to the deflection at yielding in order to give the results in a dimensionless form. Values are given for times of rise to maximum pressure, measured in units relative to the natural period of vibration of the structure, of 0, 0.5, 1.0, and 1.5T. Intermediate values could be computed but the general influence of the data is seen from the table, and further calculations would not indicate any new trends. The data given are sufficient to indicate the sensitivity of the results to the various parameters.

Although for structures in general, ranges outside of those tabulated would be of interest, it is not of importance in connection with the field test program to go beyond the range in values of peak pressure related to yield resistance shown in the data.

4.3.2 Effects of Slow Rise

The influence of the time of rise of a loading curve without precursor is indicated by the values in Table 4.1 and by Figs. 4.6 and 4.7. When the time of rise is small compared with the natural period of the structure the influence on the maximum deflection is slight . However, as the rise time approaches the natural period, this influence becomes very large and in some cases may be even infinite in magnitude. When the rise time becomes longer than the natural period of the structure, the maximum deflection may actually be greater than for a rise time equal to the natural period.

There is in general a variation in the influence of rise time, with the maximum reduction in response occurring for rise times which are integral multiples of the natural period of the structure. However, rise times much longer than those indicated in the figure are generally not of major practical interest. The greatest effect of

rise time is noted for the case where the maximum loading applied to the structure is exactly equal to the yield resistance. Under these conditions, for an infinite pulse length, the response of the structure is infinitely large for a zero rise time, but the response is equal precisely to the elastic deflection when the rise time is an integral multiple of the period. However, when the maximum load is even infinitesimally greater than the yield resistance of the structure, the maximum response is infinite for all values of rise time, when the pulse is of infinite duration.

When the maximum load is greater than the yield resistance of the structure, the influence of rise time becomes less important, but the response becomes large unless the total duration of the loading is relatively short. When the maximum intensity of loading is less than the yield resistance of the structure the maximum response is bounded even for infinitely long pulses, and the range between the maximum response for a zero rise time and for a finite rise time decreases also.

Unfortunately, the period for most underground structural elements is likely to be fairly short because of the high resistance and stiffness which such structures must have to resist the loading applied to them. Because the duration of the loading will generally be long compared with the period of the structure, for any operational weapon, it will be necessary for the resistance of the structure to approach in magnitude the maximum dynamic loading which will be applied to the structure. Consequently, the region of practical interest in the design of underground structures is the region surrounding the value of 1.0 for the ratio of maximum load to yield resistance. However, it is precisely this region where the greatest uncertainty exists in the effect of time of rise of the pressure. In order that the structure be capable of resisting all types of forces applied to it, it should apparently be designed for an instantaneous rise. However under these circumstances it is quite possible that the effect on the structure for the conditions when the rise is relatively low will be very much less than the effect for which the structure is designed.

4.3.3 Effect of Positive-Phase Length

The influence of length of the positive phase of the blast is determinable from Table 4.1, or by comparisons of the different curves in Figs.4.6 and 4.7. It can be seen that as the duration of the loading increases, the maximum deflection increases also, and in general, the relative change in maximum deflection is approximately equal to or less than the relative change in duration of the positive phase. In other words, a 20 per cent increase in duration will produce generally less than a 20 per cent increase in maximum deflection except under certain circumstances where, because of the effect of variation in rise time, an unusual condition occurs. This conclusion does not mean to state that the effect of duration is unimportant. It maybe of very great importance. However, small changes in duration will not affect the maximum deflection materially. It will require changes of

the order of magnitude of a doubling of duration to produce significant changes corresponding to a doubling of maximum deflection. An exception to this rule is noted in the case where the rise time is equal to the natural period of the structure. Under these conditions, the duration of the positive phase after the peak has no influence whatsoever on the maximum deflection. This maximum deflection is reached at the point where the maximum load is reached, and no further deformation takes place if the maximum load is less than or even equal to the yield load of the structure.

4.3.4 Effect of Yield Point of Material

The magnitude of the yield point of the material is one of the major variables in determining the magnitude of the response of the structure. It has the same influence as the intensity of peak pressure. In general, both of these variables produce an effect on the maximum deflection greater by far than the effect produced by a relative change in the duration, or any other variable. For example, for an infinitely long pulse having an infinitesimal rise time, when the yield point is 10 per cent greater than the peak force, the maximum deflection is of the order of five times the elastic deflection. However, under the same conditions, if the yield point is decreased by 10 per cent so that the new yield point is equal to the peak pressure, the response becomes infinitely large.

Similar influences can be noted in the case of finite duration, for example where the duration is 10 times the natural period of the structure. Under these conditions, the maximum deflection changes by a factor of approximately 2 for a 10 per cent change in yield resistance.

It maybe more meaningful to discuss the relative change in the strength of the structure as measured by the magnitude of the peak loading that it can sustain, rather than to discuss the maximum displacement of the structure. With this point of view in mind, it turns out that the change in strength is precisely equal to the change in yield resistance when the latter is subject to variation. Moreover, the change in required strength caused by a change in duration of the positive phase is much less than the change in duration. The strength required is influenced to a smiler extent than is the maximum deflection, for changes of any of the variables considered.

4.3.5 Effects of Precursor Plateau

The influence of the precursor plateau shown in conventionalized form in Fig. 4.5, may affect materially the response of the structure to the later shock. Although the effect of the precursor depends both on the strength of the precursor shock and on its duration, the latter produces the most unusual and variable effects. Because the precursor in the field test program had a relatively small strength compared to the structural resistance, the calculations made herein were all for a precursor strength of just 25 per cent of the

yield strength of the structure. This factor corresponds closely with the field conditions.

The maximum deflections tabulated in Table 4.1 give the responses for shocks of various durations ranging from 3 to 10 times the natural period of the structure, and include precursor durations of 0, 1/4, 1/2, and 3/4 the natural period. The effects of longer precursors, for shocks of the shape shown in Fig. 4.5, may be obtained by noting that the effect of a precursor of duration nT + to has the same effect as a precursor of duration t_o.

The rise times considered in Table 4.1 cover the range of 0, 1/2, 1, and 1 1/2 times the natural period of the structure. The values of main shock strength listed in the table range from 0.8 to 1.5 times the yield resistance.

In general the results shown In Table 4.1 indicate that for a sharp rise following the precursor, the precursor plateau reduces the influence of the shock, and the reduction is quite large when the shock strength is about the same as the yield resistance, which is the range for the M and P beam strips in the field tests. For example, a precursor lasting for a time T/2 shows a maximum deflection reduced by a factor of 2 or more from the deflection without precursor.

For long rise times, however, the precursor effect may be in the other direction, and an increased deflection may result. For the precursor strengths studied the absolute maximum effect with a precursor and delayed rise main shock is never very much greater than the maximum deflection for a shock with a fast rise time and no precursor.

As an illustration of the way the precursor influences the structural behavior consider Fig. 4.8. The solid lines marked "load" indicate the loading considered, with a precursor plateau as shown. The solid line marked "deflection" shows the response and indicates the fact that a preliminary maximum deflection is reached in the precursor stage, followed by a minimum during the initial stages of the main shock, and a maximum a short while later.

The dashed line representing the deflection without a precursor goes to a greater maximum, as shown in the figure. Both curves correspond to the same yield resistance which is slightly larger than the peak value of the load in the main shock.

TABLE 4.1 - Ratios of Maximum to Yield Deflection for Finite Rise Time and Precursor Shocks

Relative Peak Pressure p_m/q_e	Relative Rise Time t_r/T	Relative Shock Duration t_1/T = 3, Relative Precursor Duration t_i/T				Relative Shock Duration t_1/T = 5, Relative Precursor Duration t_0/T			
		0	1/4	1/2	3/4	0	1/4	1/2	3/4
0.8	0.0	1.8	1.5	1.0	1.4	2.0	1.6	1.0	1.5
	0.5	1.4	1.1	1.7	2.0	1.5	1.2	1.9	2.2
	1.0	0.8	1.2	1.5	1.1	0.8	1.2	1.5	1.2
	1.5	0.9	0.9	1.2	1.2	0.9	1.0	1.3	1.4
1.0	0.0	3.6	2.9	1.7	2.5	4.8	3.8	2.1	3.4
	0.5	2.9	1.9	3.2	4.0	3.5	2.3	4.1	5.2
	1.0	1.0	2.0	2.8	2.0	1.0	2.2	3.3	2.2
	1.5	1.3	1.0	1.4	1.9	1.4	1.2	1.8	2.5
1.1	0.0	5.4	4.4	2.7	3.9	8.3	7.0	4.2	6.1
	0.5	4.6	3.0	4.7	6.0	6.8	4.6	7.2	9.0
	1.0	1.6	3.1	4.4	3.5	2.1	4.4	6.4	4.9
	1.5	1.8	1.3	1.7	2.4	2.6	1.7	2.3	3.8
1.25	0.0	9.9	8.7	5.9	7.4	L9	17	12	15
	0.5	9.3	6.5	8.6	10.8	L7	13	17	20
	1.0	4.8	6.4	8.7	7.9	L0	13	16	15
	1.5	3.6	4.2	4.4	3.6	8	9	9	8
1.5	0.0	24	22	L8	20	54	52	45	47
	0.5	23	19	21	25	53	46	50	56
	1.0	17	17	21	21	42	43	50	50
	1.5	11	15	L7	L4	52	39	42	37

TABLE 4.1 (CONTINUED) - Ratios of Maximum to Yield Deflection for Finite Rise Time and Precursor Shocks

Relative Peak Pressure p_m/q_e	Relative Rise Time t_r/T	Relative Shock Duration t_1/T = 7, Relative Precursor Duration to/T				Relative Shock Duration t_1/T = 10, Relative Precursor Duration to/T			
		0	1/4	1/2	3/4	0	1/4	1/2	3/4
0.8	0.0	2.1	1.6	1.0	1.6	2.2	1.7	1.1	1.6
	0.5	1.5	1.2	1.9	2.2	1.5	1.2	2.0	2.4
	1.0	0.8	1.2	1.5	1.1	0.8	1.2	1.5	1.2
	1.5	1.0	1.0	1.4	1.4	1.0	1.0	1.5	1.4
1.0	0.0	5.7	4.3	2.4	4.1	6.9	5.4	2.9	4.9
	0.5	4.0	2.6	4.8	6.0	4.7	3.0	5.8	7.2
	1.0	1.0	2.5	3.6	2.3	1.0	2.7	4.0	2.5
	1.5	1.5	1.3	2.0	3.0	1.7	1.5	2.3	3.5
1.1	0.0	11.2	9.1	5.7	8.4	16	13	8.6	12
	0.5	9.0	6.1	9.6	11.8	13	9.0	14	17
	1.0	2.8	6.0	8.3	6.3	4.2	8.4	12	8.9
	1.5	3.6	2.2	3.2	5.3	5.4	3.4	4.7	7.9
1.25	0.0	29	26	20	24	50	46	37	42
	0.5	27	21	27	31	46	39	46	52
	1.0	17	21	26	24	32	37	44	41
	1.5	15	16	16	10	29	29	30	22
1.5	0.0	95	92	82		180	176	162	
	0.5	94	84	89	98	178	164	172	184
	1.0	79	81	90	89	157	159	173	172
	1.5	65	75	79	72	136	150	156	147

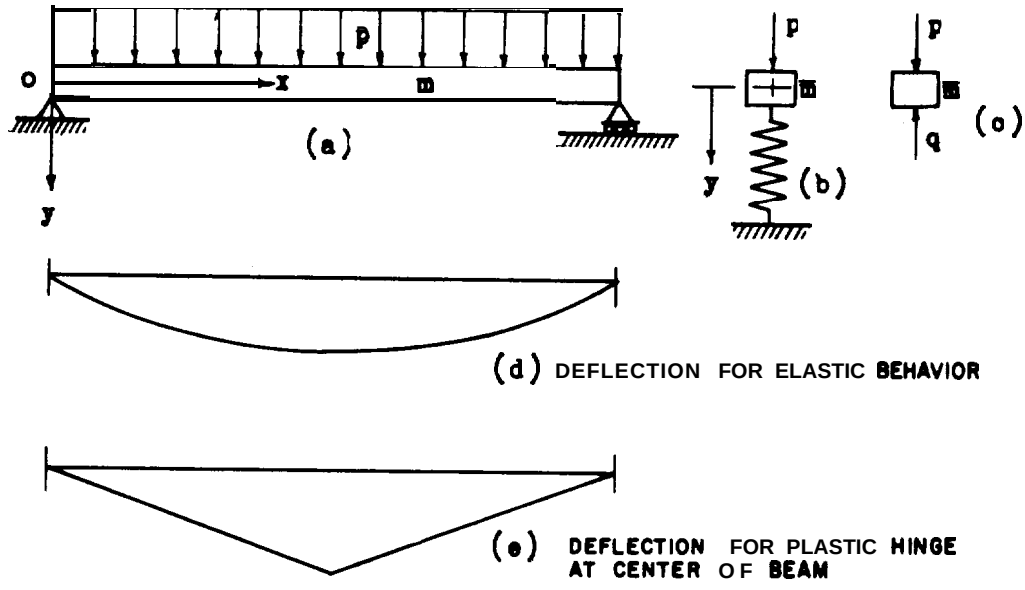

Fig. 4.1 Beam and Replacement Simple Structure

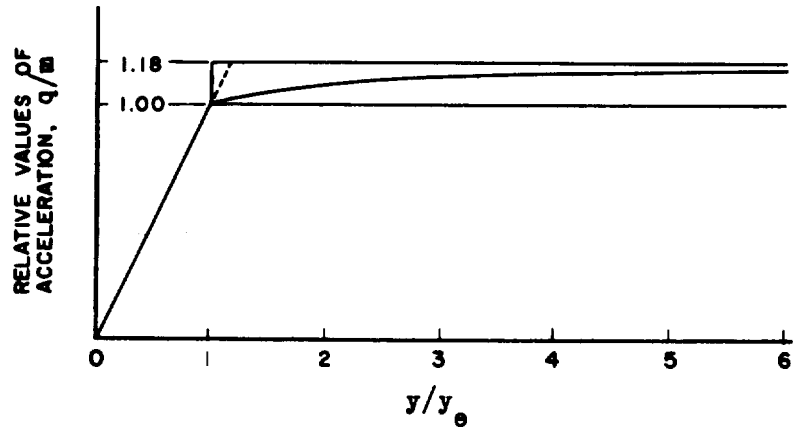

Fig. 4.2 Modification of Acceleration as a Function of Deflection

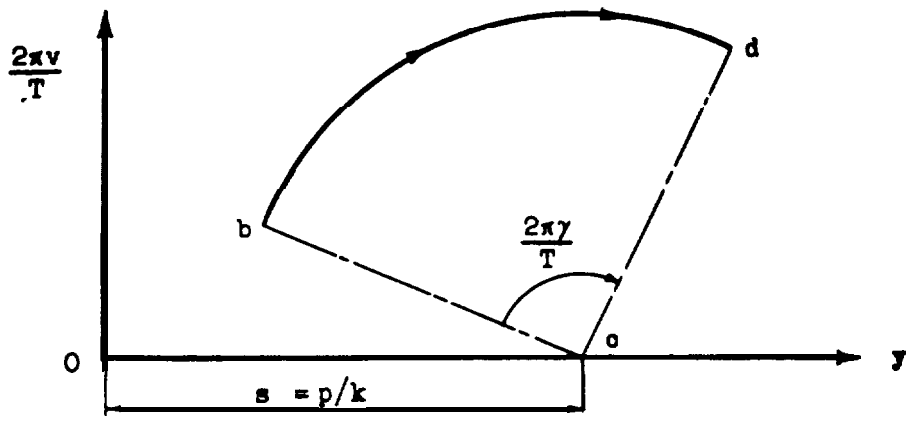

Fig.4.3 Illustration of Gyrogram Construction

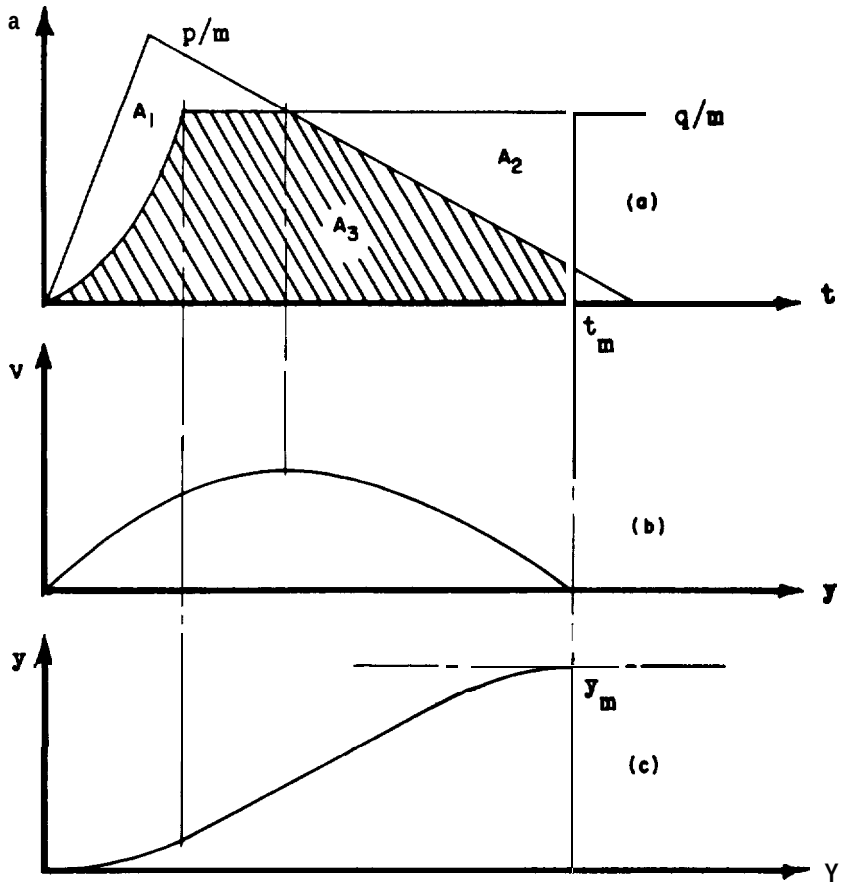

Fig. 4.4 Relations Among Acceleration, Velocity, and Displacement

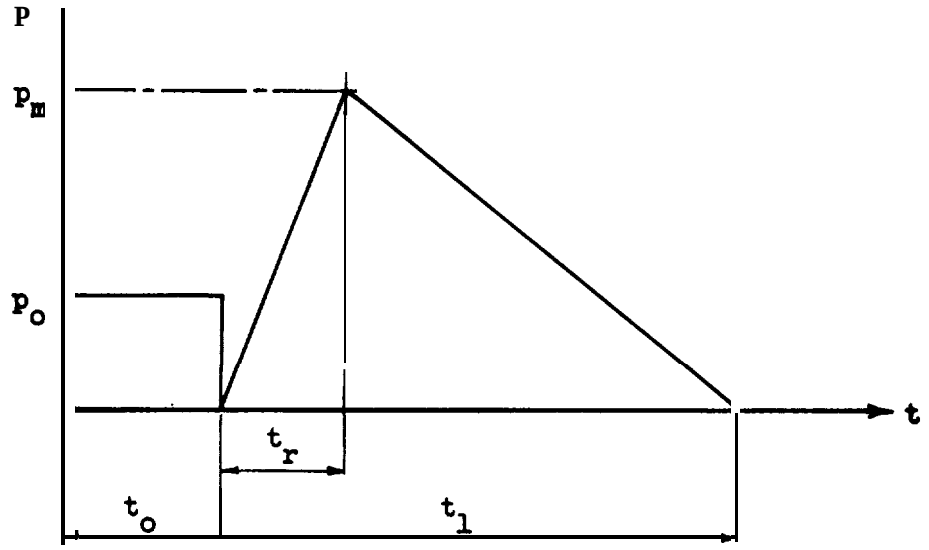

Fig.4.5 Simplified Loading Considered

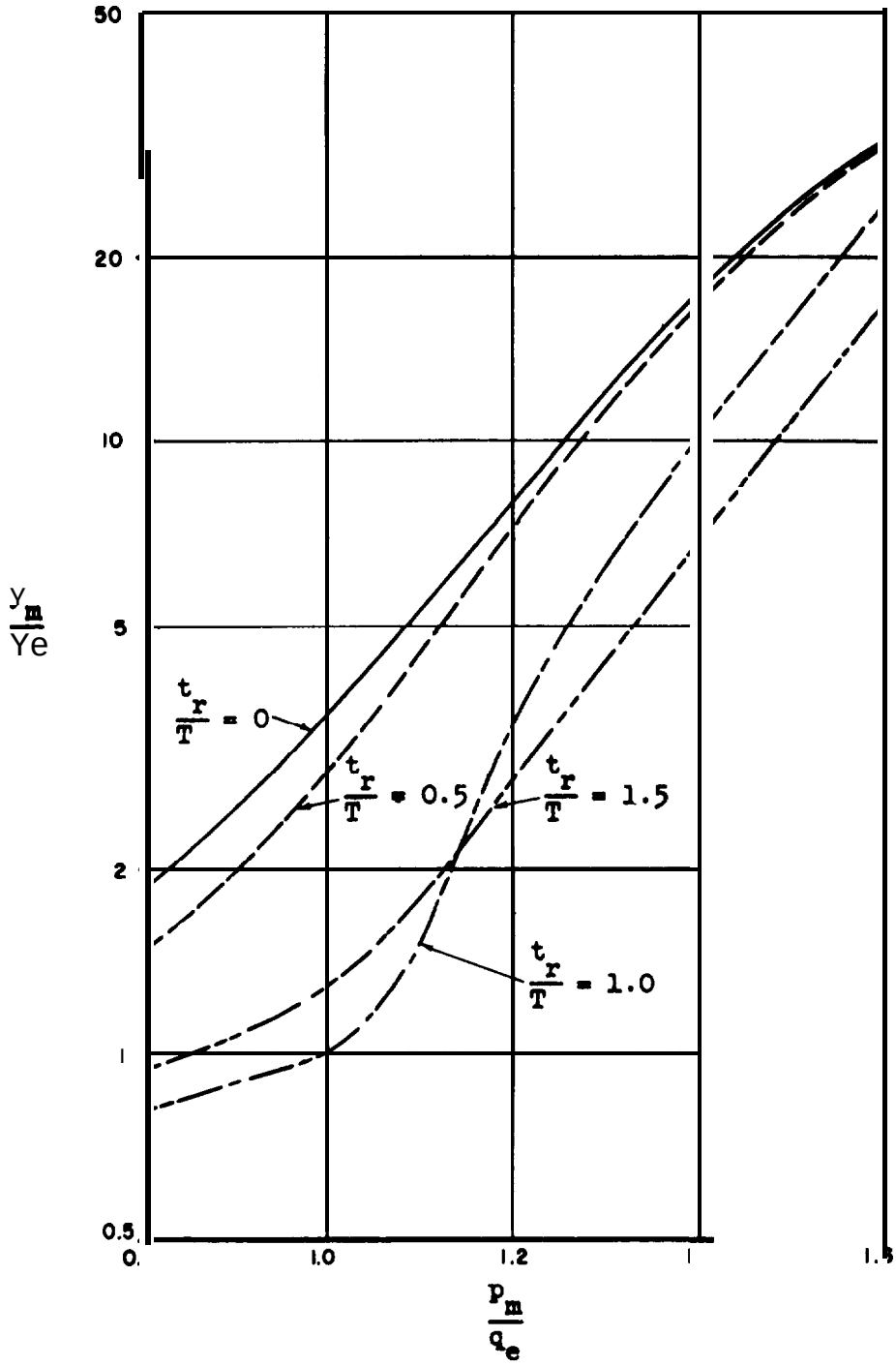

Fig.4.6 Response of Elasto-Plastic System to Slow Rise Shock--$t_1/T = 3$

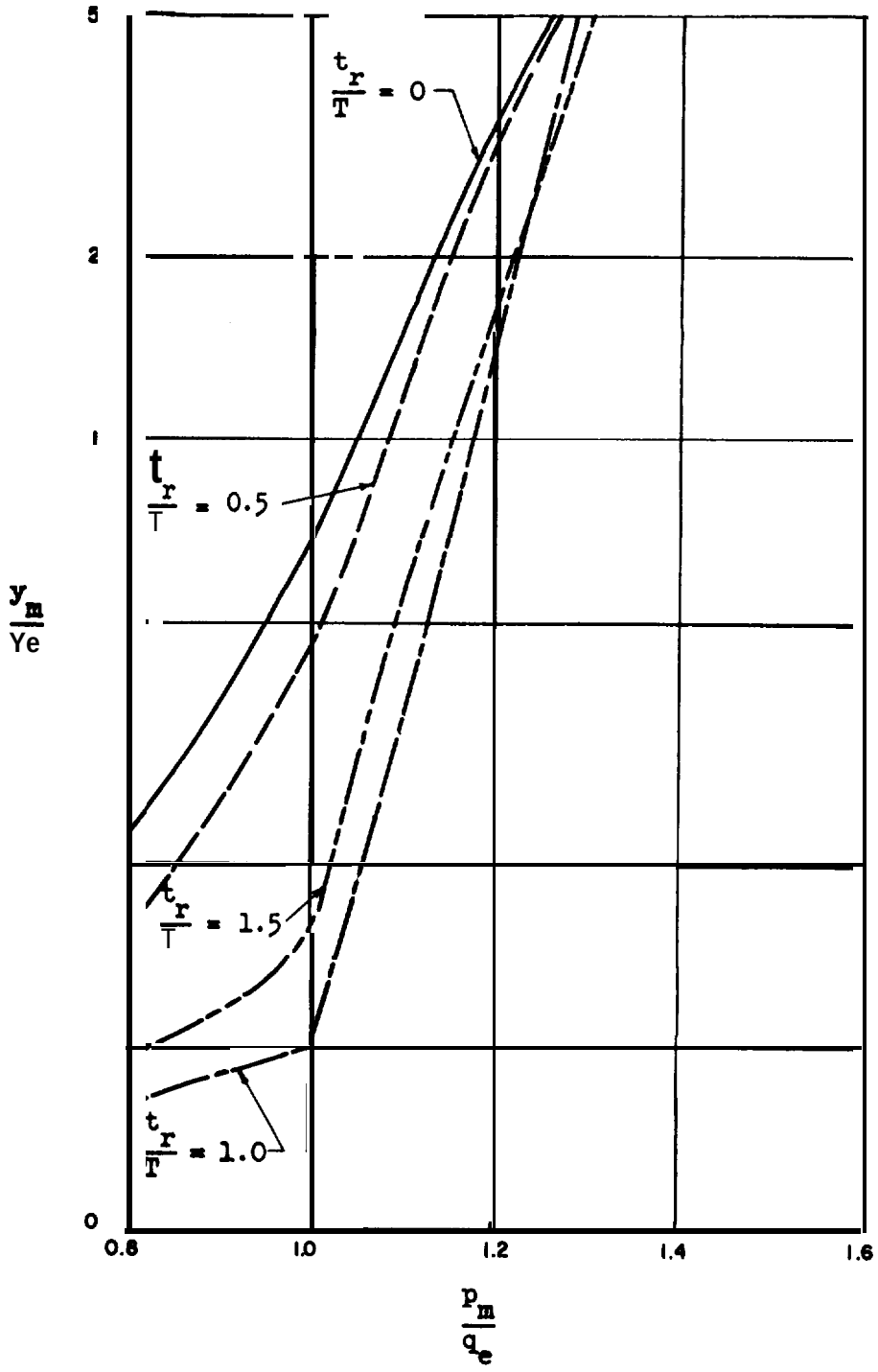

Fig. 4.7 Response of Elasto-Plastic System to Slow Rise Shock--$t_1/T = 10$

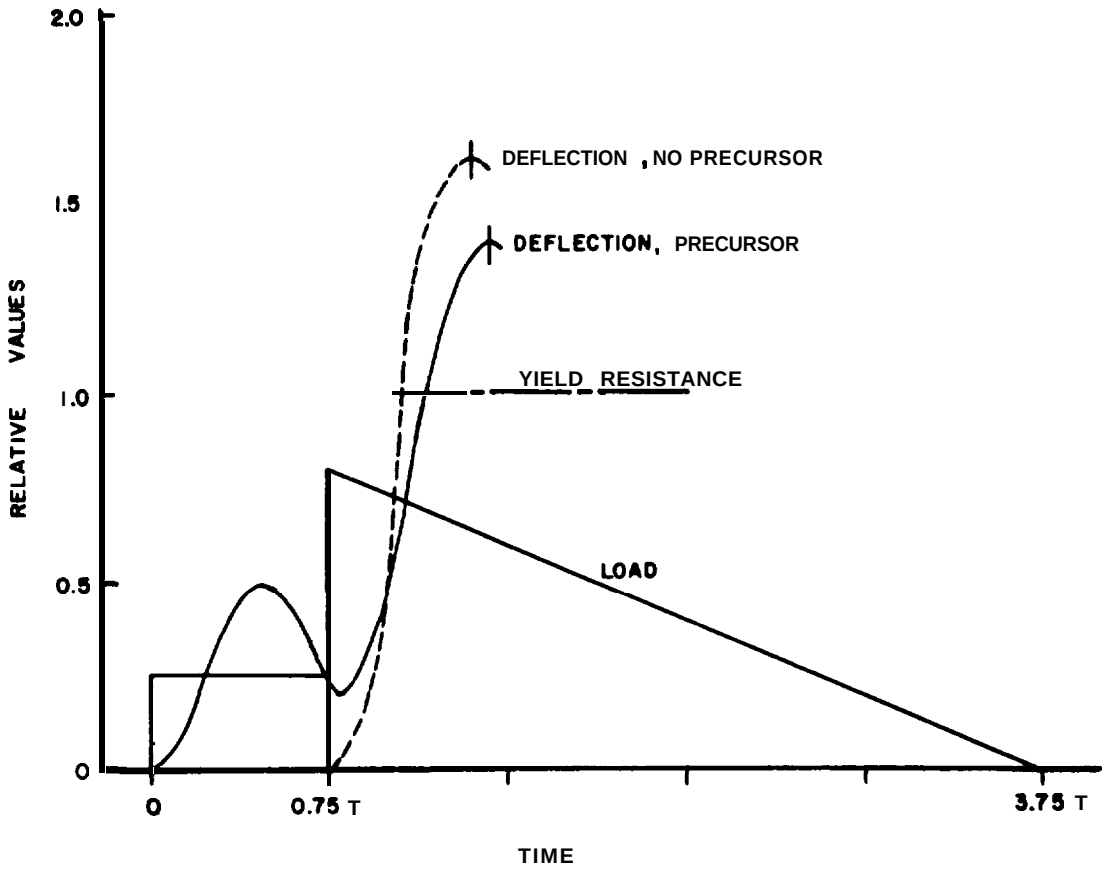

Fig.4.8 Effects of Precursor Shock

CHAPTER 5

LABORATORY TESTS

5.1 GENERAL DESCRIPTION

In order to interpret the results of the field tests, complete knowledge is required of the physical properties of the material and the characteristics of the behavior of the beam strips. Because of the variability in the properties of structural steel it was necessary to identify the properties of all of the different pieces that enter into the principal parts of the structures tested. For this purpose, standard ASTM tensile coupon tests were made of the various pieces of beam and plate entering into all of the beam strips in the structures. These data were intended to give the comparative strengths of the different beam strips in order to permit information to be used from all of the beam strips in the structure including those not instrumented as well as those fully instrumented. The data serve as a basis for the interpretation of future tests that may be made with this array of beam strips.

In addition to the control coupon tests, tests were made of complete beam strips supported on standard shoe supports as in the test chambers, and loaded to extremely large deflections. These tests should have been made before the location of the structures was chosen for the field test. However, because of the time schedule required for this program, it was necessary to make the control tests of the specimen beam strips after the field tests were completed.

Tests were made on Beam Strips CE1, CM1, and CP1, respectively representative of the test beam strips for the E,M, and P beams. One additional specimen of a P beam strip, CP2, has not yet been tested but is available for special test if further tests are performed on the structures in the field.

These laboratory tests were made for several reasons: (1) to furnish information as to the actual yield point of the material in the beams under conditions similar to those applying to the test conditions; (2) to relate the strains In the flanges to the deflection In order to furnish information of value in interpreting the test data; and (3)to determine the relationship between strains in the supporting shoes for the beam strips and the reactions on these shoes,

for use in checking the theoretical relations between strains in and reactions for the shoes. These laboratory tests were all made in the Talbot Laboratory at the University of Illinois under the general direction of Professor W. E. Black of the Department of Theoretical and Applied Mechanics.

5.2 STANDARD CONTROL COUPONS

Standard tensile tests were made on 112 specimens from 5 samples of the steel plate and 12 samples of the rolled sections which made up the main structural elements of the beam strips. From 6 to 9 specimens, all longitudinal to the direction of rolling, were cut from each sample of rolled channel or I-beam. Five specimens, of which 3 were longitudinal and 2 were transverse, were cut from each plate sample.

The tensile tests were performed in a 120,000 lb capacity Baldwin-Southwark hydraulic testing machine with movement pacer and microformed strain gage recorder. All tests were run at a platen speed of 0.2 in. per min. Strains were automatically recorded with an 8 in. microformed strain gage up to a strain of approximately 1.0 per cent. While still within the yield shelf or range, the test was momentarily stopped while the microformed gage was removed and replaced by an 8 in. C-type gage, the reading of which was determined from an SR-4 Strain Indicator. The test was continued at the same rate of loading and strains were measured with the C-gage up to a strain of about 10 per cent. At this point the C-gage was removed and the test continued to rupture.

Because of lack of material in the sample for Beam Strips 1P1 and 4P1, specimens cut from this sample required the use of a 2 in. microformed gage and 2 in. C-gage. All specimens were made to conform as nearly as possible to ASTM standard dimensions. In general the coupons from the beam webs and from the plate were 1 1/2 in. wide, and those from the beam flanges were 3/4 in. wide. The results of the tests on tensile coupons are summarized in Table 5.1.

In all of the rolled sections, it was noted that the yield point was lower for those specimens cut from the thick portion of the flange near the junction with the web than for specimens cut from the thinner portions of the section in the web and near the toes of the flanges. For example, in sample A3 of the 7 in. channel section, the yield point for coupons cut adjacent to the heel of the flange was about 42,000 psi whereas the yield point of coupons cut from the web or adjacent to the toe of the flange was about 49,000 psi.

Properties obtained from the plate coupons were very uniform, and showed no influence of the direction of rolling. In these tests, the yield point was determined as that stress at which the strain began to increase without increase in load, or the stress at a value of 0.2 per cent offset in strain, whichever occurred first.

The average yield point of the 7 in. channel was considerably higher than that of the 8 in. or 15 in. I-beams or of the plate. The differences between the ultimate strength values were not so pronounced. The average properties of flanges, webs, and of the 1/2 in. plate

can be compared in Table 5.1.

The specimens, cut from the 7 in. channel rolled by the Columbia Steel Co. and used in Beam Strips 1P1 and 4P1, had much higher values of yield point and ultimate strength than the other specimens. However, no measurements were made on the beam strips containing these channels, either in the laboratory tests or in the field tests; consequently, the higher yield point should have had no influence upon any of the test results of the beam strips.

5.3 TESTS OF BEAM STRIPS

5.3.1 Test Procedure

Beam Strips CM1 and CP1 were tested in a 300,000 lb Riehle testing machine, and CE1 in a 3,000,000 lb Baldwin-Southwark hydraulic testing machine. The loading system used is shown in Fig. 5.1. In order to simulate a uniformly distributed load, a four-point loading system was chosen because it was possible to select such a system to produce the same maximum moment and maximum shear values as the uniform load. In the elastic range, the four-point system causes 2.5 per cent greater deflection at the center of the span than does the same total load distributed uniformly.

As large deflections of the beam strip were obtained, the two lower loading beams shown in Fig. 5.1 had a tendency to become inclined. Therefore, at the rollers between the two tiers of loading beams, provision was made for approximately 4 in. of relative longitudinal movement between the upper and lower loading beams. In the test of Beam Strip CP1 a movement of this magnitude actually occurred. Despite the large rotations and relative displacements of the loading beams that accompanied large deflection of the test strips, the resultant force transmitted by each of the upper rollers continued to pass approximately through the quarter point of the beam, thus insuring nearly equal distribution of the load among the four load points.

Electric resistance strain gages (SR-4) were located on each of the beams in locations identical to those used in the field tests. Type A-5 gages were used at these locations since the gage length is nearly the same as that of the gages used in the field tests. Other strain gages, mostly type A-11, were installed at various points on the cross-sections of the beam at midlength and at one quarter point to evaluate better the behavior at these two sections. In the tests of CP1 and CE1, additional gages were installed on the shoes to aid in evaluating shoe reactions.

In order to provide a check on the electric strain gages and to permit the recording of strains beyond the range of the SR-4 equipment, holes were drilled to permit the measurement of strain on the upper and lower surfaces of the beam strips with a 2 in. Berry type gage and a 2 in. direct reading strain gage equipped with a 0.001 in. Ames dial.

Vertical deflection of the bottom surface of the lower flanges of the beam strips was measured by means of Ames dials reading to 0.001 in. Ten dials were used, five beneath each beam. The dials

measuring deflection in the center portion of the beam strip had a travel of 4 in. In the test of Beam Strip CP1, in which deflection in excess of 6 in. was recorded, deflections beyond about 3.5 in. were measured by means of a steel scale to the nearest 0.01 in., measuring upward from the bed of the testing machine. Figure 5.1 shows the locations of the deflection measurements for the three beams.

Load was applied to the beam strips in a series of increments, the size of the increments in the elastic range being determined to provide at least five increments prior to the initiation of yielding. After yielding first had occurred the load was increased to a predetermined value and maintained at that value until the strain and deflections readings became stationary or nearly so before any readings were taken. The size of the load increments in this range was determined so that no increment of deflection was more than twice the preceding increment.

5.3.2 General Nature of Test Results

In the test of CM1, the loading was continued until failure of the shoes occurred, as shown in Fig. 5.2. In order to prevent the longitudinal movement associated with this type of failure in the later tests, a jacking frame was devised to resist this movement, which could not occur so readily in the field structures because of possible restraint from the parapets and filler strips and the definite restraint of the earth cover. This frame was used successfully in the test of Beam Strip CP1, and the test was continued until a deflection of over 6 in. was reached, at which time the test was discontinued because of interference between the bottom flange and the shoe bolts at one end of the span. Maximum load had not been reached at this stage, but a good deal of plastic deformation had occurred.

In the test of Beam Strip CE1, failure of the expansion shoe occurred at a load of 470,000 lb, before any yielding of the beam itself had been detected. This shoe was then cut off and replaced by a stronger support detail. The test then was continued, starting again from zero load. At a load of 550,000 lb there was evidence of impending failure of the fixed shoe, the test was again stopped, and the fixed shoe was reinforced by welding plates to it. During this operation the load dropped to 350,000 lb. The test then was continued, with no attempt at further measurement of the shoe reactions, until the fixed shoe failed above the reinforcement. At the final load of 660,000 lb plastic action had been initiated in the beam.

With longitudinal motion prevented as in the field test, the shoe strengths are entirely adequate for the P and M beams, but may require strengthening for the E beams if these are to be loaded to the plastic range by a subsequent test well above the load for which the UPSHOT-KNOTHOLE program was planned. For peak pressures less than about 200 psi, no strengthening appears to be required for the E beams.

In general, at the first indications of yielding in the beams,

detected by large departures from linearity in the readings of the strain gages on the lower flanges of the beams, there was very little departure from linearity in the relation between load and deflection. However, as the load was increased further, the load-deflection relations began to show more evidence of yielding until finally a definite departure from linearity was reached. The sharp bend in the relationship between load and deflection did not occur until yielding had extended well through the flange and up into the web of the section, at loads of the order of 40 per cent greater than those that corresponded to initial yielding.

5.3.3 Load-Deflection Relations

The relationship between load and deflection was normal for the type of structure, showing a linear relationship up to initial yielding and then only a slight departure from linearity through general yielding of the flanges and part of the web. Load deflection curves for each of the beams are shown in Fig. 5.3. It is of interest to note that in no case was a true maximum load reached even though large deflections were obtained in Beam CP1. The rate of increase of load was slow in the latter stages of the test of the two beams which developed considerable yielding. It is of interest to note that the actual load-carrying capacity of Beams CM1 and CP1 were almost the same, although the theoretical values, corresponding to their section moduli, differ by nearly 40 per cent. This difference is due to the fact that the yield point of the material in Beam CP1 was greater than that in Beam CM1, although a difference of this order of magnitude is not indicated by the yield point of the test coupons.

The results of the load-deflection tests are summarized in Table 5.2. It appears from this table that the initial yielding of the two beams occurred at about the same loads, at a stress that corresponded to the coupon yield point of the flange material for Beam CP1, but at a stress considerably lower than the coupon yield point of the flange material for Beam CM1. The yield points detected by the first departures from linearity in the deflection curve corresponded very closely with the yield points determined from the strains in the flanges. The deflections at these points were computed by means of the coefficients given in Table 2.1, and the values corresponding to the yield point loads indicated in Table 5.2 are, respectively, for the P, M, and E beams, 0.303, 0.205, and 0.153 in. The first two values are in excellent agreement with the observed values and the latter is somewhat less than the value for the E beam, and may be accounted for by the vertical deformations in the shoes of the E beam which increased the measured deflections relative to the base of the testing machine. A deflection curve plotted relative to the end deflection gages, with the appropriate correction for the deflection between this point and the end, shows a closer agreement with the theoretical value.

The "knee" of the load-deflection curves is difficult to define unequivocally. However, one can take for this point the load

corresponding to the intersection of the two straight line components of the load-deflection curve. At these values, the apparent stresses computed from the section moduli were, respectively, 59,000, 45,100, and at least 48,000 psi for the P, M, and E beams. These values are, of course, not true measures of the yield point. They are obtained by taking the loads that correspond to the "knee" of the load-deflection curve, and computing for these loads the stresses by the usual straight-line stress distribution formula of the ordinary theory of flexure. It is likely that the yield point is of the same order of magnitude as the stresses tabulated in Table 5.2 for initial yielding, but because of the non-linearity of the stress distribution as the yielding progresses through the depth of the beam, there is an apparent increase in yield point corresponding to the load at which the deflections begin to grow increasingly large. This apparent increase in yield point is not associated with dynamic loading at all since it is observed in static tests. However, it is this apparent yield point which determines the load at which large deflections, or plastic deflection characteristics, are developed in the actual structure.

5.3.4 Distribution of Strain on Cross-Section

The distribution of strain over the cross-section of the beam strips followed the same general pattern in each of the three beams. The strains measured on the inner faces of the top and bottom flanges were slightly higher and those measured at the extreme fibers were slightly lower, on the average, than the corresponding values computed on the assumption that the flexural strains are linearly distributed. A typical plot of the strain distribution at several loads is shown in Fig.5.4, for Beam Strip CP1. The distribution is nearly linear but not completely so. One effect of this non-linearity is, of course, to change the values of the curvatures computed from the extreme fiber strains in such a way that the deflections computed from the strains measured in the field tests are not an accurate measure of the actual deflections. However, the corrections are not large, and in view of the uncertainty as to-the position of the neutral axis under dynamic loading, and in view of other major uncertainties in the field test data, no correction for this effect appears to be warranted.

5.3.5 Strains in Supporting Shoes

In order to serve as a calibration on the readings of the reactions indicated by the strain gages on the supporting shoes of the beams in the field, tests were made in the laboratory to indicate the reactions by similar arrangements of strain gages in the supporting shoes of Beams CP1, CM1, and CE1. In the field tests, the SR-4 gages were arranged in groups of four or eight including two or four vertical and two or four horizontal gages on a shoe arranged so that equal numbers of gages in the same direction were on opposite sides of the web of the shoe, and connected so as to have a common output. Strains in each group of gages were read as a unit using a four arm bridge

which recorded a quantity proportional to the sum of the strains in the vertical direction minus the sum of the strains in the horizontal direction. The horizontal strains normally would be expected to be in the opposite sense to the vertical strains and of magnitude equal to the vertical strains times the value of Poisson's ratio. If the value of Poisson's ratio is designated by the symbol μ, the ratio of the vertical strain indicated by the bridge reading to the true vertical strain would be the quantity $2(1 + \mu)$. This quantity is the so-called "bridge factor." The value of Poisson's ratio normally lies between 0.25 and 0.30, consequently the bridge factor varies from 2.5 to 2.6. A value of 2.5 was used in analyzing the field test data.

In the laboratory each gage was read individually. The individual readings were combined to give a total output for the gages connected in the same manner as in the field. In general, this total output was linear with regard to the reaction or to the applied load, up to the point where the shoe began to fail in the case of Beams CM1 and CE1, and up to practically the maximum load on the structure in Beam CP1. However, the ratio of the strains in the vertical and horizontal directions indicated an effective value of Poisson's ratio of less than 0.25, which is reasonable because of the restraint to lateral deformation offered by the heavy flanges of the shoe and by the welded connection to the beam at the top of the shoe. This restraint was less in the expansion shoes than in the fixed shoes, and the ratio of the horizontal to vertical strains in these shoes, especially for Beam CE1, approached 0.25. The output of the four or eight gages, used as a measure of end reaction and in analyzing the field data, was analyzed to determine the adequacy of the average bridge factor of 2.5 for the shoes of the various beams when the gages were connected in the way in which they were read in the field test. The total loads on each of the Beam Strips CE1, CM1, and CP1 were determined from the bridge readings and plotted against the total applied load in the static tests, in Fig. 5.5. The agreement is remarkably good even for total loads approaching those at which the deflections were 3 in. or more. There was less than a 10 per cent departure of the computed from the actual loads at total loads corresponding to average applied pressures of 100, 96, and at least 200 psi, respectively for Beam Strips CP1, CM1, and CE1.

It can be concluded that the strains in the shoes serve as a good measure of the reactions on the beam strips up to a range of reaction at which plastic behavior is induced in these shoes either from the overall vertical compression or from local flexure of the shoes. The expansion shoes, being subjected to less flexure than the fixed shoes, were more reliable at the higher loads. However, the shoes were capable of recording reactions up to very nearly the maximum loads which it was possible to put on the beams.

Similar phenomena in terms of effective Poisson's ratio and corresponding bridge factor were observed in the flanges of the beam strips. There appeared to be a considerable lateral restraint in the top flange of Beam CP1, and the effective bridge factor for this beam appeared to be somewhat less than the assumed value of 2.5. However, the difference is not important for the *major* part of the readings

TABLE 5.1 - Properties of Tensile Test Coupons

Specimens From	Representative of Beams Listed	No. of Tests	Yield Pts., ksi			Mean Ult. Strength, ksi	Elong. in 8 in., %
			Mean	Min.	Max.		
Beam Flanges	CE1, 1E1, 1E2, 4E1, 4E2 8E1, 8E2, 8E3 (part)	12	39.8	36.4	45.4	63.0	26.1
	1E3, 4E3, 8E3 (part)	6	36.0	34.7	39.1	60.4	28.3
	CM1, 1M1, 1M2, 1M3, 4M1 4M2, 4M3, 8M1, 8M2, 8M3	18	38.9	34.8	43.2	60.7	25.6
	CP1, CP2, 1P2, 1P3, 1P4, 4P2, 4P3, 4P4, 8P1, 8P2, 8P3, 8P4	20	45.4	41.1	52.7	65.4	23.5
	1P1, 4P1	4	50.8	46.7	55.2	70.6	24.6*
Beam Webs	CE1, 1E1, 1E2, 4E1, 4E2, 8E1, 8E2, 8E3 (part)	6	44.2	40.2	52.5	66.5	28.3
	1E3, 4E3, 8E3 (part)	3	36.0	35.1	36.8	60.4	28.3
	CM1, 1M1, 1M2, 1M3, 4M1, 4M2, 4M3, 8M1, 8M2, 8M3	6	41.7	37.4	44.0	60.4	26.6
	CP1, CP2, 1P2, 1P3, 1P4, 4P2, 4P3, 4P4, 8P1, 8P2, 8P3, 8P4	10	49.9	47.4	52.2	67.9	22.1
	1P1, 4P1	2	52.0	51.6	52.4	71.7	31.4*
1/2 in. Plate	All Beams - Longitudinal	15	38.5	36.0	40.5	62.8	28.1
	Transverse	10	39.1	37.4	40.8	62.6	29.1

* Elongation in 2 in. length.

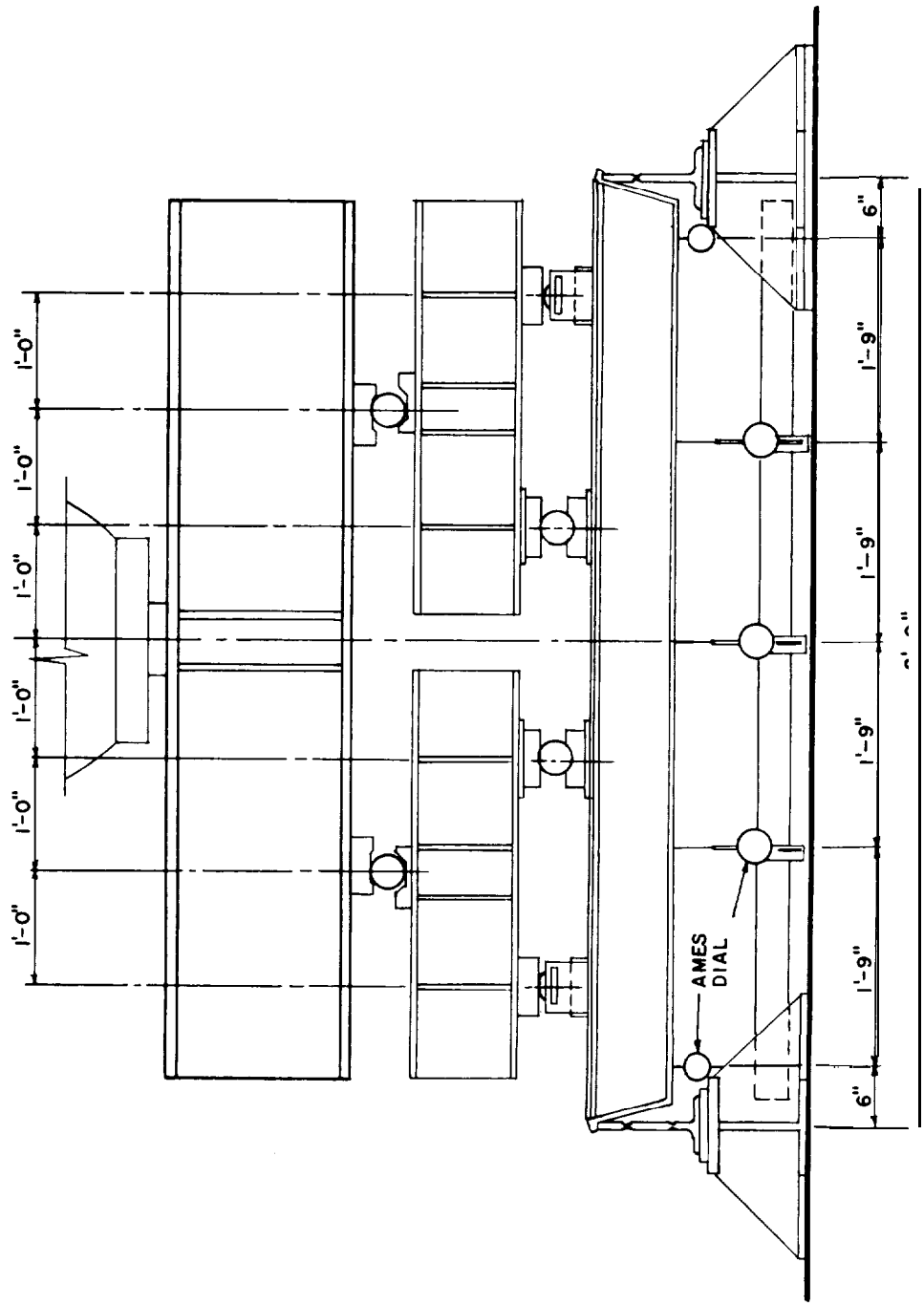

Fig. 5.1 Test Setup for Beam Strips

obtained, and consequently no change in the calculations appears to be required. An effective bridge factor of 2.5 was used in converting all of the data obtained from the strain gage bridges.

TABLE 5.2 - Results of Load-Deflection Tests of Beam Strips

Item	Beam Strip		
	CP1	CM1	CE1
At Yield Pt. (Apparent)			
Deflection, in.	0.300	0.215	0.170
Total Load, 1000 lb.	115	110	450
Equiv. Unif. Load, psi	54.4	54.6	195.3
Flange Stress, ksi	45.1	33.1	35.9
Coupon Yield pt., ksi	45.4	38.9	39.8
At Knee of Load-Defl. Curve			
Deflection, in.	0.64	0.43	0.36*
Total Load, 1000 lb	150	150	600 *
Equiv. Unif. Load, psi	71.0	74.5	261
Flange Stress, ksi	59.0	45.1	48.0
At Deflection of 1.0 in.			
Total Load, 1000 lb	159	166	
Equiv. Unif. Load, psi	75.3	82.4	
At Deflection of 3.0 in.			
Total Load, 1000 lb	177	198	
Equiv. Unif. Load, psi	83.7	98.3	

* Values not accurately defined.

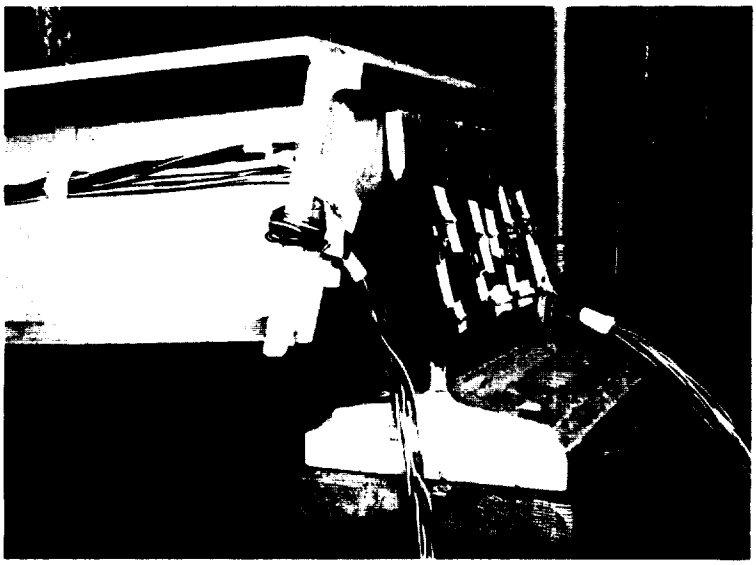

Fig.5.2 Failure of Shoe in Beam CM1

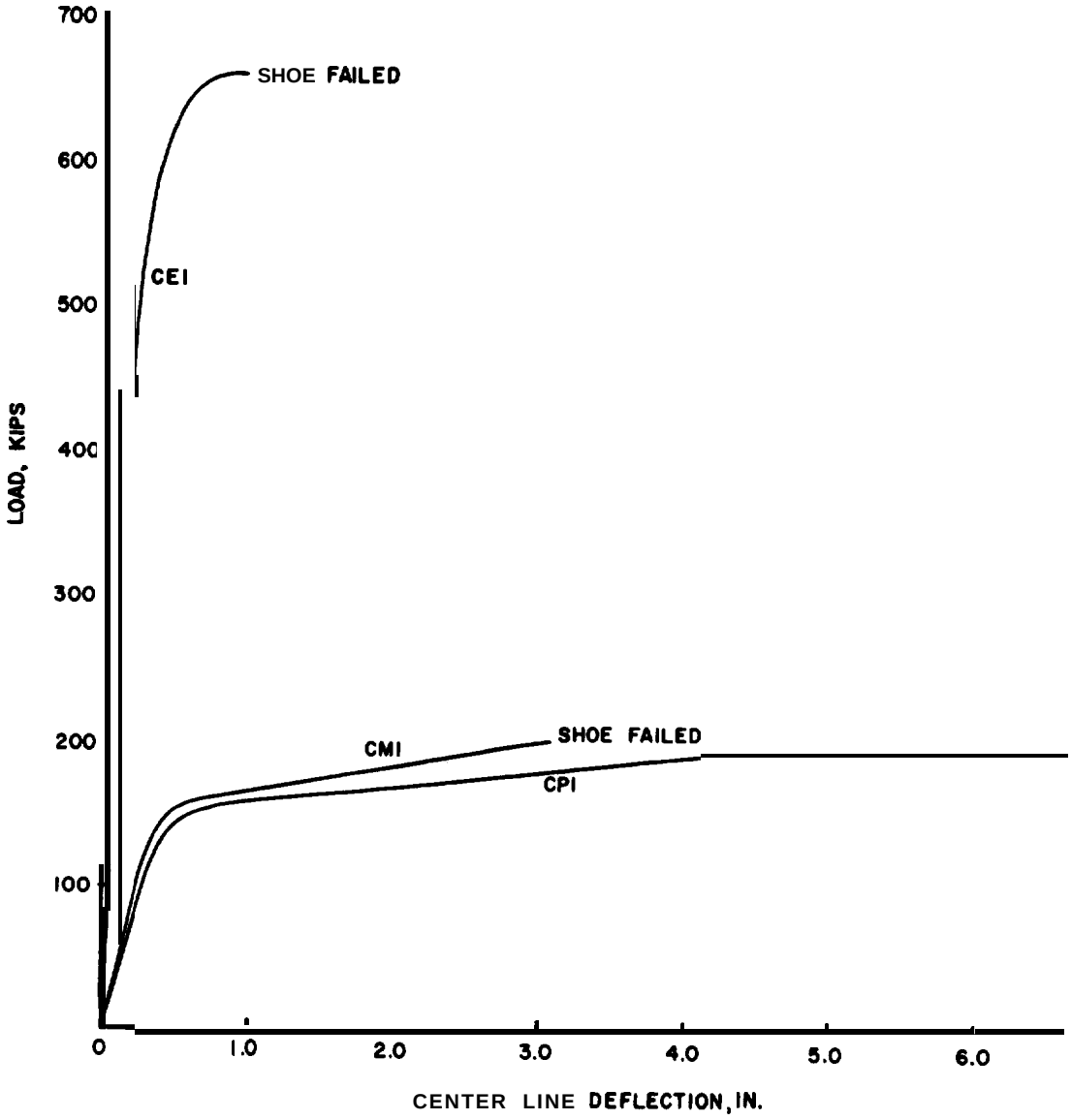

Fig.5.3 Load-Deflection Curves for Beam Strips

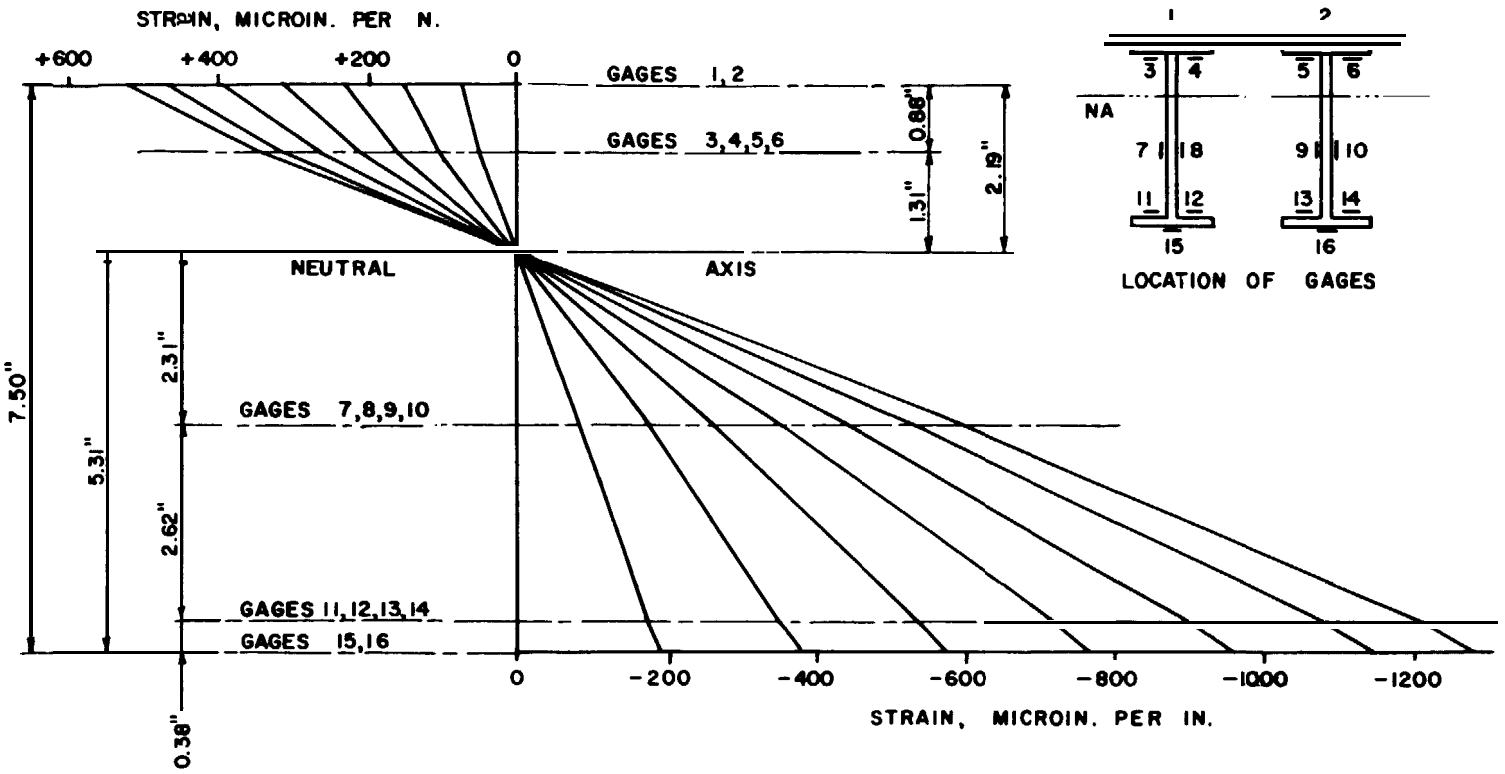

Fig. 5.4 Strain Distribution on Center Cross Section of Beam Strip CP1

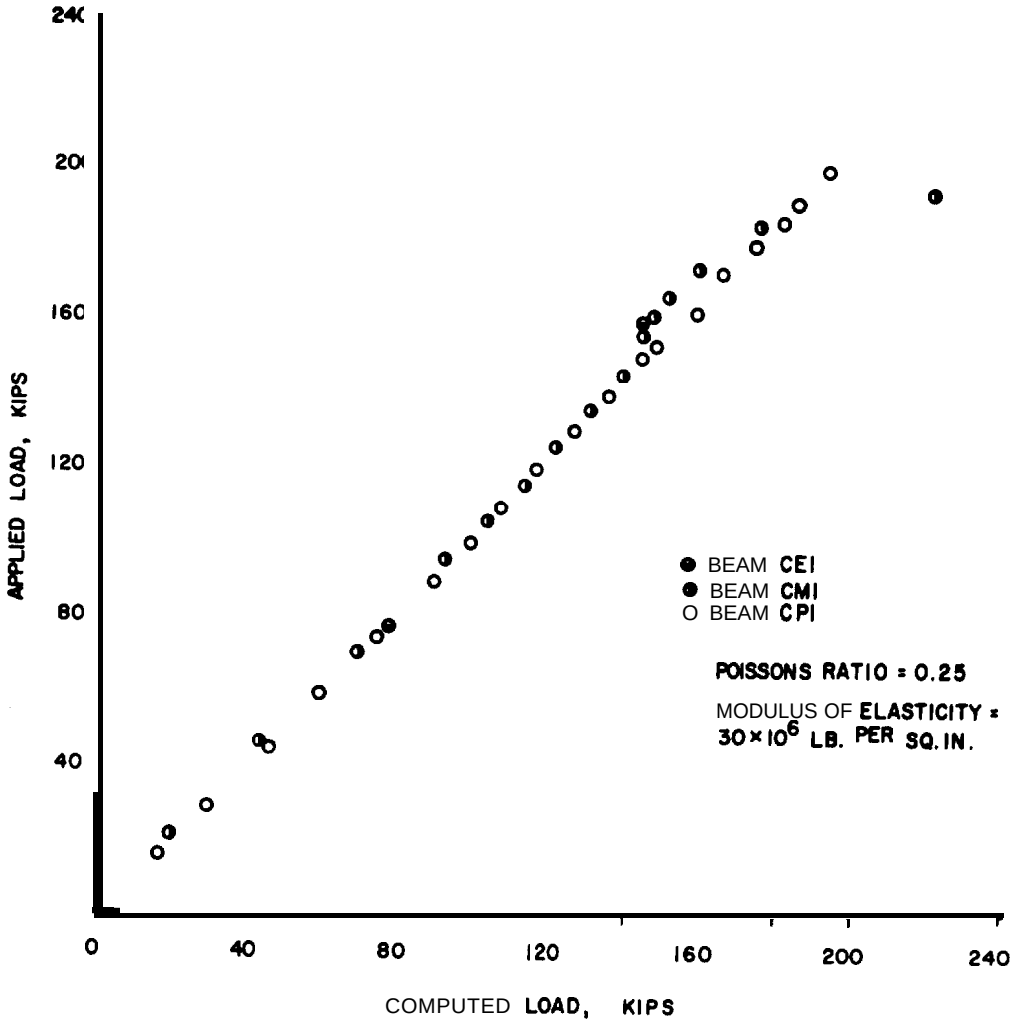

Fig.5.5 Load vs Reaction Indicated by Strain Gages *on* Shoes

CHAPTER 6

CORRELATIONS AND COMPARISONS OF DATA

6.1 PRESSURES ON SURFACE

The air pressures on the ground surface are shown in Figs.3.1 and 3.2 for Shots 9 and 10 respectively. In this chapter only the data for Shot 10 are considered because of instrumentation failures which made correlation with other records impossible for the data of Shot 9. Three records of pressure are plotted in Fig. 3.2. All three gages were located in the same general area and gave similar records. However, because the various other records obtained for Project 3.8 came from BRL, and because of the good correlation among the three ground pressure gages, the BRL record was used for all the comparisons made herein. The BRL ground surface air pressure record is repeated in Fig. 6.1.

6.2 PRESSURES IN FREE EARTH

The pressures recorded by the gages at various depths in free earth are shown in Fig.6.1. The general shapes of the pressure-time curves are similar for all of the depths at which measurements were made. It can be noted that there is a slight lag in the time to reach corresponding points on the curve as the depth increases, indicating the finite time of travel of the pressure wave through the earth. Moreover, there seems to be a reduction in intensity of pressure and a marked reduction in the duration of the positive phase of the pressures, with depth below the surface.

The decrease of pressure with the depth is also indicated by the plot of intensity of peak pressure as a function of depth, shown in Fig. 6.2. The points represent the peak pressures as measured by the gages at the various depths in free earth for this project. There seems to be little difference in pressure from the ground surface to a depth of something over 4 ft, only a slight reduction to a depth of 8 ft, and a large reduction below this depth. Data on the attenuation of free earth pressure with depth were also reported by Mr. W. R. Perret of the Sandia Corporation in UPSHOT-KNOTHOLE Report WT-716. The empirical relation developed in WT-716 for decay in vertical

pressure with depth is shown in Fig. 6.2 for comparison with the experimental data for Project 3.8. *The data are* roughly comparable, although the attenuation at shallow depths differs herein from that given by the empirical relation taken from Report WT-716.

A similar but smaller reduction in pressure with depth is noted for the precursor phase of the pressures in Shot 10, as indicated in Fig. 6.2. Because of the length of this precursor phase, these data can be considered almost as indicative of the effects of a low pressure shot, and the data are therefore useful as a replacement for the missing data for Shot 9.

Although the data are not reliable enough to determine wave velocities, one can note from Fig. 6.1 that the front of the pressure wave appears to travel downward at roughly 1000 ft per sec, but the peak of the pulse travels much more slowly. One can also note that the pulse length appears to become shorter with increasing depth. The latter is also consistent with the data reported in WT-716.

6.3 VERTICAL PRESSURES ON STRUCTURES

6.3.1 Pressures on Top of Beams

The pressures measured at the various points on the surfaces of the beams of the three structures at different depths all had in general the same major characteristics, and these were similar to the pressures at the ground surface. Pressure-time diagrams for the quarter points of the P beam strips, which are typical of all the other records, are shown in Fig. 6.3 for each of the depths. There is a marked oscillation in the record for the 1 ft depth, but this is damped out markedly for the 4 ft depth, and almost completely for the 8 ft depth. The recorded peak pressures are respectively 120, 76 and 59 psi for the 1 ft, 4 ft, and 8 ft depths, but the first value is not reliable. It appears from the curves that the impulse, or area under the pressure-time curve, is almost the same for the three depths. Moreover, if the curves are approximated by triangular pulses, the peak pressures are very nearly the same for all three depths, and are approximately equal to the surface peak pressure of 63 psi. The major difference is in the longer rise time for the deepest structure, which is of the order of 35 millisec., compared with about 6 millisec. for the shallowest structure and about 15 millisec. for the intermediate structure. The positive phase duration for the equivalent triangular pulse is about 125 millisec. for all three depths.

From the data shown in Fig. 6.3 and the similar records for the other pressure gage measurements on top of the beams, the following summary is made:

(1) The arrival time for the pressure pulse is to some extent a function of depth, but the relation is obscured by the fact that the deeper structures *were* closer to ground zero than the shallowest structure, and the pressure actually reached the deepest beams first.

(2) The precursor pulse duration appears to be of the same length for all pressures on all beams.

(3) The time to reach the peak pressure from the beginning of the pulse is between 70 and 80 millisec. for both the 1 ft and 4 ft depths of cover, but is approximately 10 to 20 millisec. longer for the 8 ft cover.

(4) The total positive phase duration is of the order of 250 to 300 millisec. for the two shallower structures, but is about 50 millisec. longer for most of the beams in the deepest structure.

To indicate the possible influence of the differences in rigidity of the beam strips and the differences in depth, there is shown in Fig. 6.4 a comparison of the peak pressures on the various beams of all of the structures which were instrumented. The figure shows the peak pressures in both the precursor phase and the main pulse only for Shot 10. The data recorded indicate a more or less random variation in pressure which shows no correlation with rigidity of the beams on which the gages were mounted, or with the depth of cover. No general conclusions appear possible. It might have been expected that the pressures measured near the supports of the E beams would show the greatest peaks, because of the reflection of the pressure from the more rigid surface. However, the differences in measured pressures could not in general be attributed to the differences in stiffness of the elements to which the pressure gages were attached, except possibly in the precursor phase, and even here the evidence is not striking. The same phenomena were noted for Shot 9 as for the precursor of Shot 10.

In contrast to the situation in free earth, it appears that the pressure is transmitted through the earth to structural elements without substantial reduction; or alternatively if there is any attenuation, it is recovered by a reflection of the pressures from the beams. In effect, the beams appear to be subjected to pressure pulses of about the same intensity as the pressure pulse applied to the ground surface. No explanation can be offered for the difference between the pressure variation with depth as measured by the gages in free earth and that as measured by the gages mounted on the top surface of the beam strips. The accuracy of the latter readings is attested to by their general consistency with other measures of forces acting on the beams, namely the beam reactions, deflections, and strains. Nevertheless, among all these quantities, the pressure gages showed the greatest variations and appeared to be the least reliable. No other types of data are available for correlation with the readings of the gages in free earth. It is possible that such gages give inaccurate results because of their construction and the way in which they must be set in place. On the other hand, with regard to attenuation, the data reported herein even for gages in free earth do not show *any* appreciable attenuation for depths of 4 ft *or* less. But 4 ft is still several times the size of the pressure gage. It is not unreasonable that there should be no attenuation of pressure on a structure of a span of 8 ft until a depth of cover of several times this span is reached.

The matter of a possible reflection of pressure from the top of the structures cannot be settled from these data. There is no

physical reason to expect an increased reflection as a function of depth only, in a manner different in the structures from that on the gages used to measure free earth pressures. Yet if one assumes attenuation of the vertical stress with travel through the earth, in order to explain the free earth pressure measurements, then increased reflection coefficients with depth are required to explain the measured pressures and other phenomena for the beam strips in the roofs of the test chambers. However, the shapes of the pressure-time curves do not seem to indicate a reflection.

In an elastic medium loaded at a free surface, where there is a rigid immovable surface at some depth, there should be a reflection involving a doubling of the pressure at each instant at the rigid surface, and this doubling should last for a time equal to that for the reflected wave to travel to the surface and back again to the rigid surface, but the second time as a tensile wave because of the condition at the free surface. The latter wave is combined with the free surface loading existing at the time the wave gets to the free surface.

The data in Figs. 6.3 and 6.4 do not support a contention that there were pressure spikes lasting roughly twice the travel time to the free surface, of magnitude equal to twice the incident pressures. There was erratic variation in the pressures, but no indication of a systematic reflection.

One should expect a reflection in a rigidly supported element which, because of the rigid support, does not deform as the surrounding medium when a pressure wave strikes it. However, the structures move bodily in about the same way as the surrounding soil, because the net density of the structures is nearly the same as (actually slightly less than) the surrounding soil. Moreover, the roof beams are in no case perfectly rigid, but deform even in the case of the elastic beam strips, and this deformation takes place rapidly because of the short period of the beams themselves. Therefore one should not expect any material reflection phenomena in these structures, nor in general for underground structures subjected to vertical pressures arising from air blast.

It is entirely possible that a true shock wave with a steep front, in earth, may show a reflection phenomenon when it strikes an object of greater rigidity than the earth. However, a pressure pulse with a slow rise may not indicate a similar phenomenon, because of the relative properties of the structure and the earth. In any case, there is no evidence from these tests of any of the following: (1) attenuation of pressures on the structures with depth; (2) arching with consequent relief of pressures near the center and increase in pressure near the supports, in the main shock of Shot 10 (although there are indications of arching in Shot 9 and the precursor of Shot 10);(3) differences in effect of roof flexibility, *or* of a reflection phenomenon from the roof of the test chambers.

With regard to attenuation of peak pressure with depth, the data in Fig. 6.4 *are* particularly important. On the whole, there is no evidence of a reduced peak pressure from the reliable gage

readings, as a function of depth. Whether structures buried more deeply would show a decreased pressure is another question which the present data cannot answer. It should be pointed out again that all of the measures of structural response, including beam reactions, beam deflections, and beam strains, give results consistent with the pressure measurements on the tops of the beams. There may well be an attenuation of pressure with depth in free earth. There is no reasonable way of interpreting the data on the structures to indicate an attenuation of pressure on the structures with depth, at least up to a depth of cover equal to the span of the structure.

6.3.2 Pressures on Base of Structures

The pressures on the bottom of the structures, measured by the gages embedded in the floor, also were similar to the pressures measured at the ground surface except for a difference in magnitude. The base pressure curve obtained for Structure 3.8b is shown in Fig.6.5. It is noted that the magnitude of the pressure on the base was about 3/4 the pressure on the ground surface. For Structure 3.8a it was about half this much, if the record is reliable. The time rate of variation of the pressures on the base was similar to those on the roofs of the structures, but with a somewhat longer rise time to the maximum value.

The differences in dynamic pressures at the top and under the bottom of the test chambers produce accelerations of the test chamber. If the roof and the floor of the structure were rigid, these accelerations could be computed directly from the pressures and the mass of the structure. However, because of the flexibility of the roof, even though the floor is fairly rigid, this calculation cannot be performed accurately by a direct method. It is necessary to use instead the reactions of the beam strips on the concrete test chambers, which differ from the static reactions corresponding to the roof beam loading because of the time it takes for the beam strips to respond to the roof pressures. Ordinarily, if the pressures were instantaneous in their application there would be large discrepancies between the reactions and the instantaneous pressures on the roof beam strips. However, because of the relatively slow rise in the pressure the measured reactions are approximated fairly well by the equivalent static reactions for the loadings applied to the beam strips of the roof. Therefore, it should be possible to compute the accelerations of the entire structure from the differences in the pressures applied to the top and bottom surfaces. (This approach neglects any influence of dynamic shearing forces applied to the sides of the structure, which are probably very small.) Because of the uncertainties in the pressure-time curves, the instantaneous values of acceleration computed in this way have no resemblance to the recorded acceleration curves. An approximate calculation of maximum acceleration can be made, however.

The total weight of the test chamber is less than the weight of the soil displaced by the chamber. The effective density of the test

chamber is, on the average, 77.5 lb per cu ft or approximately 69 per cent of the density of the displaced soil. The differences in forces on the top and bottom surfaces at corresponding times, divided by the mass, gives the acceleration of the test chamber at each instant. To compare the order of magnitude only, one can compute the maximum acceleration from the maximum values of the forces applied and the mass of the test chamber. Summaries of the maximum forces are tabulated in Table 6.1. The calculations made with these entries are described in the discussion of the computed and measured accelerations contained in Section 6.5.

6.4 HORIZONTAL PRESSURES ON STRUCTURES

The horizontal pressures on the vertical walls at the ends of the test chambers were measured at a number of points. The general nature of the measurements is indicated by the typical curve plotted in Fig. 6.6 for Structure 3.8a. In general, all of the side pressures have the same general shape and show a remarkable consistency in pattern. The peak values were relatively small. A tabulation of the peak pressures on the sides of the chambers, in both the precursor phase and in the main blast pulse of the shock in Shot 10 is given in Table 6.2. The ratio of the horizontal pressures to the vertical ground pressures ranged from 13 per cent to 25 per cent for the precursor, and from 11 per cent to 16 per cent for the main shock. These data are consistent with the data reported in WT-716, and give consistent indications that in this type of soil, at least, the horizontal pressures induced in the earth by air shock do not reach high magnitudes compared with the vertical pressures.

6.5 MOTION OF ENTIRE STRUCTURE

Acceleration measurements were made on all of the structures in order that the motion of the structure as a whole could be determined and taken into account if it proved necessary. The measurements were not as dependable as the other measurements which were made, judging from discrepancies between records that should have been the same, and between two reproductions of one of the records for acceleration in Structure 3.8b.

Measurements of transient accelerations obtained by the electronic gages and those obtained with the ERA accelerometers appeared to correlate fairly well although the time scales between the two types of instruments did not correlate as well as the maximum values of acceleration. An acceleration record is shown in Fig. 6.7 for Structure 3.8a. Corresponding curves for Structure 3.8b did not appear to be dependable after a rerun of this acceleration record was obtained.

In order to obtain a measure of the maximum velocity and displacement of the concrete test chambers, integrations were performed on the acceleration records originally obtained. Although these records were made obsolete by the rerun records furnished later, the results are indicative of the order of magnitude of the transient

motions, and are reported in Table 6.1 for that purpose only.

As another indication of the adequacy of the acceleration readings for the purpose of defining the transient motions, a further check of maximum accelerations was made by computing the acceleration corresponding to the maximum unbalanced force on the chambers, divided by the mass of the structure. For this calculation, the downward forces arising from the beam strip reactions are summarized in Table *6.3* for use in the calculations shown in Table *6.1.* Where the air pressures at the ground surface were used, the mass considered was that of the structure and the earth above it. The values reported in Table 6.1 appear reasonable. Unfortunately no more reliable values *can* be *given* as adequate records of forces at the top, forces at the bottom, and accelerations of the test chamber, do not exist for any one structure although good records for some of these data are available for different structures.

The permanent deflections of the structures and of the earth surface were determined relative to bench marks located as shown in Fig. 2.10. There was no relative permanent deformation of the bench marks at different elevations, nor of the bench mark at the surface relative to the datum points underground. There was some small permanent deflection in the structures themselves relative to these bench marks. With some allowance for the errors inherent in the survey measurements the permanent displacements were determined as approximately 0.25 in. upward for Structure 3.8a, and less than 0.05 in. downward for the two deeper structures.

6.6 POSSIBLE EFFECT OF TYPE OF SOIL

Many of the phenomena discussed in this chapter are dependent on the characteristics of the soil. Certainly the material either in its natural state or as remolded in the backfill differs from other soils such as sand or clay. One would expect the amount of arching to increase with the shearing strength, in general. Since the strength of the backfill material was quite high, it was expected that a maximum arching effect would be obtained in this experiment. Because no significant arching was noted, it is reasonable to assume that for most other soil types there would be no dynamic arching either, at least up to the depth-span ratios used in these tests.

With regard to the differences in strength of the backfill and the surrounding natural deposit, it is likely that these differences were not as great after Shot 9 *as* is indicated by the tests of samples reported in Chapter 2. The presence of shrinkage cracks and of fissures induced by the blast would make the backfill have more nearly the same properties as the original natural soil. Moreover, because of the way in which the backfill was placed, the structures should act as if they were placed in a deposit having properties throughout the same as those of the backfill. The flaring out of the backfill from the structure was chosen so as to avoid having planes of shear failure or of relative soil motion intersect the natural soil. The earth pressures on the beam strips and the other measures of force

TABLE 6.1 - Base Pressures and Peak Accelerations for Test Chambers

Quantity	Structur		
	3.8a	3.8b	3.8c
Peak Air Pressure at Ground - Shot 10, psi	63	63	63
Max. Pressure Top of Beams Ave.* for Shot 10, psi	62	61	63
Pressure Corr. to Max. Reactions Ave. for Shot 10, psi	69	85	72
Peak Base Pressure - Shot 10, psi	24	47	
Approx. Max. Acceleration, g.			
from Ground Pressure, incl. Earth Mass and Struct.Mass	7.5	2.1	
from Beam Pressure and Struct. Mass only	8.6	3.1	
from Reactions and Struct. Mass only	10.1	8.6	
Max. Meas. Accel., g	7.6	6-10**	1.0
Max. Accel. in Obsolete Record, g	8.3	5.9	
Calc. Max. Veloc., ft per sec.	4	3	
Calc. Max. Displ., in.	2.1	2.5	

* Ave. for all values not beyond calibration range.

** Peak greater than 10g on rerun, but nearly 6g on original record.

TABLE 6.2 - Values of Peak Side Pressures on Test Chambers

Structure	Gage No.	Depth Gage below surf., ft.	Peak Reading, psi	
			Precursor Shot 10	Main Shock Shot 10
3.8a	E7	3.0	2	10
	E8	5.75	2	7
	E9	8.5	0	10
3.8c	E6	11.75	4	8

transmitted to the beam strips indicated that this experiment design was successful, and that over the whole surface of the structures there was no net arching, either positive or negative.

With regard to the horizontal pressures on the vertical surfaces, one would expect these to be nearly equal to the vertical pressures in a medium behaving much like a fluid, or in a saturated soil. They would be expected to be of the order of half the vertical pressures in a cohesionless material such as sand. The actual measured horizontal pressures were very low in this test. However, it is not considered safe to expect that they would always be so low in other types of soil.

TABLE 6.3 - Average Shoe Reactions on Beam Strips

Struct.	Beam Strip	Shoe	Max. Meas. or Computed Values - Shot 10		
			Strain microin. per in.	Reaction, kips	Equiv. Static Press., psi
3.8a	1P3	Fixed	370	76	69
		Exp	460	102	93
	1M2	Fixed	240	44	42
		Exp	370	80	76
	1E2	Fixed	60*	*	*
		Exp	250	78	65
	Ave.				69
3.8b	4P3	Fixed	450	92	84
		Exp	440	97	88
	4M2	Fixed	50*	*	*
		Exp	400	85	81
	4E2	Fixed	280	103	86
		Exp			
	Ave.				85
3.8c	8P3	Fixed	510	103	94
		Exp	400	83	75
	8M2	Fixed	380	80	76
		Exp	260	56	53
	8E2	Fixed	70*	*	*
		Exp	230	72	60
	Ave.				72

* Poor records, not used in averages.

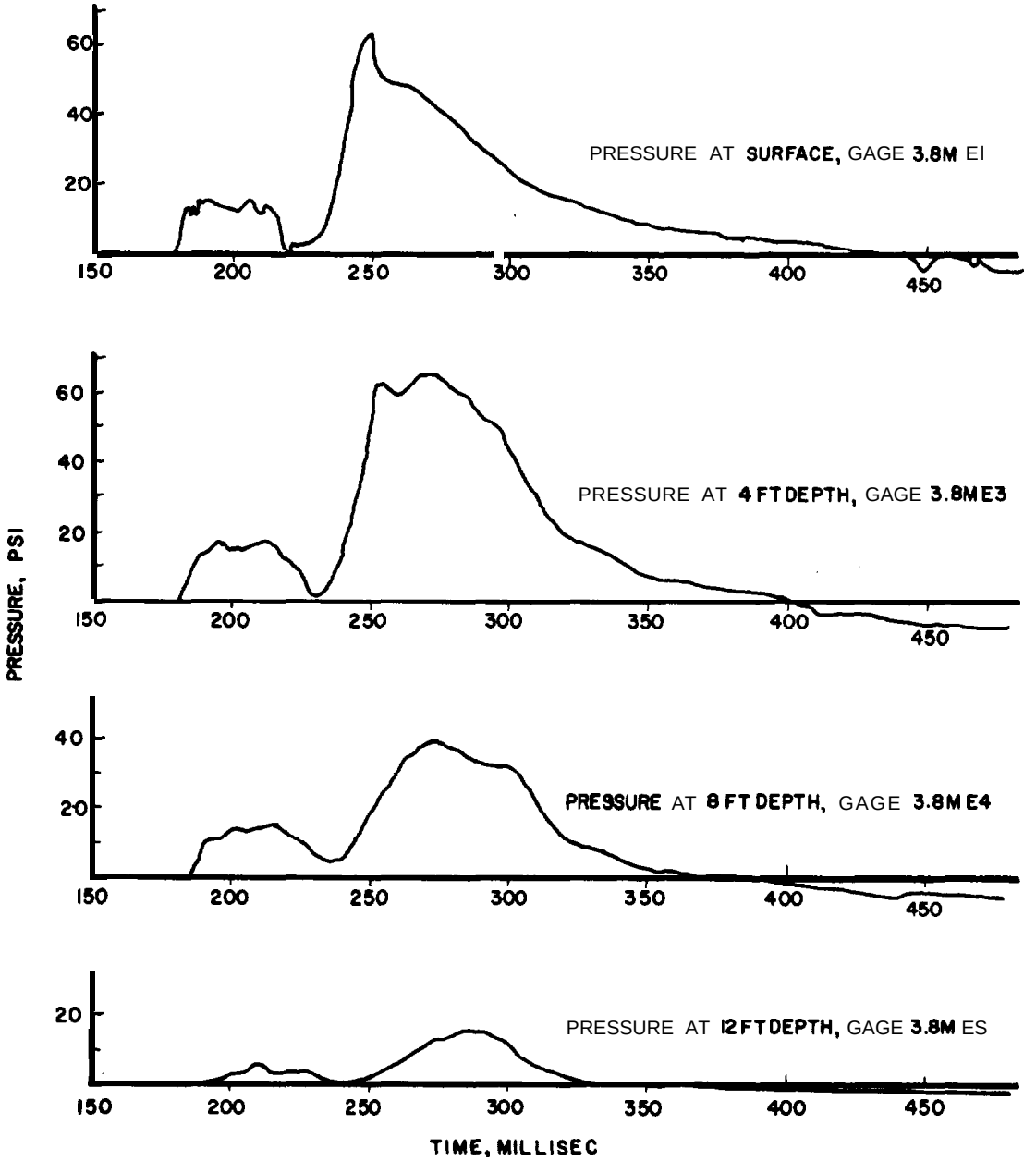

Fig.6.1 Pressures in Free Earth

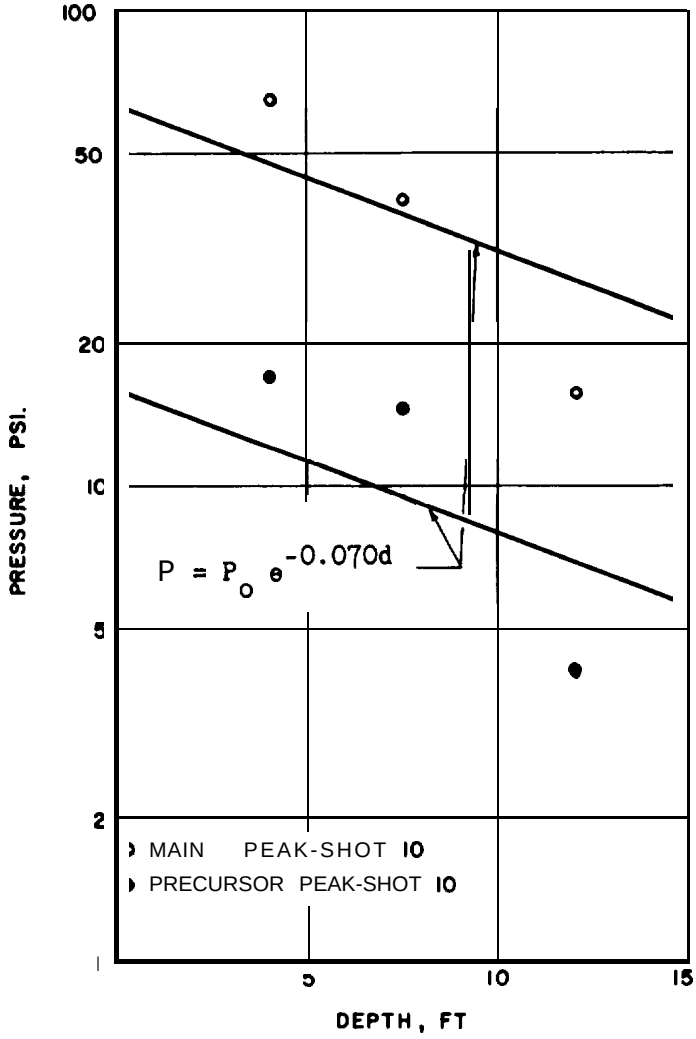

Fig.6.2 Variation of Peak Pressure with Depth

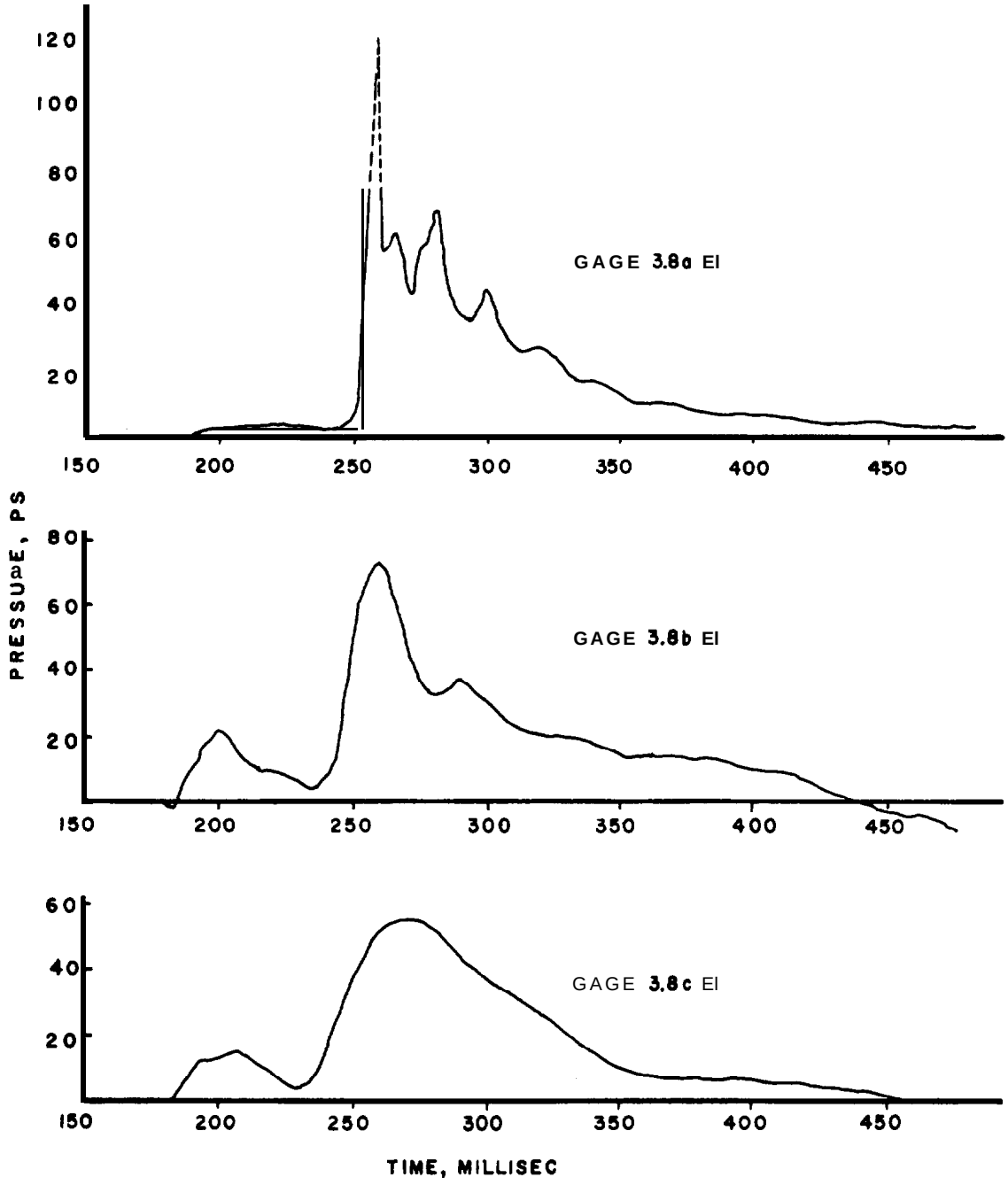

Fig.6.3 Pressures on Beam Strips at Quarter-Point of P Beams

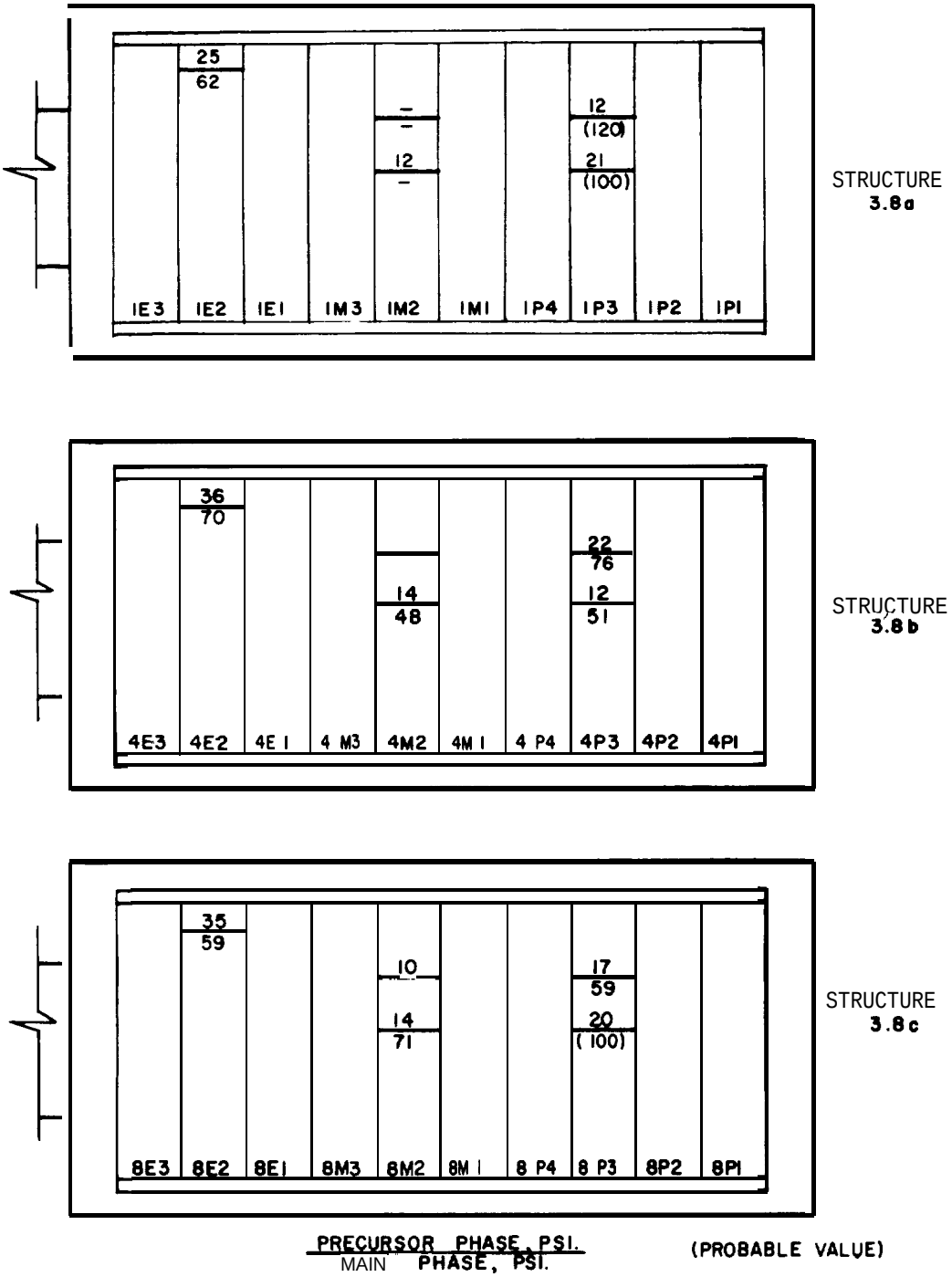

Fig.6.4 Comparison of Peak Pressures on Beams

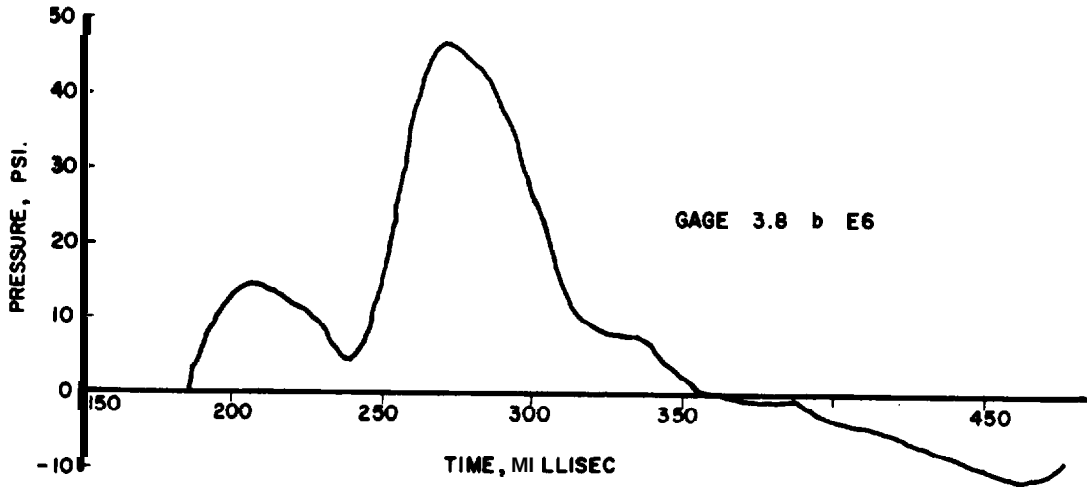

Fig.6.5 Base Pressure on Structure 3.8b

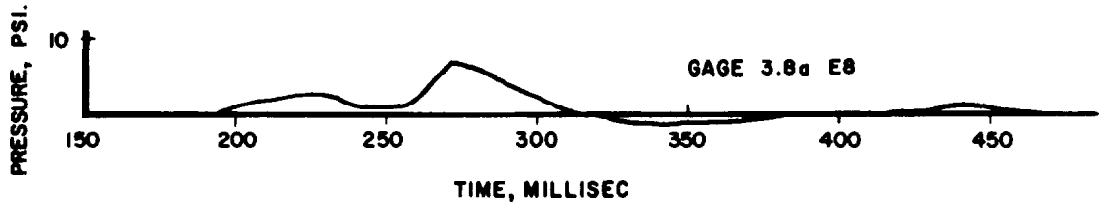

Fig. 6.6 Side Pressure on Structure 3.8a

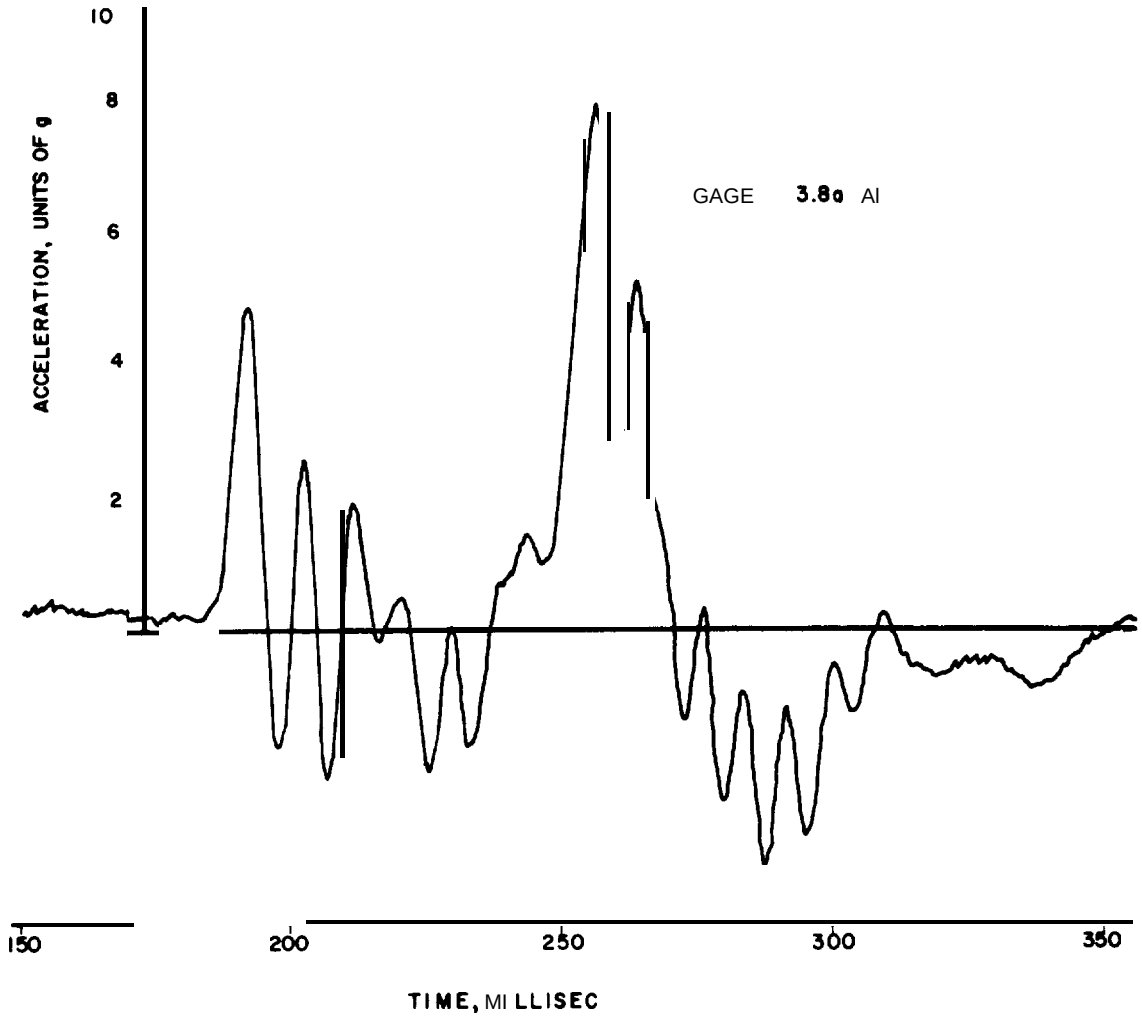

Fig.6.7 Acceleration Record on Structure 3.8a

CHAPTER 7

BEAM STRIPS

7.1 STRAINS IN BEAM STRIPS

7.1.1 General Discussion

Transient strains were measured in the beam strips by means of gages located on the top of the lower flange, and on the bottom of the top flange of the beam sections, at locations described in Chapter 2. Typical records of strain are shown in Fig. 7.1, which gives the strain in the top flange of Beam Strips 1P3 and 8P3 for Shot 10. The strains in the bottom flanges went beyond the yield point. The vibration in Beam 1P3 is evident. Otherwise the curves are quite similar.

Because of the short period of vibration of the beams (5 to 11 millisec.), the response to a dynamic pressure is quite rapid and the strains in the beams, therefore, reflect quite well the shape of the loading curve on the surface of the beams. Since these are also similar in shape to the ground surface loading, the beam strains are similar in general characteristics to the external loading. Because of the similarities, it is not necessary to present in detail all the strain-time curves obtained in the test. For convenience in reference, however, the maximum transient strains recorded for each part of each test beam are given in Table 7.1 for all instances where reliable records were obtained. Because the strains were relatively small, only the values of strain for the main pulse in Shot 10 are included in Table 7.1. The designations near and far refer to the location of the two beams of the pair making up the beam strip, with respect to the entrance to the test chamber.

In this section the measured strains are discussed primarily in terms of their correlation with other quantities. One of these possible correlations is with the deflections. There are a number of different ways in which the deflections can be computed from the various other measured quantities. All of the various methods lead to results which are compared later in Section 7.3 of this chapter. The determination of deflections from strain involves in part a determination of the strain distribution over the cross section, or an estimate

of the location of the neutral axis in the beam. Therefore, consideration is given to this relationship in this section of the report.

Attempts to determine the initiation of yielding from the measured strains are not too fruitful, but a record of the results is also included in this section.

7.1.2 Location of Neutral Axis

Because strains were measured only near the top and bottom of the beam cross-section, the distribution of strain on the cross-section could only be inferred by assuming a linear distribution between the two points at which measurements were taken. The position of the neutral axis can be computed from the maximum transient strains, recorded in Table 7.1, assuming (as was evident from the records) that the maximum strains in the upper and lower flanges occurred at the same time. By a linear interpolation between the recorded strains, the values obtained for the neutral axis location are reported in Table 7.2. The theoretical values of the neutral axis location, taken from Table 2.1, *are also* indicated in Table 7.2 for comparison. It appears that the neutral axis location is reasonably close to the theoretical position. In several cases only the strain in one flange was available, and the calculation of the neutral axis position could not be attempted. In view of the nature of the results, it was decided to use in all cases the theoretical position of the neutral axis in determining curvatures from strains and in the consequent determination of deflections from strains. This approach permitted the strains to be used in every case where even one record existed, and perhaps was as accurate as the *use* of the actual measured position of the neutral axis as determined by the strain measurements because of the fact that the strain distribution may not have been completely linear over the cross-section.

7.1.3 Correlation with Pressures on Top of Beams

As an indication of the relationship between strains and pressures on the top of the beams, the maximum strains recorded in Table 7.1 can be converted to corresponding equivalent peak pressures, acting statically on the surface of the beam. This correspondence is not unreasonable because of the fact that the period of the beam is so short that it can be considered to respond almost instantaneously to the pressure curve on top of the beam. The pressures so calculated are recorded in Table 7.3 and are useful in comparing that table with the measured peak pressures at the beam surface shown in Fig. 6.4. The agreement is reasonably close for the values determined from bottom flange strains. The discrepancies are a measure of the lack of reliability of the measurements either of strain or of pressure. However, no criterion is available to decide which of the measurements is more reliable.

7.1.4 Yielding in Beam Strips

Because of various reasons involving to a minor degree the precursor, the slow rise of the pressure, and the short duration of the *main* pressure pulse, and to a major degree because the plastic beam strips had relatively a much higher yield strength than the other beam strips, the magnitude of yielding in the beam strips was much less than was expected for the pressures which were recorded. However, there was evidence of yielding in the plastic beam strips and in the intermediate beam strips. The presence of such yielding can be inferred from the presence of permanent strains. The transient records of strain in the beams are not reliable as a measure of permanent strain. However, survey measurements of permanent strain were made with two different types of strain gage, and the values obtained from these measurements can be used as an indication of permanent deformation and consequently of yielding. The results of the permanent strain measurements with both the mechanical direct reading gage and the Whittemore gage are recorded in Table 7.4. The Whittemore gage readings are the most reliable in the range of strains noted, and therefore all further use of the data is based on these readings. There is only general qualitative agreement between these two measures of permanent strain, but there is positive evidence of yielding in all of the plastic beam strips and in at least one of the intermediate beam strips.

Because of the fact that the recovery from the maximum transient strain to the permanent strain is presumably elastic unless there is a reversal in direction of loading on the beam, the dynamic yield point can be inferred approximately from the difference between the strains recorded in Table 7.1 and in Table 7.4. Since these were measured on different sides of the flanges, the former values have to be extrapolated to the extreme fiber.

The best estimates of the yield stress computed from the recovery in strain are given in Table 7.5. Some of the values in this table are questionable and are so indicated. The evidence appears to be that yielding occurred at stresses of the order of 50,000 to 70,000 psi in the various beams. This is not greatly higher than the values reported in Table 5.2 for the stresses at which appreciable yielding is noticed, and the difference is consistent with the effect of rate of straining.

7.2 REACTIONS

The reactions measured on the beam strips as determined by the strains in the shoes supporting the beam strips were in general consistent with the other data. A typical record of reaction is shown in Fig. 7.2 for the expansion shoe of Beam Strip 8P3. The record is similar to the other quantities measured. The maximum intensity of reaction determined from the dynamic records is shown in Table 6.3 for Shot 10.

Although the reaction on the beam is not directly related to the

instantaneous value of the load on the beam, because of the nature of the loading curve and because of the high frequency of vibration of the beam, the maximum reactions recorded should show a reasonably good correlation with the maximum values of pressures on the surface of the beams. The effective pressures determined from the reactions, corresponding to the static pressure intensity on the surface of the beams required to give the measured reaction, are repeated in Table 7.6 from Table 6.3. *These* values are compared in Table 7.6 with the maximum values of pressure on the beam as given in Fig.6.4. There is a reasonably good agreement.

It should be noted that the reactions are affected by the deflection of the beam, and the transient reaction cannot be developed without a corresponding deflection having been developed. Therefore the ratio of the equivalent pressures determined from the reactions to the pressures corresponding to the loading is a measure of the dynamic amplification factor for the loading. Moreover, if the beam strips behave plastically, without strain hardening, the maximum reaction that can be developed is a measure of the yield point of the material. Therefore, values of stress in the bottom flanges of the beam strips are computed for the instantaneous values of the reactions in Table 7.6, and are tabulated therein. These values are a measure of the yield point if yielding actually occurs, and may be compared with the values tabulated in Table 7.5. The results agree very well.

7.3 DEFLECTIONS

7.3.1 Measured Values

The dynamic deflections recorded in the test *were* determined by two types of gage. Typical records of the deflections obtained in Shot 10 are shown in Figs.7.3 and 7.4 for the P beams and the M beams in Structures 3.8a and b. In general, the deflections of the beams show the same general characteristics as all of the other measured quantities and appear to correlate very well in shape with the pressures on the beams. The deflections in the shallowest structure show the typical vibrations for all the readings for that structure. The deflections for the deeper structures are smoother.

The maximum transient deflections recorded in the test for Shot 10, for both the precursor and main shock are summarized in Table 7.7, where they are compared among themselves and with deflections computed from other data. There is a discrepancy between the deflections recorded by the two types of deflection gages in the measurements for the M beams where both types were used. The values given by the BRL gage are consistently higher than those given by the linear differential transformer gage. The discrepancy can only be interpreted as indicating that the recorded deflections are subject to errors of as much as 25 per cent. However, other measures of deflection obtained from strains, reactions, and other data, appear to indicate a greater reliability of the linear differential transformer gage. This

means that possibly the deflections recorded by the BRL gages were as much as 25 per cent too large in general.

Permanent deflections were determined from the difference of survey elevation readings made on the beam strips before and after each shot. However, the permanent deflections were so small that they could not be determined accurately by the measuring techniques used. Deflections smaller than 0.03 in. are probably not reliable. In any case, the fact that the permanent strains are relatively small would indicate that the permanent deflections would have to be negligible.

The best values of permanent deflection determined from the survey measurements are given in Table 7.8. Only the P and M beams showed enough permanent deflection to indicate reliably that yielding had been reached. The deflections obtained were sufficiently large to develop almost complete static arching at the centers of the P and M beam strips.

7.3.2 Calculation of Deflection From Strains

There is a direct correspondence between the strains measured in the flanges of the beams and the deflections of the beams. The measured strains correspond to curvatures along the length of the beam. These curvatures in turn correspond to deflections at the center of the beam. If the distribution of moment along the length of the beam, and consequently the distribution of curvature, is known, then the deflections can be computed directly. The discussion of the analysis of the dynamic response of the beams given in Chapter 4 indicates that the shape of the deflection curve is very nearly a sine curve, or also very nearly the same as the shape of the static deflection curve. With this assumption, one can determine directly the deflection for a given measured strain by proportion to the deflection computed for a given theoretical strain corresponding to a particular value of uniform load. With this type of calculation, the deflections can be determined directly and the values so computed are also tabulated in Table 7.7 for comparison with the measured values. The values given are computed using the tabulated values of transient strain in Table 7.1 for either the upper or lower flange or both, and taking into account the theoretical rather than the "actual" position of the neutral axis. The computed values take into account the effect of shear.

7.3.3 Calculation of Deflection From Pressures

The transient deflections determined by measurement can be checked by other means as well. One of the checks that can be made is to compute the deflections from the applied pressures. Pressures were recorded on the surface of the beam strips, and also on the surface of the ground. In the case of the pressures recorded on the surface of the beam strips, the calculations can be made directly, because of the short natural period of the beam and the general character of the pressure curves, by determining the deflections from the instantaneous

values of the maximum pressures. However since the average pressures are so nearly equal to the ground surface pressures, the tabulated values are recorded for a static pressure of 63 psi, assuming in one case elastic behavior of the beam strips, and in another case inelastic action with the relation between load and deflection given by the static test data plotted in Fig.5.3.

As a further measure of the deflections, values are computed for the "static" deflections consistent with the average reaction pressures shown in Table 7.6, based on an assumed elastic behavior of the beam strips, and these are shown in Table 7.7. The deflections should exceed these values if plastic behavior was reached. The results are consistent.

The values of deflection given in Table 7.7 for the precursor phase are interesting. Since the structures were unquestionably elastic in the precursor, and because the loading was very nearly a step pulse of loading, one would expect the responses to be very nearly twice the elastic responses computed for a static load equal to the applied pressure. For most of the recorded deflections the values are almost precisely twice those computed for a 16 psi static pressure, in agreement with the theory.

The computation of the deflections from the pressures recorded on the ground surface must be made by means of a dynamic analysis taking into account the mass of the soil and the properties of the beam strip with the soil acting on it. Calculations were made by numerical procedures taking into account the measured load on the ground surface, the properties of the beam strips, the mass of the soil supported by the beam strips, and considering the beams to behave elastically up to some definite yield point. The pressures used in these calculations are given in Table 7.9. The results of the calculations are shown in Table 7.10. Entries are given in this table assuming elastic behavior of the beam strips in every case, and in some cases assuming plastic deformation occurring at the yield value recorded in the table. For the calculations involving yielding, the beam was assumed to act plastically beyond the yield point with a constant resistance.

A number of assumptions were made for the calculations reported in this table. In the first case, the pressure curve used in the calculation had a peak of only 61 psi because this was the only pressure curve available at the time the calculations were made. The rerun value of the pressure curve arrived too late for the calculations to be redone. Consequently, the data are consistent with values of peak pressures about 3 per cent less than those which appear to be consistent with the latest records available. A 3 per cent increase in yield point together with the same increase in load would leave the deflections virtually unchanged, and consequently the data recorded in Table 7.10 can be used without serious discrepancy in the form in which they are given.

In the tabulated values, two assumptions are made concerning the supports of the beam strips. In the first assumption the supports are assumed rigid and non-deflecting. This corresponds to the

condition where the concrete test chamber does not move during the application of the loading, or more precisely during the time that the beam is reaching its maximum deflection. This assumption is not entirely valid but is almost correct in view of the small corrections due to the accelerations which were experienced by the concrete test chamber. However, in the case where acceleration records were available, and where these appeared to be reasonable in value, corrections were made taking into account the effect of the movement of the supports. This calculation was made by a numerical procedure, using the measured acceleration curves and considering that the supports of the beams moved in accordance with these accelerations at the same time that the pressures were acting on the surfaces of the beams. The calculations differ somewhat from and in general are less than those computed on the basis of rigid supports. The acceleration records used were not available in accurate form at the time the calculations were made. The maximum values of acceleration used are recorded to indicate the qualitative applicability of the data to the problem. However, because the time scale, as well as the scale of ordinates for the acceleration curves, is not accurate, possibly the numerical results are not dependable quantitatively for the condition of moving supports.

In each of the entries for the plastic and the intermediate beam strips, the calculations are given assuming that the beams remained elastic, and the maximum recorded stresses are tabulated on the basis of this assumption. Calculations are also given assuming plastic behavior of the beam strips with yield stresses of both 50,000 and 55,000 psi in the case of the plastic beam strips, and 40,000 and 50,000 psi in the case of the intermediate beam strips.

It is interesting to note that the calculations indicate a greater deflection with depth in the case of the plastic beam strips. Because of the increase in dead load, the increment in yield resistance available to resist dynamic loads is smaller for the beams that are buried more deeply. The nature of the measured results, however, indicates that possibly there was some absorption of energy in the deeper cover, because the deflections did not increase with depth.

7.3.4 Significance of Yield Point of Material

A comparison of the deflections recorded in Table 7.7 and 7.10 indicates that the values computed from the time-pressure curve for the ground surface agree quite well with the measured deflections.

This agreement is best if a yield point of the order of 55,000 psi is used for the plastic beams, and a yield point of approximately 40,000 is used *for* the intermediate beams. These yield points are greater than the indicated yield points of the flange material in the beams determined by laboratory tests, and reported in Chapter 5. The laboratory tests indicated flange yield points of the order of 45,000 and 39,000, respectively, for the plastic and the intermediate beams. However, the beam strip static tests reported in Table 5.2 indicated yield points of the order of 45,000 and 33,000 psi for initial

yielding of the material. The load deflection curve at this magnitude of stress was still substantially a straight line as indicated by Fig. 5.3. The knee of the load deflection curve, corresponding to the laboratory test data, for both of these beams occurs in the neighborhood of a load of 150 kips which corresponds to an equivalent uniform pressure respectively of 71.0 and 74.5 psi over the surface of the full width of the beam strips. These pressures correspond to effective yield points of the material of approximately 59,000 psi and 45,000 psi. The later values are in substantial agreement with the values for which the calculations reported in Table 7.10 give the best agreement with the measured deflections. However these values are

TABLE 7.1 - Maximum Transient Strains in Beams, Main Shock, Shot 10 Only

Struct	Beam of Pair	Strains in Flanges of Beam Strips, microin. per in.					
		P		M		E	
		top	bottom	top	bottom	top	bottom
3.8a	far	480	----	190	510	100	340
	near	630	2040	380	2620	---	---
	Ave.	560	2040	290	1570	100	340
3.8b	far	---	----	---	----	150	380
	near	---	4020	350	2080	---	---
	Ave.	---	4020	350	2080	150	380
3.8c	far	440	2000*	280	1280	130	40*
	near	690	4530*	380	1570	---	---
	Ave.	570	3270*	330	1430	130	40*

* Value uncertain.

TABLE 7.2 - Locations of Neutral Axis From Measured Strains

Struct.	Beam Strip	Dist. Neutral Axis to Bottom Fiber, in.	
		From Max. Strains Table 7.1	From Theo. Props. of Section
3.8a	P	5.20	5.31
	M	6.47	5.83
	E	11..26	9.71
3.8b	P	-----	5.31
	M	6.55	5.83
	E	10.48	9.71
3.8c	P	5.71	5.31
	M	6.24	5.83
	E	-----	9.71

TABLE 7.3 - Pressures Computed From Measured Strains

Struct.	Beam Strip	For Ext. Fiber, Top Flange: strain, microin. per in.	stress, ksi	pressure, psi	For Ext. Fiber, Bot. Flange: strain, microin. per in.	stress, ksi	pressure, psi
3.8a	P	930	27.9	81.6	2190	*	----
	M	445	13.3	47.9	1690	50.6	83.6
	E	119	3.6	32.8	364	10.9	59.2
3.8b	P	---	----	----	4320	*	----
	M	537	16.1	57.9	2250	*	----
	E	178	5.3	48.4	406	12.2	66.2
3.8c	P	946	28.4	83.0	3510	*	----
	M	507	15.2	54.7	1540	46.2	76.3
	E	154	4.6	42.0	----	----	----

Notes: Strains extrapolated to extreme fiber from data in Table 7.1, using theoretical position of neutral axis.
Stress computed with $E = 30 \times 10^6$ psi.
* Designates stress above yield point.
Pressures computed assuming elastic behavior.

TABLE 7.4 - Permanent Strains From Whittemore and Direct Reading Gages

Struct.	Beam Strip	Beam of Pair	Perm. Strain, Bot. Flange, microin. per in.: Whittemore rt.	Whittemore left	Whittemore ave.	Direct Rdg. rt.	Direct Rdg. left	Direct Rdg. ave.
3.8a	P	far	1100	1050	1075	1000	*	1000
		near	-150	-100	-125	0	-500	-500
	M	far	-100	**	-100	500	**	500
		near	-750	**	-750	-500	**	-500
3.8b	P	far	1400	2250	1825	2500	2500	2500
		near	3400	650	2025	3000	-1000	1000
	M	far	1500	**	1500	4000	**	4000
		near	350	**	350	-1000	**	-1000
3.8c	P	far	2200	-350	925	500	500	500
		near	1100	1200	1150	2500	2000	2250
	M	far	50	**	50	500	**	500
		near	-100	**	-100	1000	**	1000

* Reading obviously unreliable.

** Only one reading taken along c.l. of flange.

less than the yield points indicated by recovery of strain, in Table 7.5, or from measured reactions in Table 7.6.

It maybe inferred that the yield points recorded in the field are modified from the actual yield values of the material to the extent of corresponding more accurately to the load deflection curve obtained by static test, which may be the same in effect as a dynamic increment in yield point. These two phenomena may occur more or less independently, however. There may be an actual increase of the order of 25 per cent in the yield point under the conditions of speed of loading in the field tests. This increase in yield point may however be effective only for a very short time and the beams would act as if the load-deflection curves under dynamic conditions were substantially the same as those under the laboratory test conditions, with the exception that the curves would rise somewhat more linearly to the yield values and would then bend over much more abruptly but would follow about the same trend from that point on. In any case, the effective yield points obtained from the calculations are not inconsistent with those which can be attributed to the difference between the maximum transient strain and the permanent strain, if proper allowance is made for inaccuracies in the recorded data.

TABLE 7.5- Estimated Dynamic Yield Strengths
Computed From Recovery in Strains

Struct.	Beam Strip	Beam of Pair	Strains, Bot. Flange, microin. per in.			Min. value yield point ksi
			Max.* transient	Perm. set	Recovery Strain	
3.8a	P	far	----	1075	----	----
		near	2190	-125	2315	69.5
	M	far	550	-100	650	19.5
		near	2830	-750	3580	**
3.8b	P	far	----	1825	----	----
		near	4320	2025	2295	68.9
	M	far	----	1500	----	----
		near	2250	350	1900	57.0
3.8c	P	far	2150	925	1225	36.8
		near	4870**	1150	3720	**
	M	far	1380	50	1330	39.9
		near	1690	-100	1790	53.7

* Values extrapolated to extreme fiber from data in Table 7.1, using theoretical position of neutral axis.

** Value obviously unreliable.

TABLE 7.6 - Maximum Dynamic Reactions on Beam Strips and Corresponding Loads

Structure	Beam Strip	React. Press. from Table 6.3, psi			Press. from Fig. 6.4, psi			Bot. Flange Stress, ksi, Elastic Action		
		Fixed End	Exp. End	Ave.	at c.l.	at q.p.	Ave.	For React. Press.	For Ave. React. Press.	For 63 psi Load
3.8a	P	69	93	81	(100)*	(120)*	--	67.3	57.4	52.4
	M	42	76	59	---	---	--	35.7	41.8	38.2
	E	--	65	65		62**	62	12.0	12.7	11.6
Ave. (wt'd)				69			62			
3.8b	P	84	88	86	51	76	64	71.5	70.6	52.4
	M	--	81	81	48	---	48	49.1	51.5	38.2
	E	86	--	86		70**	70	15.8	15.7	11.6
Ave. (wt'd)				85			61			
3.8c	P	94	75	85	(100)*	59	59	70.6	59.8	52.4
	M	76	53	65	71	---	71	39.4	43.6	38.2
	E	--	60	60		59**	59	11.0	11.1	11.6
Ave. (wt'd)				72			63			

* Values in parentheses beyond calibration range, not used in averages.

** Measurements made near support.

TABLE 7.7 - Maximum Values of Transient Deflection Determined by Various Means

Item	Deflection of Beam Strip, in.								
	1P3	4P3	8P3	1M2	4M2	8M2	1E2	4E2	8E2
Precursor - Shot 10									
Meas. by BRL Gage	0.23	0.17	0.18	0.23	0.14	0.11			
Meas. by Lin. Diff. Transf. Gage				0.08	0.08	0.09	0.02	0.02	-----
Comp. for 16 psi Static Press.	0.09	0.09	0.09	0.06	0.06	0.06	0.012	0.012	0.012
Main Shock - Shot 10									
Meas. by BRL Gage	0.57	0.59	0.51	0.56	0.50	0.38			
Meas. by Lin. Diff. Transf. Gage				0.31	0.45	0.31	0.07	0.07	-----
Comp. for 63 psi Static Press. - Elastic Action	0.34	0.34	0.34	0.23	0.23	0.23	0.05	0.05	0.05
Comp. for 63 psi Static Press. - Fig. 5.3	0.38	0.38	0.38	0.27	0.27	0.27	0.06	0.06	0.06
Comp. from Top Flange Strain	0.44	----	0.45	0.18	0.21	0.20	0.02	0.04	0.03
Comp. from Bot. Flange Strain	0.43	0.85	0.69	0.31	0.41	0.28	0.05	0.05	----
Comp. from Reaction Pressures - Elastic Action	0.37	0.46	0.39	0.25	0.31	0.26	0.05	0.07	0.06

TABLE 7.8 - Permanent Deflections of Beam Strips

Structure	Type of Beam Strip	Perm. Defl., in., for Beam Strip No. 1	2	3	
3.8a	P	0.00	0.07	0.01	0.01
	M	0.00	----	0.01	
	E	-0.01	-0.03	0.01	
3.8b	P	0.04	0.07	0.06	0.10
	M	0.09	----	0.06	
	E	0.00	0.02	0.02	
3.8c	P	0.06	0.06	0.06	0.09
	M	0.08	----	0.01	
	E	0.00	0.01	-0.01	

TABLE 7.9 - Ground Pressures Used in Calculation of Theoretical Deflection

Time, millisec.	Pressure, psi	Time, millisec.	Pressure, psi	Time, millisec.	Pressure psi
180	10.0	220	2.2	255	45.7
185	11.0	225	1.6	260	43.3
190	11.8	230	7.0	265	40.0
195	10.5	235	20.3	270	37.0
200	10.1	240	44.0	275	32.6
205	11.9	245	61.0	280	28.0
210	10.5	250	47.7	285	25.8
215	5.5			290	21.9

Note: Pressures tabulated are average values over a 5 millisec. interval with center at the time indicated after the blast. Values were taken from original record, not rerun.

TABLE 7.10 - Maximum Values of Dynamic Deflection
Computed From Ground Pressures

Beam	Supports Rigid			Supper Moving			
	Yield Point, ksi	Time after Blast, millisec.	Max. Defl., in.	Max. ** Accel.,	Yield Point, ksi	Time after Blast, millisec.	Max. Defl., in.
1P3	72*	250	0.47	8.3	74*	249	0.48
	55	251	0.51	8.3	55	250	0.50
	50	253	0.53	8.3	50	251	0.54
4P3	80*	254	0.51	5.9	69*	252	0.43
	55	258	0.57	5.9	55	253	0.44
	50	262	0.69	5.9	50	254	0.45
8P3	92*	257	0.57				
	55	269	0.80				
	50	273	0.90				
1M2	45*	248	0.27	8.3	41*	248	0.24
4M2	66*	251	0.39	5.9	45*	249	0.26
	50	252	0.40				
	40	257	0.49				
8M2	63*	255	0.36				
	50	255	0.37				
	40	261	0.42				
1E2	13*	246	0.053	8.3	15*	245	0.059
4E2	15*	247	0.060	5.9	16*	249	0.062
8E2	15*	247	0.059				

* Max. stress reached for elastic condition.

** Obsolete values used as rerun records not available when calculations were made. No record available for entries left blank.

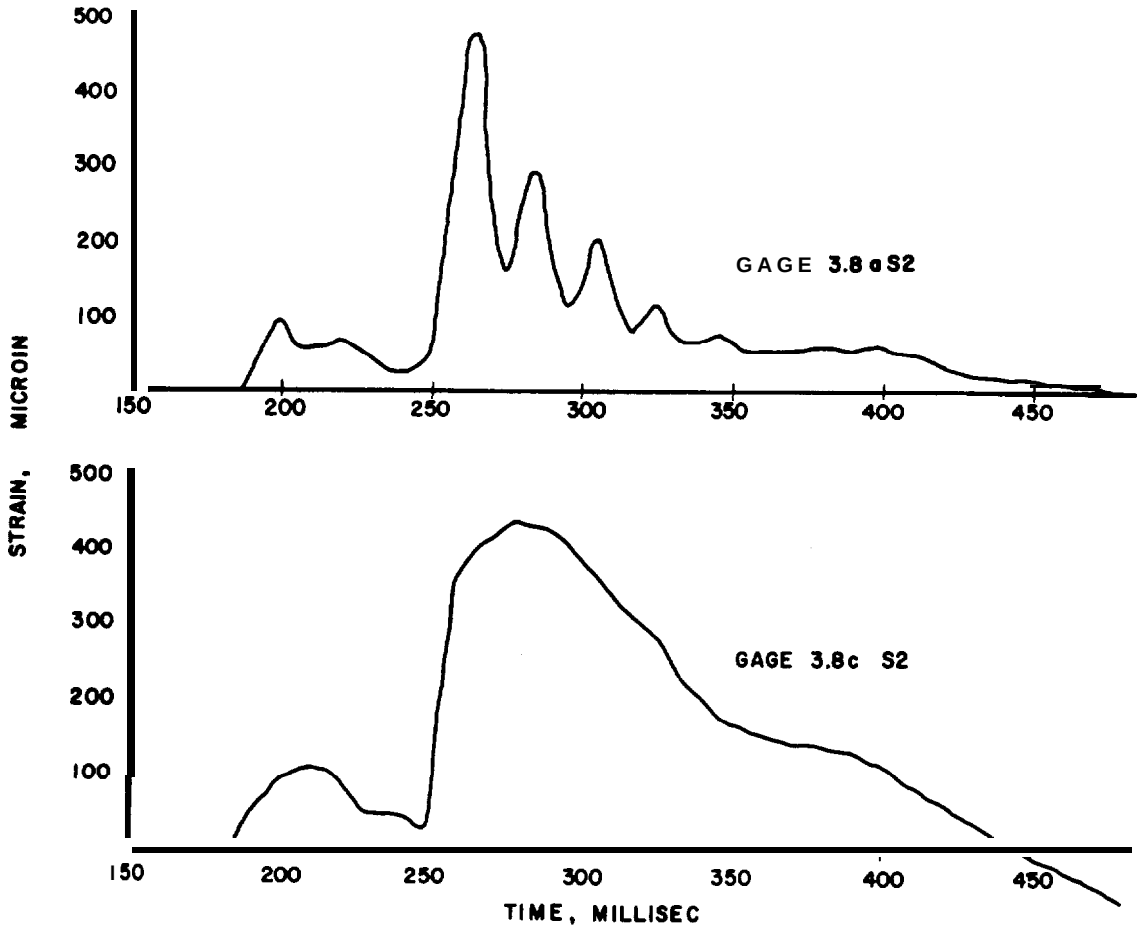

Fig. 7.1 Strain-Time Relation for Top Flange of P Beams at 1 ft and 8 ft depths

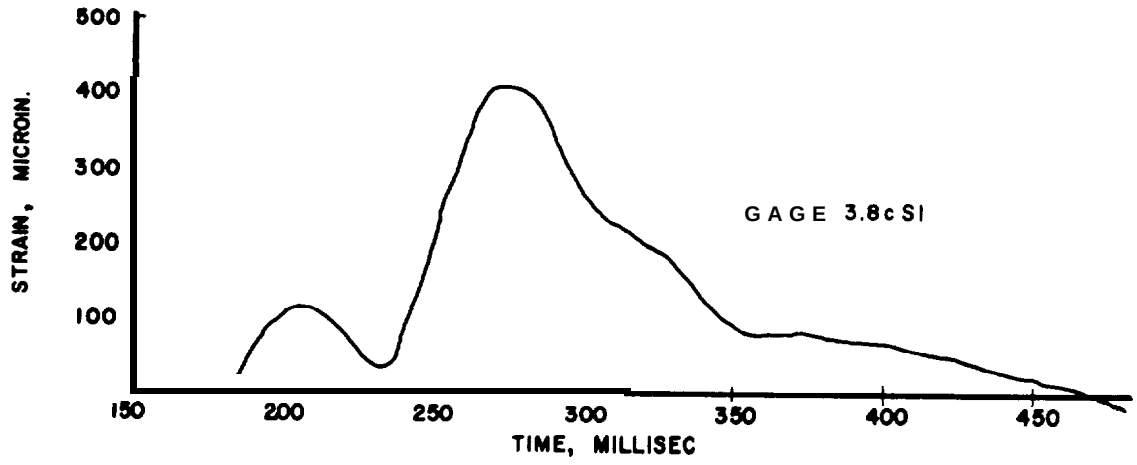

Fig. 7.2 Reaction-Time Relation for P Beam Strip in Structure 3.8c

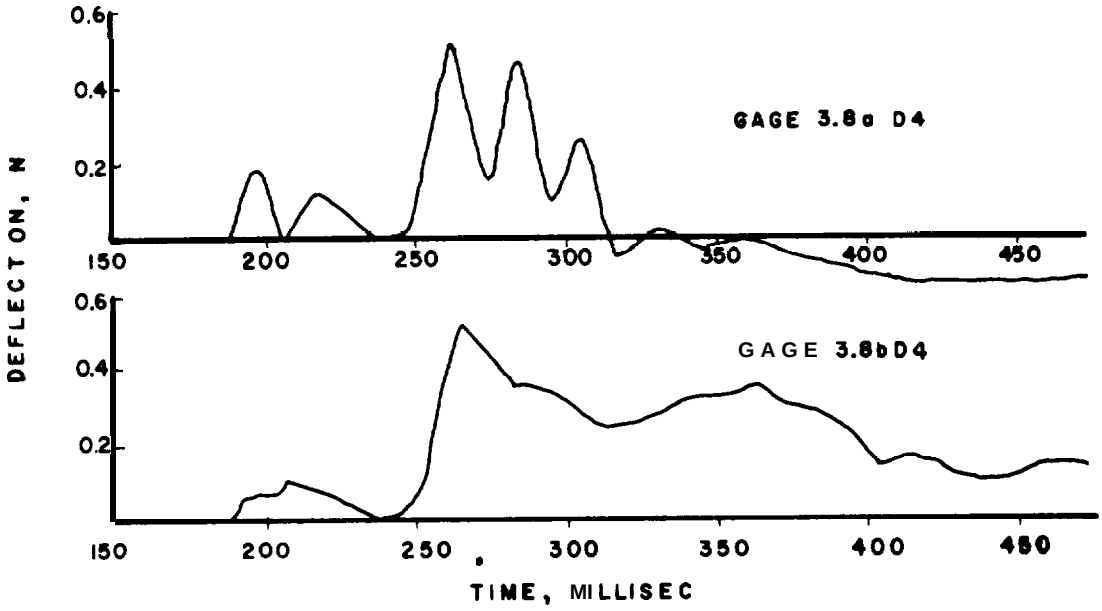

Fig.7.3 Deflection-Time Relations for P Beam Strips in Structures 3.8a and 3.8b

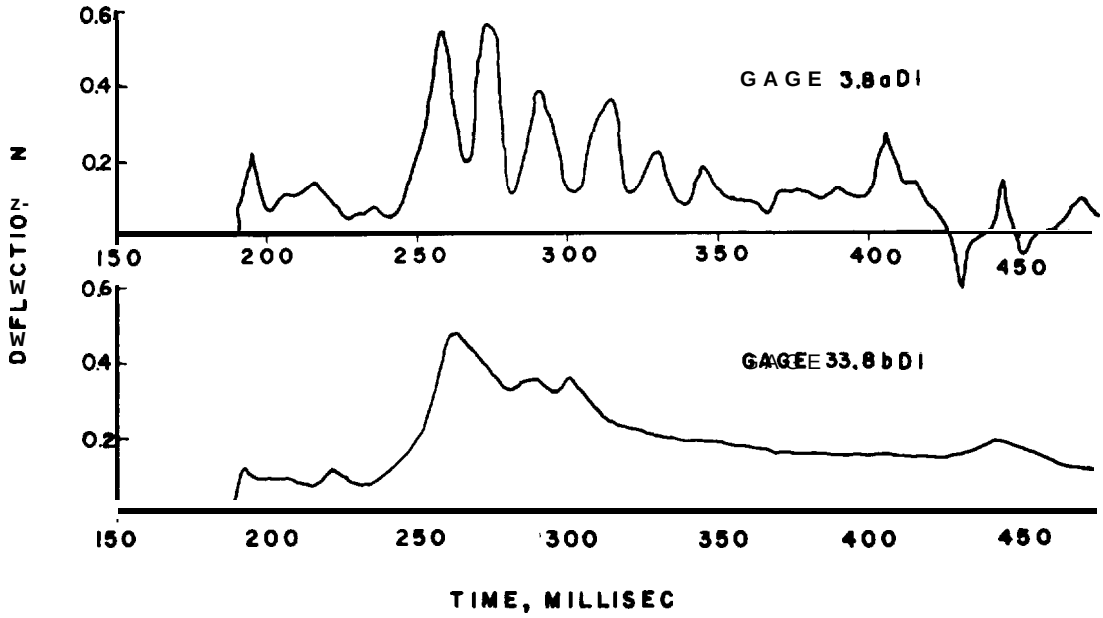

Fig.7.4 Deflection-Time Relations for M Beam Strips in Structures 3.8a and 3.8b

CHAPTER 8

SIGNIFICANCE OF RESULTS OF TESTS AND ANALYSES

8.1 PRACTICAL CONSIDERATIONS

The design of underground protective construction to resist the air blast from atomic bombs presents difficulties only where the pressures are extremely high. For low pressures, of the order of 20 to 30 psi, in general the amount of cover required for radiation protection is great enough so that the static strength of the structure required to support the cover, under the usual working stresses, will generally be sufficient to resist the dynamic forces, although special consideration may have to be given to the effects of very long duration pulses of pressure resulting from the blast of extremely large bombs. If there is only a light cover, it is a simple matter to make the structure heavy enough to resist these moderate pressures. However, when the pressures are extremely high, in the neighborhood of 100 psi, then some special consideration may be required because the reserve strength required for normal design under static conditions would not be sufficient.

There are many factors which influence the behavior of underground structures subjected to blast forces. The response of the parts of the structure are affected very materially by the shape of the pressure-time pulse which reaches the structure. It is reasonable in design to use as a criterion the magnitudes of pressure and duration which are most probable, but also to consider that the pulse might have a shape such that the maximum effect is produced. In other words, it is not desirable to discount the effect of the blast by considering extremely long rise times or precursor pulses, which in general lessen the response of the structure. The design should be sufficiently strong to take account of possible conditions where these mitigating influences are not obtained.

In general, the main structure used in underground construction will be very heavy, and it will be desirable to limit the deflections to relatively small quantities. This is the case for reinforced concrete construction because with deep sections the amount of deflection that is possible before fracture is much smaller than for shallow sections or for steel members. Therefore the test data obtained in this

field test are probably directly applicable to design conditions where heavy roof construction is required, because arching should in general be small on account of the small permissible deflection.

One must take into account the nature of collapse of structural elements used in construction. Wherever possible one should use materials and types of fabrication that permit the absorption of energy without brittle fracture. Finally one should take account of the fact that vibrations are likely to occur under dynamic conditions and that reinforcement and anchorage should be provided to resist the full effect of reversal in the elastic range. In other words, a structure designed for downward loading may often be subjected to an upward loading consistent with an elastic vibration just equal to the yield deflection of the structure. If the structure is not so designed it may suffer secondary collapse which in some cases may be serious.

8.2 SUMMARY OF CONCLUSIONS FROM DATA AND ANALYSES

The following conclusions appear to be warranted by the field test data, the analyses of these data, and the analytical studies reported herein.

(1) In silty subsoil which is well compacted, there is little if any attenuation with depth of the effective pressures applied to an underground structure. There may be more attenuation in granular material or in cohesive clays. However, in the light of present knowledge, it does not appear desirable to consider attenuation of pressure in design procedures for buried structures. Although there was apparently some attenuation of vertical pressure with depth in the free earth pressure measurements, there was no attenuation even for these pressures at depths of 4 ft or less. Some of the attenuation noted for the greater depths could possibly be due to unavoidable discontinuities introduced in the soil mass by the placement of the gages.

(2) Either because of combined attenuation and reflection, or more likely because there was neither attenuation nor reflection of the vertical pressures in the soil acting on the structure, the beam strips appeared to respond as if they were loaded with the vertical forces acting on the earth surface immediately over the structures.

(3) Increases in pressure applied to a structure because of reflections of pressure from the structure apparently are negligible or very small for pressure pulses transmitted through earth, possibly because of the slow rate of rise of the pressure pulses, or because the impedances of the soil and the structural elements of the roof are of the same general order of magnitude.

(4) There was no evidence of dynamic arching in these tests. On the other hand none of the beams deflected more than about 0.5 per cent of their span, and none of the depths of cover used was more than the span length. Whether dynamic arching might occur for much larger deflections or much greater depths of cover is still an open question. For practical design conditions it does not seem advisable to count on dynamic arching to reduce the design loads.

(5) The influence of the over-all accelerations of a structure buried in soil acts to reduce the influence of the pressures applied to the top of the structure but this influence is not large and should be neglected in design.

(6) The lateral earth pressures exerted on vertical faces of a buried structure, produced by air pressures applied at the top surface of the soil, are relatively small for well compacted silty soils when the vertical pressures are high. It appears that pressures of the order of 15 per cent of the vertical force are reached in the horizontal direction for such soils. However, this ratio may be higher for plastic clays or for granular materials of the nature of sand or gravel, and would probably be much higher for material carrying water under pressure or for material with voids completely filled with water.

(7) The upward pressures exerted on the bottom of buried structures are of the same order of magnitude as the pressures on the roof. A base pressure of about three-quarters the roof pressure appears to be sufficient for design purposes unless the duration is extremely long. This will take into account the absorption of pressure producing acceleration of the top surface of the structure, and that which produces acceleration of the structure as a whole.

(8) More favorable distribution of forces on a buried structure may be obtained by arching the outer contour of the surface in such a way that the pressures act relatively uniformly on all surfaces. Then the structure will be subjected primarily to compression rather than to flexure.

(9) Design criteria should be selected which correspond to conditions at yielding or at limit behavior of the structure. In selecting the collapse loads or limit loads, consideration should be given to the probable actual strength of the material under the conditions applying to the structure in practice. The increased dynamic yield point of structural steel may be considered. However it is probably more reasonable to use the apparent increased yield corresponding to the actual static strength of the structural elements considered. Both increases should not be taken into simultaneous account, however.

8.3 DESIRABLE FURTHER INFORMATION

Because experimental data are lacking in the range of structural action approaching collapse, or for large deflections, it is desirable to obtain further information on these structures. The influence of "arching" on the behavior can be obtained by subjecting the test structures to further tests with pressure levels of the order of 75 psi to 150 psi. The conditions can be fairly critical, and even an 80 psi pressure level with a relatively long duration and a sharp rise could cause large deflections in the plastic and intermediate beam strips.

It is unfortunate that the plastic and intermediate beam strips have very nearly the same resistance. If the yield points of the two beam strips had been the same, the resistances would have been more

nearly in proportion to the design values. These beams can be put more in line with the intended design, however, by removing some of their lower flange area.

Because the elastic beam strips are highly resistant, it is possible for them to carry surface loads of the order of 150 to 200 psi without suffering severe damage. Consequently, even though the plastic and intermediate beam strips may fail under such high loads it would be desirable to make an additional test even if the pressures expected would range considerably higher than those recommended above.

In such further tests information of great value could be obtained with only measurement of permanent deformations as established by survey measurements before and after the test. However a pressure-time record of the overpressures on the ground surface would be required. Transient measurements of deflection, reaction, acceleration, and possibly of strain would be helpful in interpreting the data but all of these are not absolutely essential to the development of further useful information. As a minimum, transient deflections and reactions should be measured.

In order to investigate the possible reduction in design pressures that would be permitted by dynamic arching, it is desirable to plan further tests with structures similar to those tested in this program. Such future tests should include greater depth to span ratios and should also include a range in roof flexibilities. If it is possible, a range in soil types should be used, including sand, clay, and different degrees of compaction of the backfill. Such tests should go to pressure ranges as high as practicable.

Further additional information that would be helpful in defining the proper design procedures for underground construction need not be associated with field tests but may be obtained from basic studies in the laboratory. Such studies are:

(1) Studies of pressure transmission through different types of soil, with and without the presence of free water in the soil, by means of a sort of earth shock tube. The attenuation of pressure with distance, and the change in character of the shock front, are the particular variables to be studied.

(2) Studies in the same sort of apparatus of the lateral pressures induced by transmitted longitudinal pressure pulses.

(3) Studies of the motion required to buildup various degrees of arching, under both static and dynamic loading, in different types of soil. Static studies may even be carried out in one of the field structures in order to obtain data for the particular soil used in this test program. However, a simpler laboratory program would be preferable.

(4) Studies of the reflection of pressures from elements of various flexibilities when the pressures are applied as pulses through soil. Again a sort of soil shock tube may be used. Both steep front and varying rise shocks of different strengths should be considered.

8.4 DESIGN RECOMMENDATIONS

The following tentative recommendations are made for the design of buried structures, in the light of present knowledge. These recommendations are based on the assumption that the vertical pressure acting on the ground surface is transmitted downward to the structures without attenuation or reduction in magnitude, and the further assumption that there is no reflection of pressure from the structure.

(1) Buried structures having horizontal upper and lower surfaces should be designed for pressure pulses acting on the upper surface equal to those acting on the ground surface, but assuming that the mass of the covering material acts with the upper surface to increase its mass. Such a calculation is safe because It neglects the possible transfer of pressure laterally by arching around the structure, and it neglects the helpful effect of the accelerations of the supports of the roof as the whole structure is deflected downward. However, such a design procedure is probably not unduly conservative in the light of present information unless the depth of *cover* is extremely large compared with the span.

(2) The bottom or floor of such structures should be designed for upward pressures of the order of three-quarters the downward pressure applied to the top. For extremely long pulses, however, the bottom should be made as strong as the top.

(3) The side walls of buried structure should be designed for approximately one-quarter of the pressures applied to the top surface, unless the material has voids completely filled with water, in which case the side walls must be designed for the same pressure as the top.

(4) In all cases the structure should be designed for a condition corresponding to general yielding of the materials or elements used in it, taking into account the dynamic conditions and the increase in yield point under such conditions compared with static behavior.

(5) For very long pulses, the structure should be designed for the pressures described above, acting as static pressures, for stresses at least 10 per cent below those corresponding to general yielding. For structures at or very close to the surface, the design stresses should be at least 20 per cent below those corresponding to general yielding.

APPENDIX A

INSTRUMENTATION

The instrumentation for the 3.8 structures included the electronic recording of the output from 99 gages for Shot 9 and 101 gages for Shot 10. The installation and operation of the gages and recorders used for both shots was the responsibility of the Ballistic Research Laboratories of the Aberdeen Proving Ground. Permanent personnel from these laboratories with the assistance of military personnel performed the work, all of which was under the direction of Mr. J. J. Meszaros.

The recording equipment used was the Webster-Chicago Tape Recording type which had been modified by Crescent Industries of Chicago, Illinois. Since this equipment is a phase sensitive type on which long leads could not be used, all of the recording equipment and the associated power source for the 3.8 structures was located in an instrument shelter approximately 150 ft from the test chambers. The gages in the test structures were connected to the recording equipment by shielded cable which was buried at a minimum depth of 18 in. Each of the recording units used was capable of recording the intelligence from 22 gages onto a 1 in. magnetic tape. BY running a tape through play-back equipment the intelligence from the tape was transferred to oscillograph records. This method makes it possible to prepare records having almost any desired time basis after a test has been completed.

After each gage had been connected to a recorder with the cables which were to be used during the test, it was calibrated. The cable was then placed in a trench and the gage installed in its proper location. Table A.1 summarizes the location and calibrated range used for both shots for all of the gages. All gages of a particular type were numbered consecutively within the associated structure. Therefore, to designate a gage completely, the particular structure, the letter designating the specific type of gage, and the number of the gage must be given. In stating the location of the SR-4 strain gages the terms "near" and "far" have been used to designate the specific I-beam of the beam strip which is nearest to or farthest from the entrance to the structure. The calibrated ranges given in the table are those actually used. Because of the large difference in the expected

peak pressures in the two shots it would have been desirable to calibrate each gage for a different range for each shot, or in some cases to use other gages which were designed to be used for different ranges. Unfortunately, this scheme was not feasible and was not specified.

The earth pressure gages available had a nominal range equal only to 50 per cent of that desired for more than half of the gages for Shot 10. Since they were buried in the earth and on the exterior of the structures it was possible to calibrate them only once. It was also impractical to supply an equal number of gages having a much lower range to be used for Shot 9. Therefore the following procedure was used for these gages. It was assumed after limited tests on one gage that the gages could be calibrated up to 150 per cent of their nominal range without damaging them. This was done with the expectation that the range would be high enough for most of the gages but probably not high enough for all of them. During the calibration of these gages many more levels of calibrating pressure were used in the low range, with the expectation that amplification of the records and the calibration tape would allow these gages to be used in determining pressures for Shot 9 with a fair degree of accuracy. Since all of the SR-4 strain gages were accessible from inside the structures, these gages were calibrated for different ranges for each shot as shown in the table. Unfortunately, in calibrating the 12 deflection gages incorrect values were used; these gages were set for ranges during Shot 9 which were entirely too high and therefore the readings were of no value.

The calibration of each gage was accomplished by applying a measured effect on the gage and recording the output of the gage on a magnetic tape. For a pressure gage, several levels of measured pressure were applied to the gage through an SR-4 load cell and the output of the electrical system recorded on a tape. On completion of this part of the calibration, an electrical calibrating system was set such that it would place a signal on the magnetic tape having a value between 50 and 80 per cent of the 100 per cent signal, or calibrated range, for that particular gage. A similar procedure was used for other types of gages. Each of these calibration tapes was then run through the play-back equipment, and oscillograph records containing the calibration were prepared. The information from these records and from the calibration data books were plotted in the form of calibration curves. Atypical curve is shown in Fig. A.1. The vertical scale is in fiftieths of an inch as measured on the oscillograph record prepared from the calibration tape, and the horizontal scale is the actual pressure, strain, etc. which was applied to the gage to produce the deflection on the oscillograph record. In addition to the plot of the deflection caused by a known applied physical phenomenon, each calibration curve contained in the title block the deflection caused by the application of an electrical calibrating signal. Owing to the manner in which this recording equipment operates, the calibration curves are not linear. For those gages which are calibrated for both positive and negative phenomena, the calibration curves are not

necessarily similar in the two directions.

During the period immediately preceding the test, all recording equipment was operated remotely. Approximately one-half hour before each test, relays were used to turn on all *recording* equipment and allow it to warm up. A matter of seconds before the actual test, another relay started the tape to travel through the recording head, and at a prescribed time a relay closed and placed an electrical calibrating signal on the tape. Immediately thereafter, the detonation took place and the signal transmitted from each gage was recorded. The tape continued to run until it reached its end.

After the test an oscillograph record was prepared for each gage which contained the intelligence from only portions of the magnetic tape on which the output of the gage was recorded during the test. A rough sketch of one of these records for Shot 10 is shown in Fig. A.2. The typical record illustrated is divided into five areas by large dark bands across the full width of the record. Each of these dark bands signifies a point where the paper in the oscillograph was stopped until the proper section of the tape was reached. Across the bottom of each of the sections there is a fine black line. This line acts as a base line and is used to eliminate the effects of any wobble which may have existed in the transporting of the paper during the reproduction of the record. This line should be used as a base line in making all measurements on the record. Across the top of each record, there is another line, somewhat heavier, which is wavy. This line is recorded on the tape at the same time that the signal from all the gages is recorded and serves as a check on the time basis for the record. Immediately to the left of the major signal shown in the center section of the record, there is a slight discontinuity in the line across the top of the record. The starting point of this discontinuity is the *zero* time *or* time of the detonation. On the record, from left to right, there are the following sections:

(1) The first section contains a straight line near the center of the paper. This line is made by the galvanometers with no signal applied.

(2) In the next section, this line has become slightly wavy. This shows the same galvanometers with the output from the tape being supplied to it. In the right hand part of this section, the trace takes an abrupt movement upwards and continues horizontally for some distance. This deflection is caused by the electrical calibrating signal.

(3) In the center section at the left hand side, the trace from the galvanometers has returned to a zero position and continues horizontally for a short distance. The first discontinuity in the record is caused by the effects of radiation on the recording equipment. However, this effect generally disappears rapidly and by the time the blast reaches the structure the signal has almost returned to the original zero. The remaining portion of this section represents the actual phenomena which occurred over a short period of time after the blast reached the structure. Since such a fast paper speed is used in the oscillograph, it is impractical to reproduce the entire record. Therefore, the paper was again stopped and the record was not

recorded for a period of approximately 15 sec.

(4) The fourth section of the record represents the signal from the gage after about 15 sec.

(5) The last section of the record again represents the galvanometer with no signal applied.

In examining the records produced by the above method, in order to determine both the general quality and the actual peak values of pressure and strain it is necessary to measure the height of the record above the base line at several points. These values are designated in Fig. A.2 by the letters A through G. The values A and G are used as a check to determine if the galvanometers was damaged during preparation of the specific record. The values B and C are used to determine the value of the electrical calibration on the record. The quantities D and E are two possible zero values which must be subtracted from any other heights measured on the record to arrive at a correct height for use in connection with the calibration curves. The height E should always be measured immediately before the blast arrival. The height F is used to determine any residual set or permanent effects on the gage. All of these values are measured in fiftieths of an inch because the calibration curves were plotted using this scale. Since this recording system is not linear and the only calibration signal which appears on the oscillograph record of the test phenomena is the electrical calibration, the ratio of the height of the electrical calibration signal on the calibration curve to the deflection caused by the electrical calibration on the oscillograph record must be used in determining actual values of the physical phenomena.

During the first examination of the records to determine their reliability and the peak values of each of the quantities measured, it was noticed that on many of the records for both Shot 9 and Shot 10 the heights of trace representing zero signal were different before the calibration step (B), after the calibration step (D), and just before blast arrival (E). A small difference in the values measured before and after the calibration step was assumed to be due to short-time instability in the recording channel. Any greater difference in the values measured before calibration and just before shock arrival were assumed to be due to the effects of radiation on the equipment. It was also noticed on many of the records that the height of the signal produced by the electrical calibrating system was not constant. Therefore, the height C was always measured near the start of the calibrating pulse on the assumption that this was probably the most accurate height.

After peak values were read from all of the records, it was found that very little information could be obtained from the records for Shot 9. This was due in several cases to the measured value being such a small percentage of the calibration range, but in most of the cases it was due to the effects of radiation on the equipment. On those records examined, the effects of the radiation were characterized by two distinct phenomena. One phenomenon which was present on many of the records was a large shift in the position of the galvanometer trace at zero time. After shifting positions, the trace remained

horizontal until blast arrival. Another phenomenon which appeared in many of the records was an instability which made itself evident in the form of long waves containing superimposed essentially steady state oscillations. Some of the records for one of the recorders were so bad that no corresponding oscillograph records were prepared by BRL. The peak readings as determined for Shot 9 are given in Table A.2 along with comments on the quality of the record or the reason for there being no value given. In those cases where a value is given and the remarks indicate that there was an appreciable zero shift, the height E was assumed to be the height of zero signal in entering the calibration curves. Although this is probably not the correct location of zero this was done only where the calibration curve was relatively straight, and the value is probably not too much in error.

After the records and peak values for Shot 10 were read, it was decided that although they contained many irregularities all effort should be concentrated on working with these records since they appeared to be the most promising. In general the effects of the radiation were entirely different on the records for Shot 10. In most of the records where the radiation caused the trace to deflect at zero time this effect disappeared rapidly so that by the time the blast reached the structures the signal had become almost horizontal and had returned nearly to the original zero position. Since the effect of the radiation is probably the same as an actual signal from the gage as far as the recording equipment is concerned, it should be treated as such in reducing the records. Therefore in determining the peak values for Shot 10 the height (P-D) was used to determine a total apparent pressure and the height (E-D) was used to determine a fictitious pressure caused by radiation. The fictitious pressure was subtracted from the total apparent pressure to determine the actual gage pressure. This procedure assumes the radiation effect to be constant during the time of the major transient effects.

After discussion of the irregularities and amplifications used in preparing the original oscillograph records for Shot 10 with personnel at BRL, it was agreed that they would prepare new oscillograph records for approximately 40 of the gages for Shot 10 to see if the quality of the records could be improved. These reruns were prepared in a slightly different form. Immediately after the running of the test tape from a gage through the equipment, the associated calibration tape was run through the same equipment without changing any of the adjustments so that both the test phenomena and the full calibration appear on the same oscillograph record. Since records produced by this second method should be of much better quality than those produced by the first method the values read from them have been used throughout the report where the information was received. A summary of the values for the peak readings for Shot 10 is given in Table A.3.

In this table there is a column headed "Type of Record" which refers to Fig. A.1. The symbols used are defined in the figure. Where the complete record is in the essentially linear calibration range, the data are designated by the symbol "A" and are the most reliable. Where the record goes slightly outside the nearly linear range

because of a shift in the zero value, the record type is designated as "B." Where the record goes to the extreme of or beyond the calibration range, the values are highly questionable, and the type is indicated by "C." The symbol "S" is used to indicate a very small amplitude of signal and these records are not accurate. Where the record was very noisy the type was indicated by "N." In some cases combinations of these designations were used.

The last column of Table A.1 indicates the use of either the original oscillograph record in arriving at the peak value, or the rerun oscillograph record which was provided at a later date.

In reducing the reruns for Shot 10 to actual values of the physical phenomena it was possible to obtain a measure of the reliability of the data from the original records since the electrical calibration signal from both the calibration tape and the test tape appeared on the same oscillograph record. It appeared that during the electrical calibrating step, immediately before the test, the full voltage was not applied in many cases. Therefore, this deflection is often smaller than the deflection produced on the record by the actual calibration tape. Since it is not known if this happened for those records for which reruns were not prepared, some of the values read from these records could be too high. On reruns where this could be checked, there were differences of as much as 10 per cent for *several gages.* Because of the non-linearity of the system, this could produce as much as 20 per cent error in reading the actual value of the physical phenomena *near* the end of the calibrated range of the gage. On a very few of the gages, the error due to this source could have *even a* much higher value. For three of the gages the error in the height of the electrical calibrating signal was as much as 50 per cent.

However, in spite of these difficulties, it is felt that the recorded values in Shot 10 at least are reasonably reliable. Adjustments in the values even of a minor nature do not appear necessary because of the various internal checks on consistency among the different readings. Moreover, the results achieved with this equipment appear to be better than have been obtained in the past with the same equipment.

TABLE A.1 - Summary of Instrument Locations

Type and Units	Structure	Gage Number	Gage Location	Range Setting Shot 9	Range Setting Shot 10	Record Shot 10
Earth and Air Pressure Gages, psi	3.8a	E1	q.p. of Beam 1P3	75	75	Rerun
		E2	c.l. of Beam 1P3	75	75	Rerun
		E3	q.p. of Beam 1M2	75	75	Orig.
		E4	c.l. of Beam 1M2	75	75	Orig.
		E5	Near support of Beam 1E2	75	75	Rerun
		E6	In floor slab	50	50	Orig.
		E7	2 ft 0 in. below top end wall	40	40	Orig.
		E8	4 ft 9 in. below top end wall	40	40	Orig.
		E9	7 ft 6 in. below top end wall	40	40	Rerun
	3.8b	E1	q.p. of Beam 4P3	75	75	Orig.
		E2	c.l. of Beam 4P3	75	75	Rerun
		E3	q.p. of Beam 4M2	75	75	None
		E4	c.l. of Beam 4M2	75	75	Orig.
		E5	Near support of Beam 4E2	60	60	Orig.
		E6	In floor slab	50	50	Orig.
	3.8c	E1	q.p. of Beam 8P3	100	100	Orig.
		E2	c.l. of Beam 8P3	75	75	Orig.
		E3	q.p. of Beam 8M2	75	75	Rerun
		E4	c.l. of Beam 8M2	100	100	Orig.
		E5	Near support of Beam 8E2	60	60	Orig.
		E6	3 ft 9 in. below top end wall	62.5	62.	Rerun
	3.8m	E1	Flush with ground surface	75	75	Rerun
		E2	At 1 ft depth in free earth	75	75	Orig.
		E3	At 4 ft depth in free earth	75	75	Rerun
		E4	At 8 ft depth in free earth	60	60	Rerun
		E5	At 12 ft depth in free earth	100	100	Rerun
	3.8a	P1	Near ground surface at entr. to structures B and C	80	80	Orig.
		P2	Inside structure A	10	10	Orig.
	3.8b	P1	Inside structure B	10	10	Orig.
	3.8c	P1	Inside structure C	10	10	Orig.

TABLE A .1 (CONTINUED) - Summary of Instrument Locations

Type and [illegible]	Structure	Gage Number	Gage Location	Range Setting Shot 9	Range Setting Shot 10	Record Shot 10
SR-4 Strain Gages, microin. per in.	3.8a	S1	1P3 Expansion Shoe	300	1000	Orig.
		S2	1P3 Top Fl. c.l. Far I	400	2000	Orig.
		S3	1P3 Top Fl. c.l. Near I	1000	10000	Rerun
		S4	1P3 Bot. Fl.c.l. Far I	1500	2000	Orig.
		S5	1P3 Bot. Fl. c.l. Near I	5000	20000	Rerun
		S6	1P3 Fixed Shoe	300	1000	Orig.
		S7	1M2 Expansion Shoe	300	1000	None
		S8	1M2 Expansion Shoe	200	650	Orig.
		S9	1M2 Top Fl.c.l. Far I	200	2000	Rerun
		S10	1M2 Top Fl. c.l. Near I	600	6000	Rerun
		S11	1M2 Bot. Fl. c.l. Far I	600	2000	Rerun
		S12	1M2 Bot. Fl. c.l. Near I	2000	20000	Rerun
		S13	1M2 Fixed Shoe	300	1000	Orig.
		S14	1E2 Expansion Shoe	250	650	Orig.
		S15	1E2 Top Fl.c.l. Far I	200	500	Orig.
		S16	1E2 Bot. Fl.c.l. Far I	400	1000	Orig.
		S17	1E2 Fixed Shoe	250	650	Rerun
	3.8b	S1	4P3 Expansion Shoe	300	1000	Orig.
		S2	4P3 Top Fl.c.l. Far I	2000	2000	Orig.
		S3	4P3 Top Fl. c.l. Near I	1000	10000	Rerun
		S4	4P3 Bot. Fl.c.l. Far I	1500	2000	Orig.
		S5	4P3 Bot. Fl. c.l. Near I	5000	20000	Rerun
		S6	4P3 Fixed Shoe	300	1000	Orig.
		S7	4M2 Expansion Shoe	300	moo	Orig.
		S8	4M2 Expansion Shoe	200	650	Orig.
		S9	4M2 Top Fl. c.l. Far I	200	2000	Rerun
		S10	4M2 Top Fl. c.l. Near I	600	6000	Rerun
		S11	4M2 Bot. Fl.c.l. Far I	600	2000	Orig.
		S12	4M2 Bot. Fl. c.l. Near I	2000	20000	Rerun
		S13	4M2 Fixed Shoe	300	1000	Orig.
		S14	4E2 Expansion Shoe	250	650	Orig.
		S15	4E2 Top Fl.c.l. Far I	200	500	Orig.
		S16	4E2 Bot. Fl.c.l. Far I	400	1000	Orig.
		S17	4E2 Fixed Shoe	250	650	Orig.

TABLE A. 1 (CONTINUED) - Summary of Instrument Locations

Type and Units	Structure	Gage Number	Gage Location	Range Setting Shot 9	Range Setting Shot 10	Record Shot 10
SR-4 Strain Gages, microin. per in.	1.8c	S1	3P3 Expansion Shoe	300	1000	Orig.
		S2	3P3 Top Fl. c.l. Far I	400	2000	Orig.
		S3	3P3 Top Fl. c.l. Near I	1000	10000	Rerun
		S4	3P3 Bot. Fl. c.l. Far I	1500	2000	Orig.
		S5	3P3 Bot. Fl. c.l. Near I	5000	20000	Rerun
		S6	3P3 Fixed Shoe	300	1000	Orig.
		S7	3M2 Expansion Shoe	600	1000	Orig.
		S8	3M2 Expansion Shoe	200	650	Orig.
		S9	3M2 Top Fl. c.l. Far I	200	2000	Rerun
		S10	3M2 Top Fl. c.l. Near I	600	6000	Rerun
		S11	3M2 Bot. Fl. c.l. Far I	600	2000	Rerun
		S12	3M2 Bot. Fl. c.l. Near I	2000	20000	Rerun
		S13	3M2 Fixed Shoe	300	1000	Orig.
		S14	3E2 Expansion Shoe	250	650	Orig.
		S15	3E2 Top Fl. c.l. Far I	800	500	Orig.
		S16	3E2 Bot. Fl. c.l. Far I	800	1000	Rerun
		S17	3E2 Fixed Shoe	250	650	Rerun
Deflection Gages, in.	1.8a	D1	Center 1M2, BRL Type	5.22	5.22	Rerun
		D2	" 1M2, Diff. Trans.	1.0	1.0	Orig.
		D3	" 1E2, Diff. Trans.	1.0	0.25	Rerun
		D4	" 1P3, BRL Type	5.8	5.8	Rerun
	1.8b	D1	" 4M2, BRL Type	5.8	5.8	Rerun
		D2	" 4M2, Diff. Trans.	1.0	1.0	Orig.
		D3	" 4E2, Diff. Trans.	1.0	0.25	Orig.
		D4	" 4P3, BRL Type	5.8	5.8	Rerun
	1.8c	D1	" 8M2, BRL Type	5.8	5.8	Rerun
		D2	" 8M2, Diff. Trans.	1.0	1.0	Orig.
		D3	" 8E2, Diff. Trans.	1.0	1.0	Orig.
		D4	" 8P3, BRL Type	5.8	5.8	Rerun
Accelerom., g	1.8a	A1	Sidewall away from GZ	11	11	Rerun
		A2	Sidewall nearest GZ	1	1	Rerun
	1.8b	A1	Sidewall away from GZ	1	1	Rerun
		A2	Sidewall nearest GZ	10	10	Rerun
	1.8c	A1	Sidewall nearest GZ	11	11	Rerun
		A2	Sidewall away from GZ	1	1	Rerun

TABLE A.2 - Summary of Peak Readings - Shot 9

Quantity and Units	Structure	Gage Number	Measured Peak	Remarks
Earth and Air Pressure Gages, psi	.8a	E1		Large zero shift, record uninterpretable
		E2		No pulse on record
		E3	12	
		E4	36	
		E5	36	
		E6	15	Record poor, estimated value
		E7		No pulse on record
		E8		No pulse on record
		E9		No pulse on record
	.8b	E1	30	Large zero shift, record poor, estimated value
		E2	19	
		E3	15	
		E4	15	
		E5	35	Large zero shift, estimated value
		E6	17	
	.8c	E1	10	Record poor and calibration bad, estimated value
		E2		No pulse on record
		E3		Electrical calibration data uninterpretable
		E4	16	Record poor, estimated value
		E5	35	Record Poor and calibration bad, estimated value
		E6	3	
	.8m	E1	8	Calibration data erratic, value obviously too low
		E2	7	
		E3	16	Record poor
		E4	26	Large zero shift, estimated value
		E5	3	
	.8a	P1		No record
		P2		No pulse on record, probable value zero
	.8b	P1		No record
	.8c	P1		Record confused

TABLE A.2 (CONTINUED) - Summary of Peak Readings - Shot 9

Quantity and Units	Structure	Gage Number	Measured Peak	Remarks
SR-4 Strain Gages, microin per in.	3.8a	S1		No record
		S2		No record
		S3	400	Calibration data poor, estimated value
		S4		No record
		S5	370	
		S6	80	Noisy record
		S7	130	
		S8	100	Record poor, estimated value
		S9	130	
		S10	130	Record poor, estimated value
		S11	630	Beyond calibrated range, estimated value
		S12	610	
		S13		Signal too small to interpret
		S14		Bad record
		S15	30	Record poor, zero shift, estimated value
		S16	140	
		S17	40	Calibration data poor, zero shift, estimated value
	3.8b	S1		No record
		S2		No record
		S3	400	Second peak
		S4		No record
		S5	470	
		S6	60	Second peak
		S7	90	
		S8	80	Record poor, estimated value
		S9	110	
		S10	90	Record poor, estimated value
		S11	330	
		S12	290	
		S13	110	Record poor, estimated value
		S14		No pulse on record
		S15	40	Record poor, zero shift, estimated value
		S16	100	Noisy calibration pulse, estimated value
		S17	190	Second peak

TABLE A.2 (CONTINUED) - Summary of Peak Readings - Shot 9

Quantity and Units	Structure	Gage Number	Measured Peak	Remarks
SR-4 Strain Gages, microin. per in.	3.8c	S1		No record
		S2		No record
		S3		Large oscillations, not interpretable
		S4	500	Record poor, zero shift, estimated value
		S5		Peak beyond range, record questionable
		S6		Large oscillations, not interpretable
		S7	200	
		S8	70	Record poor, estimated value
		S9	80	
		S10		Malfunction occurred at blast
		S11	370	
		S12	240	
		S13	80	Record poor, estimated value
		S14		Malfunction occurred at blast
		S15	160	Record poor, zero shift, estimated value
		S16		Large oscillations, not interpretable
		S17	60	Second peak
Deflection Gages, in.	3.8a	D1		No record
		D2		Record too small to interpret
		D3		Noise bigger than signal
		D4	0.2	Record too small for accuracy
	3.8b	D1		No record
		D2	0.1	
		D3		Value smaller than electrical oscillation on record
		D4	0.2	Noisy record
	3.8c	D1		Record poor, zero shift, uninterpretable
		D2	0.1	Value between 0.1 and 0.2
		D3		No pulse on record, zero shift
		D4	0.1	
Accelerom, g	3.8a	A1	5	Record poor, zero shift, estimated value
		A2		Beyond range
	3.8b	A1		Beyond range
		A2	4	Unusual record, only one large peak
	3.8c	A1	1	Zero shift, estimated value
		A2		Beyond range

TABLE A.3 - Summary of Peak Readings - Shot 10

Quantity and Units	Structure	Gage Number	Meas. Peak		Type Record See Fig. A.2	Remarks
			Pre-ursor	Main Shock		
Earth and Air Pressure Gages, psi	3.8a	E1	12		C	Probable peak about 120 psi
		E2	21		C	Probable peak about 100 psi
		E3				Record bad
		E4	12		C	Beyond range
		E5	25	62	A	
		E6	14	24	A	
		E7	2	10	A	
		E8	2	7	A	
		E9	0	10	A	
	3.8b	E1	22	76	A	
		E2	12	51	A	
		E3				No record
		E4	14	48	AN	
		E5	36	70	C	
		E6	16	47	A	
	3.8c	E1	17	59	A	
		E2	20		C	Probable peak about 100 psi
		E3	10		CN	Beyond range
		E4	14	71	A	
		E5	35	59	A	
		E6	4	8	A	
	3.8m	E1	16	63	A	
		E2				Record bad
		E3	17	65	AN	
		E4	15	40	A	
		E5	4	16	A	
	3.8a	P1	17			Gage ceased to function
		P2	0	0	ASN	Very noisy
	3.8b	P1	0	0	ASN	Very noisy
	3.8c	P1	0	0	ASN	Very noisy

TABLE A.3 (CONTINUED) - Summary of Peak Readings - Shot 10

Quantity and Units	Structure	Gage Number	Meas. Peak Pre-cursor	Meas. Peak Main Shock	Type Record See Fig. A.2	Remarks
SR-4 Strain Gages, microin. per in.	3.8a	S1	180	460	A	
		S2	170	480	A	Calibration data questionable
		S3	220	630	As	
		S4	840		C	
		S5	580	2040	AS	
		S6	140	370	A	
		S7				No record
		S8	80	370	A	
		S9		190	ANS	
		S10	100	380	As	
		S11	160	510	BN	
		S12	920	Note	As	TWO main peaks 1890 at 264 ms and 2620 at 278 ms
		S13	Note	240	A	Two precursor peaks 60 at 190 ms and 80 at 215 ms
		S14	100	250	A	
		S15	30	100	A	
		S16	100	340	A	
		S17	20	60	As	
	3.8b	S1	150	440	A	
		S2				Extreme oscillations
		S3			S	Values too small for significance
		S4	570		C	
		S5	390	4020	A	
		S6	130	450	A	
		S7				Record bad
		S8	90	400	A	
		S9				Record bad
		S10	140	350	As	
		S11	410		CN	
		S12	380	2080	As	
		S13	20	50	BS	Record poor
		S14				Record bad
		S15	40	150	A	
		S16	100	380	A	
		S17	90	280	A	

TABLE A.3 (CONTINUED) - Summary of Peak Readings - Shot 10

Quantity and Units	Structure	Gage Number	Meas. Peak Pre-cursor	Meas. Peak Main Shock	Type Record See Fig. A.2	Remarks
SR-4 Strain Gages, microin. per in.	3.8c	S1	110	400	A	
		S2	130	440	A	
		S3	310	690	AS	
		S4	460	2000	C	Peak uncertain
		S5	370	4530	A	
		S6	140	510	A	
		S7				Record bad
		S8	90	260	A	Uncertain calibration data
		S9	90	280	A	
		S10	130	380	AS	
		S11	380	1280	AN	
		S12	440	1570	AS	
		S13	130	380	A	
		S14	80	230	A	
		S15	50	130	A	
		S16	20	40	AS	
		S17	30	70	B	Record poor
Deflection Gages, in.	3.8a	D1	0.23	0.56	AS	
		D2	0.08	0.31	A	
		D3	0.02	0.07	A	
		D4	0.23	0.57	A	
	3.8b	D1	0.14	0.50	AS	
		D2	0.08	0.45	A	
		D3	0.02	0.07	A	
		D4	0.17	0.59	A	
	3.8c	D1	0.11	0.38	AS	
		D2	0.09	0.31	A	
		D3				No calibration data
		D4	0.18	0.51	AS	
Accelerom., g	3.8a	A1		7.6	A	
		A2			C	Beyond range
	3.8b	A1			C	Beyond range
		A2			C	Peak greater than 10g on rerun but less than 6 g on original
	3.8c	A1	0.4	1.1	A	
		A2	0.6	0.9	A	

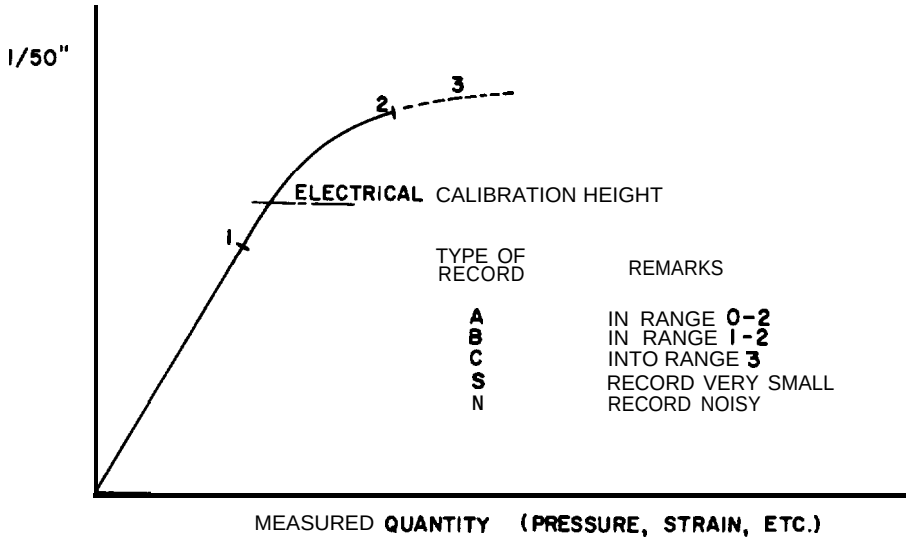

Fig. A.1 Typical Calibration Curve

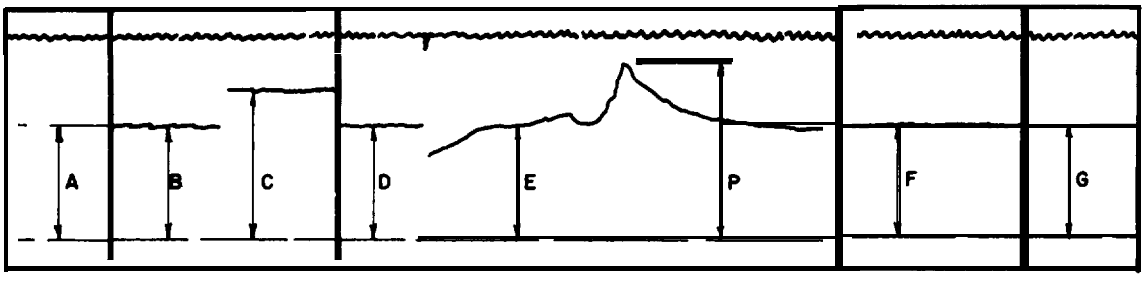

Fig. A.2 Typical Oscillograph Record for Shot 10

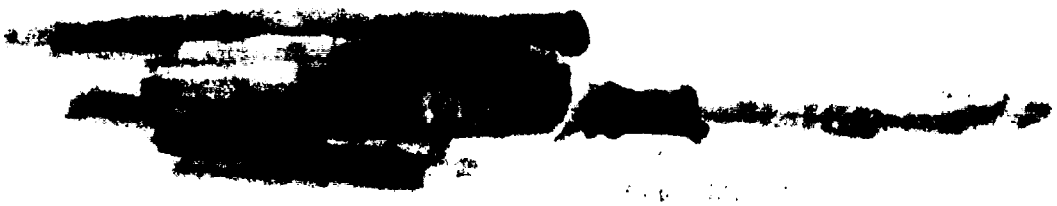

[redacted]

DISTRIBUTION

Military Distribution Category 5-60

ARMY ACTIVITIES

1 Asst. Chief of Staff, G-3, D/A, Washington 25, D.C. ATTN: Dep. CofS, G-3 (RR&SW)
Asst. Chief of Staff,, G-4, D/A, Washington 25, D.C.
2 Deputy Chief of Staff for Logistics, D/A, Washington 25, D .C. ATTN: Director of Research and Development
3 Chief of Ordnance, D/A, Washington 25, D.C. ATTN: ORDTX -AR
4- 6 *Chief* Signal Officer, D/A, P&O Division, Washington 25, D.C. ATTN: SIGOP
7 The Surgeon General. D/A., Washington 25, D.C. ATTN: Chief, R&D Division
8- 9 Chief Chemical Officer, D/A, Washington 25, D.C.
10 The Quartermaster General, CBS, Liaison Officer, Re - search and Development Div. , D/A, Washington 25, D.C.
11- 15 Chief of Engineers, D/A, Washington 25, D.C. ATTN: ENGNB
16 Chief of Transportation, Military Planning and Intel- ligence Div., Washington 25, D.C.
17- 19 Chief, Army Field Forces, Ft. Monroe, Va.
20 President, Board #1, OCAFF, Ft. Bragg, N. C.
21 President, Boarrd #2, OCAFF, Ft. Knox, Ky.
22 President, Board #4, OCAFF, Ft. Bliss, Tex.
23 Commanding General, U.S. Army Caribbean, Ft. Amador, C.Z. ATTN: Cml. Off.
24 Commander-in-Chief, European Command, APO 128, c/o PM, New York, N.Y.
25- 26 Commander-in-Chief, Far East Commend, APO 500, c/o PM, San Francisco, Calif. ATTN: ACofS, J-3
27- 28 Commanding General, U.S. Army Europe, APO 403, c/o PM, New York, N.Y. ATTN: OPOT Div. , Combat Dev. Br.
29 Commandant, Command and General Staff College, Ft. Leavenworth, Ran. ATTN: ALLLS (AS)
30 Commandant, The Artillery School, Ft. Sill, Okla.
31 Secretary, The AA&GM Branch, The Artillery School, Ft. Bliss, Tex. ATTN: Lt. Col. Albert D. Epley, Dept. of Tact ics and Combined Arms
32 Commanding General, Medical Field Service School, Brooke Army Medical Center, Ft. Sam Houston, Tex.
33 Director, Special Weapons Development Of fice, Ft. Bliss, Tex. ATTN: Lt. Arthur Jaskierny
34 Superintendent, U.S. Military Academy, West Point, N .Y. ATTN: Pro?. of Ordnance
35 Commandant, Chemical Corps School, Chemical Corps Training Command, Ft. McClellan, Ala.
36 Commanding General, Research and Engineering Command, Army Chemical Center, Md. ATTN: Deputy for RW and Non-Toxic Material
37- 38 Commanding General, Aberdeen Proving Grounds, Md. (inner envelope) ATTN: RD Control Officer (for Director, Ballistics Research Laboratory)
39- 41 Commanding General, The Engineer Center, Ft. Belvoir, Va. ATTN: A set. Commandant, Engineer School
42 Commanding Officer, Engineer Research and Development Laboratory, Ft. Belvoir, Va. ATTN: Chief, Technical Intelligence Branch
43 Commanding Officer, Picatinny Arsenal, Dover, N.J. ATTN : ORDBB -TK
44- 45 Commanding Officer, Chemical C orps Chemical and Radio- logical Laboratory, Army Chemical Center, Md. ATTN: Tech. Library
46 Commanding Officer, Transportation R&D Station, Ft. Eustis , Va .
47 Director, Technical Documents Center, Evens Signal Laboratory, Belmar, N .J.
48 Director, Waterways Experiment Station, PO Box 631, Vicksburg, Miss. ATTN: Library
49 Director, Operations Research Off ice, Johns Hopkins University, 7100 Connecticut Ave., Chevy Chase, Md. TTN
50- 56 Technical Information Service, Oak Ridge, Tenn. (Surplus)

NAVY ACTIVITIES

57- 58 Chief of Naval Operations, D/N, Washington 25, D .C. ATTN: OP-36
59 Chief of Naval Operations, D/N, Washington 25, D.C. ATTN: OP-374(OEG)
60 Director of Naval Intelligence, D/N, Washington 25, D.C . ATTN: OP-922V
61 Chief, Bureau of Medicine and Surgery, D/N, Washington 25, D.C. ATTN: Special Weapons De fense Div.
62 Chief, Bureau of Ordnance, D/N, Washington 25, D .C.
63 Chief, Bureau of Ships, D/N, Washington 25, D.C. ATTN: Code 348
64 Chief, Bureau of Yards and Docks, D/N, Washington 25, D.C. ATTN: D-440
65 Chief, Bureau of Supplies and Accounts, D/N, Washing- ton 25. D.C.
66- 67 Chief, Bureau of Aeronautics, D/N, Washington 25, D.C.
68 Chief of Naval Research, Department of the Navy Washington 25, D.C. ATTN: LT(jg) F. McKee, USN
69 Commander-in-Chief, U.S. Pacific Fleet, Fleet Post Office, San Francisco, Calif.
70 Commander-in-Chief, U.S. Atlantic Fleet, U.S. Naval Base, Norfolk 11, Va.
71- 74 Commendant, U.S. Marine Corps, Washington 25, D.C. ATTN: Code AO3H
75 Superintendent, U.S. Naval Postgraduate School, Monterey, Cal if.
76 Commanding Officer, U.S. Naval Schools Command, U.S. Naval Station, Treasure Island, San Francisco, Calif.
77 Commanding Off icer, U.S. Fleet Training Center, Naval Base, Norfolk 11, Va. ATTN: Special Weapons School
78- 79 Commanding Off icer, U.S. Fleet Training Center, Naval Station, San Diego 36, Calif. ATTN: (SPWP School)
80 Commanding Officer, U.S. Naval Damage Control Training Center, Naval Base, Philadelphia 12. Pa. ATTN: ABC Defense Course
81 C—ding Officer, U.S. Naval Unit, Chemical Corps School, Army Chemical Training Center, Ft. McClellan, Ala .
82 Commander, U.S. Naval Ordnance Laboratory, Silver Spring 19, Md. ATTN: EE
83 Commander, U.S. Naval Ordnance Laboratory, Silver Spring 19, Md. ATTN: EH
84 Commander, U.S. Naval Ordnance Laboratory, Silver Spring 19, Md. ATTN: R
85 Commander, U.S. Naval Ordnance Test Station, Inyokern, Chine Lake, Calif.
86 Officer-in-Charge, U.S. Naval Civil Engineering Res. and Evaluation Lab. , U.S. Naval Construction Bat - talion Center, Port Hueneme, Calif. ATTN: Code 753
87 Commanding Officer, U.S. Naval Medical Research Inst., Nat i onal Naval Medical Center, Bethesda 14, Md.
88 Director, U .S. Navel Research Laboratory, Washington 25, D.C. ATTN: Code 2029
89 Commanding Officer and Director, U.S. Navy Electronics Laboratory, San Diego 52, Cal if. ATTN: Code 4223
90- 91 Commanding Off icer, U.S. Naval Radiological Defense Laboratory, San Francisco 24, Calif. ATTN: Technical Information Division
92 Commending Officer and Director, David W. Taylor Model Basin, Washington 7, D.C. ATTN, Library
93 Commander, U.S. Naval Air Development Center, Johns - ville, Pa.
94 Director, Office of Naval Research Branch Office, 1000 Geary St. . San Francisco. Calif.
95-101 Technical Information Service, Oak Ridge, Tenn.

[redacted]

UNCLASSIFIED

[redacted]

AIR FORCE ACTIVITIES

102 Asst. for Atomic Energy, Headquarters, USAF, Washington 25, D.C . ATTN: DCS/O
103 Director of Operations, Headquarters, USAF, Washington 25, D.C. ATTN: Operations Analysis
104 Director of Plans, Headquarters, USAF, Washington 25, D.C. ATTN: War Plans Div.
105 Director of Research and Development, Headquarters, USAF, Washington 25, D.C. ATTN: Combat Components Div.
106-107 Director of Intelligence, Headquarters, USAF, Washington 25, D.C. ATTN: AFOIN-1B2
108 The Surgeon General, Headquarters, USAF, Washington 25, D.C. ATTN: Bio. Def. Br. , Pre. Med. Div.
109 Deputy Chief of Staf f, Intelligence, Headquarters, U.S. Air Forces Europe, APO 633, c/o PM, New York, N .Y. ATTN: Directorate of Air Targets
110 Commander, 497th Reconnaissance Technical Squadron (Augmented) , APO 633, c/o PM, New York, N.Y.
111 Commander, Far East Air Forces, APO 925, c/o PM, San Francisco, Calif.
112 Commander, Strategic Air Command, Of futt Air Force Base, Omaha, Nebraska. ATTN: Special Weapons Branch, Inspect ion Div., Inspector General
113 Commander, Tactical Air Command, Langley AFB, Va. ATTN: Documents Security Branch
114 Commander, Air Defense Command, Ent AFB, Colo.
115-116 Commander, Air Materiel Command, Wright -Patterson AFB, Dayton, O. ATTN: MCAIDS
117 Commander, Air Training Command, Scott AFB, Belleville, Ill. ATTN: DCS/O GTP
118 Commander, Air Research and Development Command, PO Box 1395, Baltimore, Md. ATTN: RDDN
119 Commander, Air Proving Ground Command, Eglin AFB, Fla. ATTN: AG/TRB
120-121 Commander, Air University, Maxwell AFB, Ala.
122-129 Coma.?. nder, Flying Training Air Force, Waco, Tex. ATTN: Director of Observer Training
130 Commander, Crew Training Air Force, Randolph Field, Tex. ATTN: 2GTS, DCS/O
131 Commander, Headquarter, Technics l Training Air Force, Gulf port, Miss. ATTN: TA&D
132-133 Commandant, Air Force School of Aviation Medicine, Randolph AFB, Tex.
134-139 Commander, Wright Air Development Center, Wright-Patterson AFB, Dayton, O. ATTN: WCOSI
140-141 Commander, Air Force Cambridge Research Center, 230 Albany Street, Cambridge 39, Mass. ATTN: CRQST -2
142-144 Commander, Air Force Special Weapons Center, Kirtland AFB, N.Mex.ATTN: Library
145 C ommandant, USAF Institute of Technology, Wright-Patterson AFB, Dayton, O. ATTN: Resident College
146 Commander, Lowry AFB, Denver, Colo.ATTN: Department of Armament Training
147 Commander, 1009th Special Weapons Squadron, Headquarters, USAF, Washington 25, D.C.
148-149 The RAND Corporation, 1700 Main Street, Santa Monica, Calif. ATTN: Nuclear Energy Division
150-156 Technical Information Service, Oak Ridge, Tenn. (Surplus)

OTHER DEPARTMENT OF DEFENSE ACTIVITIES

157 Asst. Secretary of Defense, Research and Development, D/D, Washington 25, D.C .
158 U.S. National Military Representative, Headquarters, SHAPE, APO 55, c/o PM, New York, N.Y. ATTN: Col. J . P. Healy
159 Director, Weapons Systems Evaluation Group, OSD, Rm 2E1006, Pentagon, Washington 25, D.C.
160 Armed Services Explosives Safety Board, D/D, Building T-7, Gravelly Point, Washington 25, D.C.
161 Commandant, Armed Forces Staff College, Norfolk 11, Pa. ATTN: Secretary
162-167 Commanding General, Field Command, Armed Forces Special Weapons Project, PO Box 5100, Albuquerque, N. Mex.
168-169 Commanding General, Field Command, Armed Forces, Special Weapons Reject, PO Box 5100, Albuquerque, N. Mex. ATTN: Technical Training Group
170-178 Chief, Armed Forces Special Weapons Project, Washington 25, D.C.
179-185 Technical Information Service, Oak Ridge, Tenn. (Surplus)

ATOMIC ENERGY COMMISSION ACTIVITIES

186 -188 U.S. Atomic Energy Commission, Classif ied Technical Library, 1901 Constitution Ave. , Washington 25, D.C . ATTN: Mrs. J.M. O'Leary (For DMA)
189-191 Los Alamos Scientific Laboratory, Report Library, PO Box 1663, Los Alamos, N. Mex. ATTN: Helen Redman
192-194 Sandia Corporation, Classified Document Division, Sandia Base, Albuquerque, N. Mex. ATTN: Martin Lucero
195-196 University of California Radiation Laboratory, PO Box 808, Livermore, Calif. ATTN: Margaret Edlund
197 Weapon Data Section, Technical Information Service, Oak Ridge, Term.
198-285 Technical Information Service, Oak Ridge, Tenn. (Surplus)

[redacted]

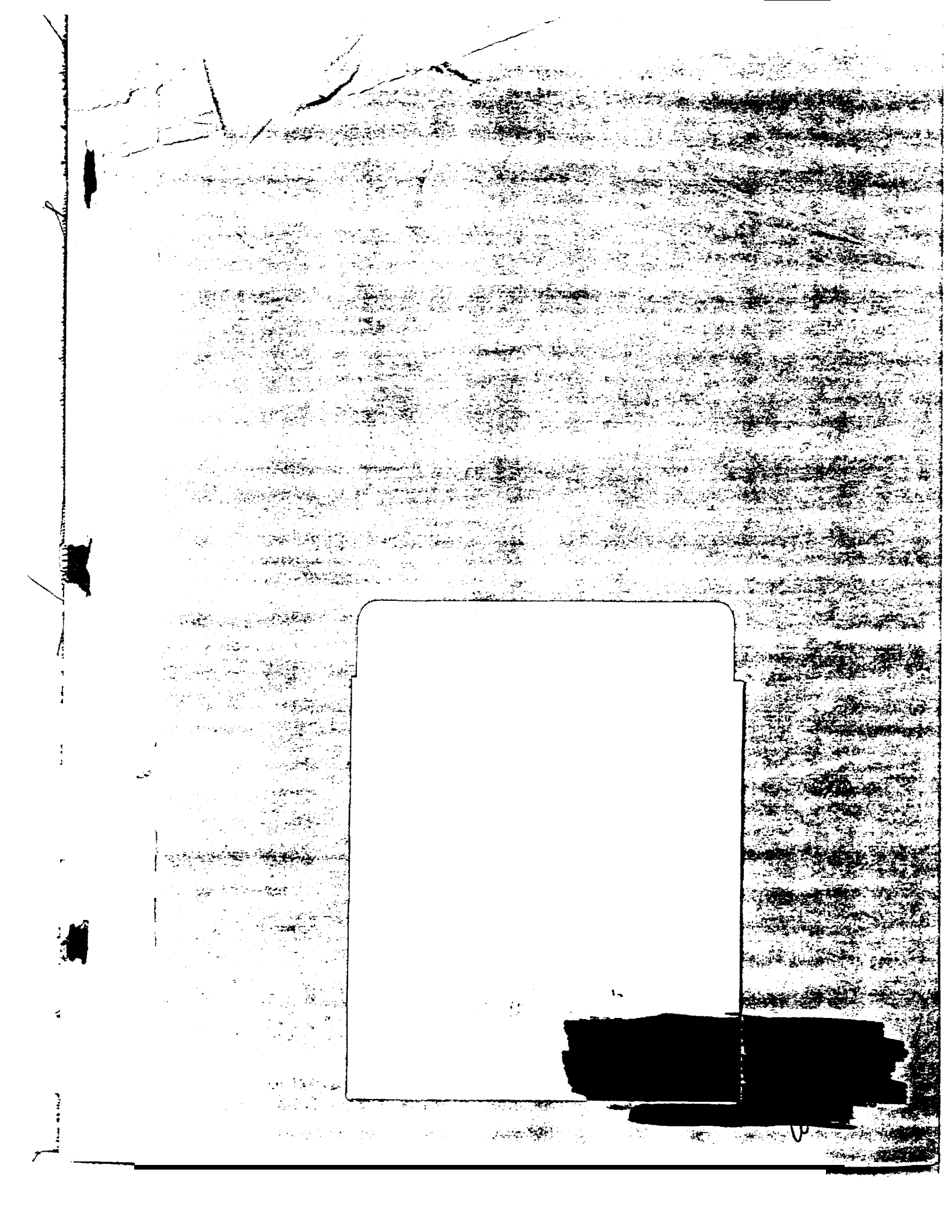

UNCLASSIFIED

[redacted]

[redacted]

UNCLASSIFIED

[redacted]

[redacted]

ea 5/6/98